EGG-TMI-7385, Rev. 1
February 1987

INFORMAL REPORT

TMI-2 CORE BORE ACQUISITION SUMMARY REPORT

E. L. Tolman
R. P. Smith
M. R. Martin
R. K. McCardell
J. M. Broughton

Idaho National Engineering Laboratory

Managed by the U.S. Department of Energy

MASTER

EG&G Idaho

Work performed under DOE Contract No. DE-AC07-76ID01570

EGG-TMI-7385
Revision 1

TMI-2 CORE BORE ACQUISITION SUMMARY REPORT

E. L. Tolman
R. P. Smith
M. R. Martin
R. K. McCardell
J. M. Broughton

Published February 1987

EG&G Idaho, Inc.
Idaho Falls, Idaho 83415

Prepared for the
U.S. Department of Energy
Idaho Operations Office
Under DOE Contract No. DE-AC07-76ID01570

ABSTRACT

Core bore samples were obtained from the severely damaged TMI-2 core during July and August, 1986. A description of the TMI-2 core bore drilling unit used to obtain samples; a summary and discussion of the data from the ten core bore segments which were obtained; and the initial results of analysis and evaluation of these data are presented in this report. The impact of the major findings relative to our understanding of the accident scenario is also discussed.

DISCLAIMER

SUMMARY

Examinations of the TMI-2 core indicated that a hard, nearly impenetrable layer of material exists across the core at approximately the mid-core elevation. It was hypothesized that this hard, basically ceramic material extended downward to about the 0.6-m elevation. Samples of this material were required to complete the end-state characterization of the core configuration, as well as to improve understanding of the physical and chemical materials interactions and fission product retention of the core materials. A core bore machine has been designed and utilized to safely and efficiently provide the desired samples prior to the commencement of bulk defueling of the core by General Public Utilities Nuclear Corp. (GPU).

The core bore machine drilled 6-ft "core" samples approximately 2.5 in. in diameter, which were later removed from the reactor vessel (RV) for detailed physical and chemical examination. The hole remaining after sample removal provided access for closed-circuit television (video) inspections of the surrounding region.

Ten samples or segments from the core, and possibly two samples of core material in the lower plenum, were obtained with the core bore machine during July and August, 1986. Visual inspections of the core bore hole and the core support assembly (CSA) were performed at all ten locations. The data obtained from this operation and subsequent analysis of the video and drilling data are presented and discussed in this document. The major research findings are:

1. A region of previously molten core materials estimated to be approximately 122 ft^2 (about 10% of the original core volume) was confirmed to be in the lower, central region of the core. This solid structure is approximately 4-ft thick in the center of the core, 1- to 2-ft thick near the core periphery, and is roughly shaped like a funnel extending down toward the bottom of the core. Intact rod stubs exist from the bottom of the core up to the previously molten ceramic material.

2. The central regions of the CSA do not contain significant amounts of previously molten fuel, which suggests that the major crust failure location was not in the central region of the core. The primary migration path of the previously molten material into the lower plenum appears to be located on the east side of the core near the periphery, primarily at assemblies P-5 and P-6.

3. Based on the limited video inspection data, the CSA appears to be undamaged in those areas where previously molten ceramic materials have frozen in place between the CSA structural members.

4. The fuel debris resting on the bottom vessel head near the center of the RV appears to be loose and relatively fine as compared with the larger agglomerated debris existing near the edge of the RV in the lower plenum.

5. The individual core bores indicate a rather homogeneous structure across the core, although detailed structural differences exist. At several core bore locations, metallic inclusions appear in the upper portion of the solid, previously molten material, while in others metallic inclusions are observed near the center and/or bottom of the previously molten regions. The shapes of the metallic inclusions vary widely.

The core bore acquisition findings summarized above provide significant insights with respect to core damage and the accident scenario. The basic features of the accident scenario and implications resulting from the core bore data are summarized below:

1. Rapid zircaloy oxidation and heatup of the upper half of the core probably occurred between 150-174 min into the accident. The rapid heating resulted in clad melting, dissolution of UO_2 fuel, and downward flow of molten zircaloy cladding and dissolved UO_2 fuel toward the bottom of the core where it eventually froze in-place. The end-state crust configuration near the

center of the vessel confirms that cooling of the bottom regions of the core (below the second spacer grid) was maintained. This is an important observation, since it allows estimates of the minimum RV liquid level during the accident. Between 150 and 174 min, continued core heatup gradually increased the size of the molten core region. By 174 min, the relocated core materials had formed a large central region of nearly solid structure composed of control rod and ceramic fuel rod materials consisting of approximately one-third of the core materials. The end-state configuration of the core indicates that the assumption of an initial core relocation to near the bottom of the core and freezing in place is sound. The intact fuel rod stubs in the lower core regions confirm that cooling in the lower 0.5 m of the core was maintained, which is consistent with previous analyses of the reactor cooling system (RCS) thermal-hydraulic response.

2. The B-2 pump transient at 174 min probably injected coolant from the B-loop cold legs into the RV. An upper-bound value of the injected coolant is approximately 1000 ft^3; however, some of this may have bypassed the RV due to the significant core blockage and steam buildup. The resulting thermal-mechanical forces from the rapid steam production are hypothesized to have shattered the remaining upper oxidized fuel rod remnants above the molten core region, forming a rubble bed on top of the solid structure. Video inspection of the core bore holes indicates that relatively large metallic structures, possibly fuel assembly spacer grids and/or remnants of fuel assembly end fittings and spiders, are embedded in the upper crust of the previously molten ceramic structure. This suggests that the upper debris bed may have vigorously mixed after the fuel rods were initially shattered and before the upper crust was completely frozen. Detailed examination of the upper core debris extracted earlier from positions H8 and G9 confirm that the debris bed was well mixed. Also, many of the particles were agglomerates consisting of essentially unrestructured fuel fragments and previously

molten ceramic fuel rod materials. The existence of agglomerated particles of this type throughout the debris bed suggests that the debris was vigorously mixed prior to the final freezing of the top crust and that some of the molten ceramic material was vigorously mixed with the fragmented fuel rod debris from above.

3. The solid structure of core material near the bottom of the core continued to heat after the pump transient, increasing the amount of molten material present in the central core. The molten material was contained within the original core boundary by a crust of solidified ceramic material at the outer edge of this solid structure of core materials. A temperature gradient within this solid structure is indicated by differences in the observed materials within the structure. The interior appears to be all previously molten ceramic material with some veins and inclusions of previously molten metal. The periphery of the solid structure is composed of fuel fragments encased within a solid matrix of previously molten ceramic material. There is no visible evidence from the video inspections that the fuel fragments are surrounded by zircaloy cladding. Apparently the zircaloy cladding was either oxidized and/or melted and incorporated into the molten ceramic material. The relatively homogeneous ceramic material in the center would have been at a higher temperature or at temperature for a significantly longer time than the agglomerated material at the periphery.

4. Data recorded by on-line instrumentation during the accident suggest that a major core relocation event occurred at approximately 224 min. Failure of the melt-containing ceramic crust at 224 min allowed the core to relocate into the lower plenum. The core bore data indicate that the flow path for relocation of molten material was on the east side of the core, probably in the vicinity of assemblies P-5 and P-6, rather than at the central region of the core as had been earlier assumed.

Damage to the core support assembly has not been observed, suggesting that the primary relocation of core materials was an event of relatively short duration.

Identification of the core structures suggesting that molten core materials relocated from the core periphery into the lower plenum indicates that the mechanisms controlling crust failure are different than had been previously envisioned. Three core crust failure mechanisms can be hypothesized to explain the peripheral core failure location. These include:

a. Thermal melt-through of the top crust caused by preferential convective heat transfer of decay heat upward to the top of the solid structure and relatively limited cooling of the top surface because of the presence of the debris bed.

b. Thermal/mechanical stress failure of the upper and/or peripheral crust.

c. Possibly eutectic interaction between the crust material and the stainless steel core former wall structures.

Our understanding of core damage during the accident is not yet complete. The most important questions remaining to be answered regarding core damage and potential failure of the RV lower head during the TMI-2 accident include:

1. What was the thermal response of the solid, degraded core structure, and did the core former wall interact thermally or chemically with the supporting crust of ceramic material to induce failure of the crust?

2. What was the impact of the coolant and RCS pressure changes on the formation and mechanical stability of the ceramic crust?

3. What are the effects of control rods and burnable poison rods on core damage progression?

4. What were the heat transfer characteristics of the debris bed and to what extent were the debris bed and the solid structure thermally and mechanically coupled?

5. What were the controlling thermal-hydraulic mechanisms that resulted in the formation and current state of the upper debris bed?

6. What was the extent of thermal and chemical interaction between the molten core materials and the core support assembly, the RV lower head, and instrument penetration nozzles and guide tubes?

7. What was the long-term thermal response (coolability) of the solid structure of core materials contained within the core region and the core debris in the lower plenum?

The examination results from the core bore samples are crucial in resolving these questions. Additional sample acquisition and examinations of core material in unique damage zones are also planned and will contribute information relative to the physical/chemical interactions and mechanisms controlling the core damage and the retention of fission products. Engineering analyses are underway to improve understanding of core damage progression and possible damage to the CSA, instrument structures, and lower head.

ACKNOWLEDGMENTS

The acquisition of the core bore samples and accompanying video inspection tapes was a joint undertaking by EG&G Idaho, Inc., and GPU Nuclear Corp. The commitment, enthusiasm, and expertise of many people from both companies were necessary to successfully complete this unique engineering task.

This report was a team effort by the TMI-2 Accident Evaluation Program staff at EG&G Idaho. M. L. Russell spent many hours viewing and interpreting the video tapes of the core bores. R. P. Smith and W. F. Downs were especially helpful in contour mapping and spatially depicting the damage core regions. M. Golusha provided support in reducing the machine drilling data, and Dr. P. Kuan has provided valuable insights in interpreting the data. Dr. J. Partin is recognized for her work in producing the enhanced video images. Recognition is also extended to N. Wade, for her excellent editing support, and to Gypsy Jones, for her graphics support.

CONTENTS

FIGURES

TABLES

TMI-2 CORE BORE ACQUISITION SUMMARY REPORT

INTRODUCTION

Introduction and Background

The TMI Accident Evaluation Program[1] is being conducted by the Department of Energy (DOE)[a] for the contribution of TMI-2 accident research toward resolution of severe accident and source term technical issues, as well as to support the TMI-2 recovery effort. This research has determined that damage to the TMI-2 core was extensive with core melting and relocation of molten core materials into the reactor vessel (RV) lower plenum. A scenario for the accident has been proposed[2] which appears to account for most of the major events and resultant core damage. However, some details of this scenario are not fully understood; and these include: (a) the physical mechanisms leading to core failure and subsequent relocation of molten materials into the lower plenum; (b) the extent of damage to the core support assembly (CSA), instrument structures, and the RV lower head; (c) the long-term cooling of the degraded core and the core debris in the lower plenum; and (d) the retention and distribution of fission products within core materials. An adequate understanding in each of these areas requires extensive physical and chemical evaluation of the core materials and RV components, together with detailed analysis and interpretation of the reactor system thermal-hydraulic measurements recorded during the accident.

A detailed sample acquisition and examination program[3] is underway to provide the requisite data to satisfy the research needs. Core boring of the damaged reactor core was selected as the appropriate means of acquiring samples of the solid structure of previously molten core

---

a. The overall TMI-2 recovery is being conducted under the auspices of the GEND organization, comprised of General Public Utilities (G), Electric Power Research Institute (E), the U.S. Nuclear Regulatory Commission (N), and the U.S. Department of Energy (D).

materials and rod stubs beneath the upper debris bed. The samples must be from well-defined locations within the core and CSA and also from the RV lower plenum at inspection locations. The core bore machine provided this capability. Core boring also provided access into the lower plenum for visual inspection in regions previously inaccessible to a closed-circuit video camera (CCTV), as well as the inside surface of the core bore holes. The original accident scenario hypothesized that voids may have existed within the solid, previously molten structure. These voids could have formed when the molten core materials relocated into the lower plenum. Details of the solid structure are important from the perspective of understanding the accident, in particular core damage progression and damage to other RV structures, as well as for core defueling and disassembly of support structures.

The primary goal of the core boring operation was to obtain physical samples necessary to spatially characterize the current chemical and physical state and distribution of core materials. Specific operational objectives were:

1. Acquire up to nine core bores from the core which are spatially distributed such that a representative sampling of core materials is obtained.

2. Acquire one core bore from core materials in the lower plenum through the lower plenum inspection port in the CSA beneath the K9 assembly.

3. Acquire a sample of core materials at the location where molten materials relocated into the RV lower plenum.

4. Obtain samples for comparison from control rod and burnable poison rod assemblies.

Assemblies were selected for drilling which satisfy these objectives. However, a number of constraints existed which restricted the available drilling locations. These constraints included:

1. Drilling was not permitted in instrumented fuel assemblies because of safety considerations related to potential failure of the instrument penetration nozzle weld joints in the lower head.

2. Drilling in the outer two rows of fuel assemblies is not possible because of hardware interface restrictions.

3. Drilling into the lower plenum was restricted to the five lower plenum inspection locations in the CSA.

4. Only twelve locations had been cleared of endfittings, spiders, and fuel debris in preparation for drilling. Drilling at other locations was considered to have a high potential for failure because of the presence of assembly endfittings and spiders.

The assemblies from which the ten core bores were drilled and their locations are shown in Figure 1. This pattern provides east-west and southwest-northeast diametral cross-sectional samples, as well as two radial sample cross sections from core center to the north and another to the southeast. A north-south sample line was also established on the eastern side of the core. These ten core bores provided two samples from the center of the core, two samples from near mid-radius, and six samples from around the core periphery. Access into the lower plenum for video inspection was obtained at three inspection locations, N12, D4, and K9, and two samples may have been obtained from the lower plenum at assemblies K9 and D4. A summary of the core bore drilling sequence, the rationale for selection of drilling locations during the operation, and the major findings for each core bore sample are given in Table 1.

A summary of the core boring hardware and operation, the data obtained, and subsequent analysis and evaluation of that data follows in this report. The core boring hardware and drilling procedures are described. The core boring data and results of the visual inspections of core bores are summarized, along with the current end-state conditions of

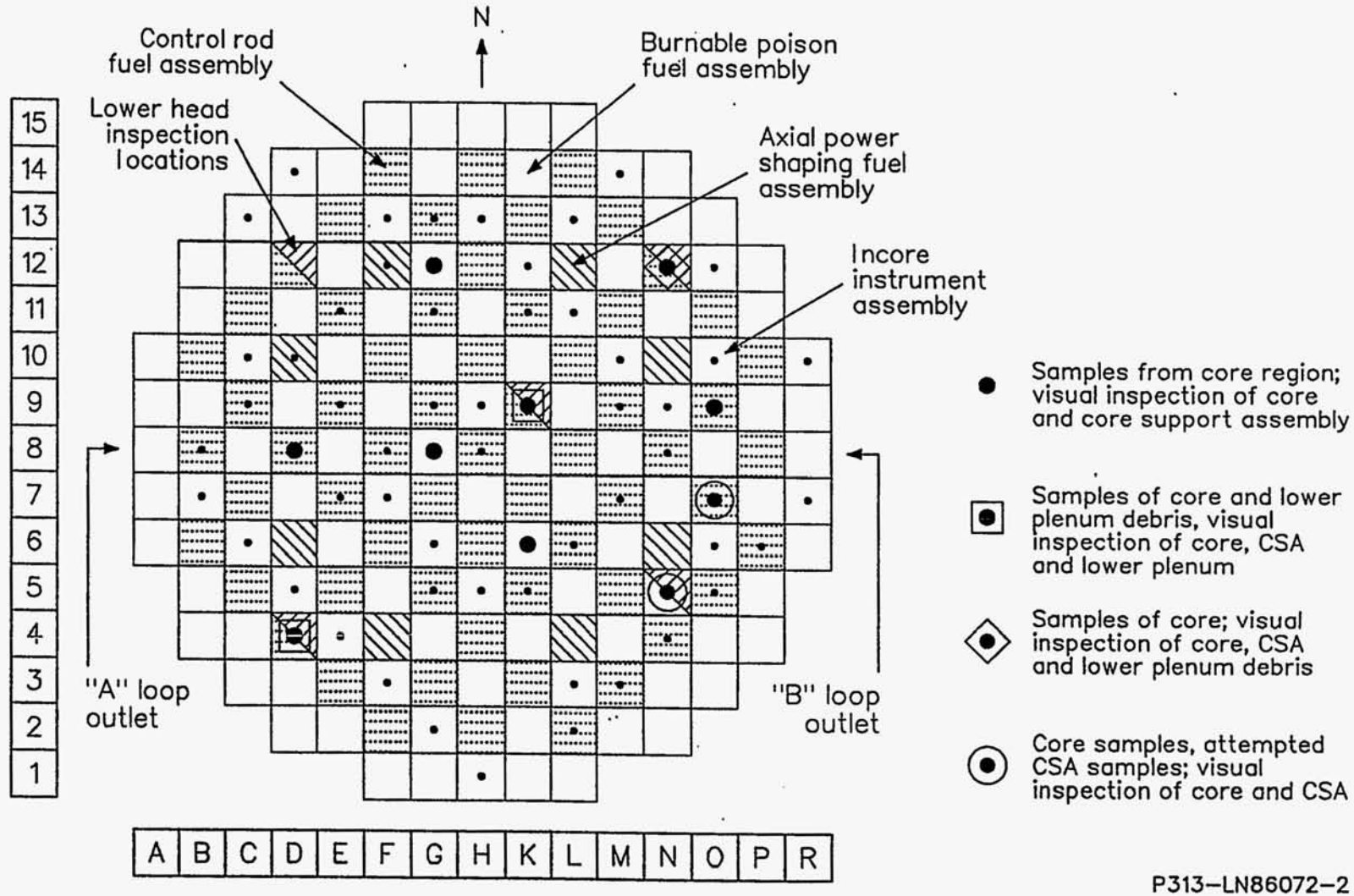

Figure 1. Ten core bore drilling locations.

TABLE 1. DRILLING SEQUENCE AND OBSERVATIONS SUMMARY FOR CORE BORE LOCATIONS

Drill Hole Number	Fuel Assembly Location	Rationale for Drill Location	Major Finding
1	N5	1. Lower plenum access position 2. Characterize SE core periphery 3. Burnable poison rod assembly	1. Localized core damage regions characterized 2. Relocated core material observed in CSA regions 3. Potential CSA damage in east quadrant near core periphery based on limited inspection data
2	N12	1. Lower plenum access position 2. Characterize NE core periphery 3. Control rod assembly	1. Localized core damage regions characterized 2. Large amounts of relocated core material in CSA regions 3. Lower plenum debris inspected 4. Potential CSA damage in east quadrant near periphery
3	G8	1. Characterize center core region 2. Burnable poison rod assembly	1. Localized core damage regions characterized 2. Only small quantity of debris in CSA 3. No damage to CSA
4	G12	1. Characterize north core periphery 2. Burnable poison rod assembly	1. Localized core damage regions characterized 2. Only small quantity of debris in CSA 3. No damage to CSA
5	K9	1. Lower plenum access position near core center 2. Control rod assembly 3. Characterize central core region	1. Localized core damage regions characterized 2. Only small quantity of isolated debris in CSA 3. No damage to CSA 4. Lower plenum debris inspected
6	D8	1. Characterize mid-core region, west quadrant 2. Control rod position	1. Localized core damage regions characterized 2. Only small quantity of isolated debris in CSA 3. No damage to CSA
7	K6	1. Characterize central-to-aid core region 2. Burnable poison rod assembly	1. Localized core damage regions characterized 2. Only small quantity of isolated debris in CSA 3. No damage to CSA
8	D4	1. Characterize SW core periphery 2. Lower plenum access 3. Control rod assembly	1. Localized core damage regions characterized 2. No damage to CSA 3. Lower plenum debris inspected
9	D7	1. Characterize east quadrant for core failure location 2. Control rod assembly	1. Localized core region characterized 2. Large amount of relocated core material observed in CSA region 3. Potential CSA damage in east quadrant near periphery
10	D9	1. Characterize east quadrant for core failure location 2. Control rod assembly	1. Localized core region characterized 2. Large amount of relocated core material observed in CSA region 3. Potential CSA damage in east quadrant near periphery

the reactor vessel and core. The hypothesized accident scenario is updated, and the primary questions which require further study are also presented.

DESCRIPTION OF THE CORE BORE MACHINE

The core bore system is a computer-controlled, electro-mechanical device specifically designed to extract samples from the normal core region of the TMI-2 reactor. The samples were to be axially continuous, stratigraphically intact cylinders cut from the damaged fuel and fuel assemblies. In addition to providing samples, needs were identified to (a) provide data on the type and elevation of material in the core region and (b) provide access for CCTV inspection of the normal core space, the regions inside the lower CSA, and the RV lower plenum space. Stringent limitations on maximum sizes, weights, geometries, forces, and operating conditions were defined and imposed as design constraints. The resulting system and its use are summarized in the following sections. More detailed technical summaries are presented in Appendix A of this report. Design details are available in Reference 4.

Drill Unit Configuration

The core bore system was developed from a commercially available unit built for the mining/geology industry and is depicted in Figure 2 as installed for the TMI-2 defueling platform. Powered by a 50-hp electric motor, the drill unit (Longyear 38-EHS), equipped with a Megalo head built by a Japanese subsidiary, consists of hydraulically driven clamps, chuck, and spindle, with adequate capacity to handle up to 4.5-in. drill rod and axial loads approaching 10 tons. With the Megalo head, the machine's operating envelope is limited to a maximum spindle speed of 500 rpm and a maximum torque of 3000 ft-lb. Control of the commercial unit was executed using standard hydro-mechanical devices and trained, experienced operators.

Due to the total lack of personnel experienced in drilling damaged reactor cores, and with an eye on obtaining "drillability" data to define the stratified structure within the core region, the commercial drill unit was modified to accept computer-based control and data acquisition systems. Process control instrumentation provided for operator interface to the drill unit and for automatic operation under certain conditions.

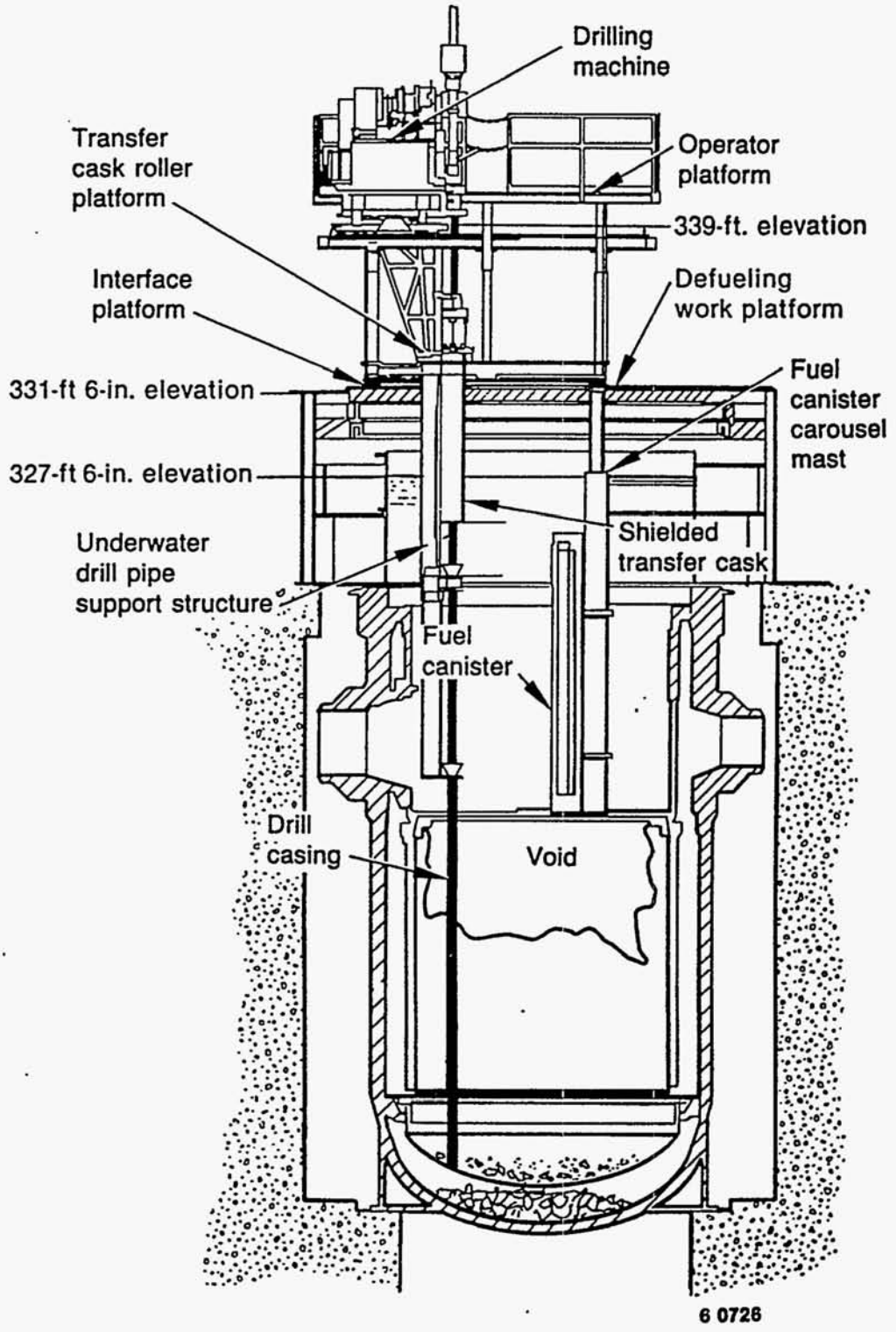

Figure 2. Schematic of core bore machine.

With this type of interface, the processor manages all safety interlocks, operates to preset parameters, controls special-condition operations, and monitors system-protection functions within the machine. Prohibited operations, system faults, or off-normal conditions result in a safe-configuration shutdown of the unit and notification to the operator of the source/type of error. The addition of a second computer and a high-density recording system provided for the monitoring and recording of drill parameters related to the qualitative assessment of "drillability" (an approach to identifying the major variations in the core strata) and provided a record of machine-related performance. Data were periodically "dumped" to tape and retrieved from the containment building for analysis. "Drillability" data, within the context of the development activities, are summarized later in this section.

Although the core barrels (i.e., core bore sample carriers), drill string, and casing were taken directly from commercial designs with little modification, the drill bits and casing shoes (the modified bit used with the casing) were substantially different from standard commercial hardware. The anticipated drilling environment at TMI-2 included hard ceramics (alumina burnable poison pellets, urania fuel, and the fuel-bearing material commonly referred to as "liquified fuel"), as well as relatively soft ductile metals [chiefly stainless steel, zircaloy, and the silver-indium-cadmium (Ag-In-Cd) poison rod material]. Numerous bit styles and designs were tested using core-region mockups containing both actual materials and suitable substitutes in place of radiologically or economically prohibitive materials. The only bit design that could successfully cut through both ceramics and metallics was the "Chrisdril," a development of Norton-Christensen of Salt Lake City, UT (see Figure 3). The face of the bit carried tungsten-carbide teeth faced with artificial diamond. The resulting combination has both extreme hardness and a very high modulus of elasticity.

A superstructure and interface plate were used to join the drill rig to the TMI-2 defueling platform. In addition to carrying the weight and forces of the drill unit, the superstructure provides radial positioning of

Figure 3. Photograph of Chrisdril bit.

the unit up to 49 in. from core center, underwater support to prevent deflections in the drill string, and a cask to transfer the loaded core barrels into a fuel shipping canister. The TMI-2 defueling platform provides an 18-in.-wide access slot, the canister "carousel" containing five fuel shipping canisters, adequate operator shielding (other than the cask), and the ability to rotate the slot in the horizontal plane through 360 degrees. The combination of platform rotation and linear translation on the superstructure was augmented with a computer-aided theodolite (CAT) system to provide precise positioning anywhere within the central 50-ft^2 of the reactor vessel.

Drilling Procedure

Following the CAT operations to position the centerline of the drill string precisely over the center of the selected fuel assembly position (procedurally referred to as "indexing"), the initial lengths of casing and drill string (with core barrel) were installed in the drill rig. The casing was adjusted to an elevation just above the debris and secured to provide lateral support for the drill string during startup operations. After the drill string had successfully penetrated the fuel assembly lower endfitting, the casing was drilled to just above the endfitting and the drill string and core barrel are extracted. The core barrel, which then contained the radioactive sample material, was withdrawn only as far as the transfer cask. Once in the cask, the combination was rolled to a position over a fuel shipping canister and the core barrel was lowered. At this point in the operations, CCTV cameras were used to inspect the spaces below the lower endfitting, including the lower RV head in those positions which permitted access completely through the lower CSA. If relocated core material was present under the sampled position, a smaller-diameter core barrel could be inserted and an attempt made to sample the material. The loaded core barrels were handled in the same manner as the larger ones. (Four such samplings were attempted during operations.) The final operations at each location involved inspecting the hole through the normal core region as the casing was withdrawn in increments and loading the bottom-most piece of casing into the canister for disposal.

Reference Drilling Data

Mockups of the anticipated core conditions were used during development of the equipment and procedures at the INEL. The mockups contained typical core materials, excluding uranium and Ag-In-Cd alloy, configured in a typical fuel assembly array and/or layered as "relocated core materials." Quartz and hard-fired alumina were substituted for urania; aluminum rod was used in place of the Ag-In-Cd. The remaining materials were either actual fuel assembly components (endfittings, spacer grids, zircaloy tube) or convenient test pieces (concrete block). The data acquisition system (DAS) was used during drilling operations to provide reference data for subsequent core bore data reduction. The important parameters logged by the DAS include spindle speed (rpm) and torque (ft-lb), penetration (in.), weight on bit (lb), and time (s).

Because of the increased number of variables associated with drilling under manual control, the DAS data were only meaningful when the rig was operated in the automatic mode. (Difficult in-core conditions at some locations precluded use of the machine in the automatic mode.) Subsequent manipulation of the data made it possible to discriminate among standing fuel, void spaces, previously molten fuel, and stainless steel and to locate the spacer grids. Substantially more information on the data-reduction activities is found in Appendix A.

UPDATED END-STATE CORE CONDITION BASED ON CORE BORE DATA

A discussion of the results of the core bore data analysis and the logical extension of that analysis to the presently known end-state condition of the TMI-2 core is presented in this section. This discussion is based on the video inspections performed immediately following each core bore. Video inspections of the interior of each core bore hole were performed to characterize the core region and the region immediately below the bottom of the core (the CSA region). In addition, video inspections of the lower plenum debris were completed at three lower head inspection locations (N12, K9, and D4). Detailed video data observations and pictures as well as drilling data for each core bore location are contained in Appendix B. Although not discussed in this section, the drilling data are in general agreement with the video data with respect to the locations of the various transition zones in the core bore holes. The following subsections summarize the condition of the core region, the CSA region, and the lower plenum region and present the results of analysis to estimate a mass balance for the presently known end-state condition of the TMI-2 core.

Core Region

Prior to core boring, it was known that the upper core consisted of an upper voided region almost entirely surrounded by standing peripheral assemblies and a region of loose debris resting on a hard crust, as illustrated in Figure 4. Conditions within the confines of the core boundary but beneath the hard crust were unknown. The RV lower plenum contained an estimated 10 to 20 tons of core debris. Based on examination of loose debris from the lower plenum, it was known that the materials were primarily ceramic fuel and cladding and that some fuel particles had reached UO_2 melting temperatures. The bulk average temperature of the debris material was estimated to be from 2200 to 2400 K.

Core boring at each location was started at an axial elevation near the hard crust and extended through the fuel assembly lower endfittings, thus providing access to the CSA region. Core boring was extended into the lower plenum debris at two locations (K9 and D4).

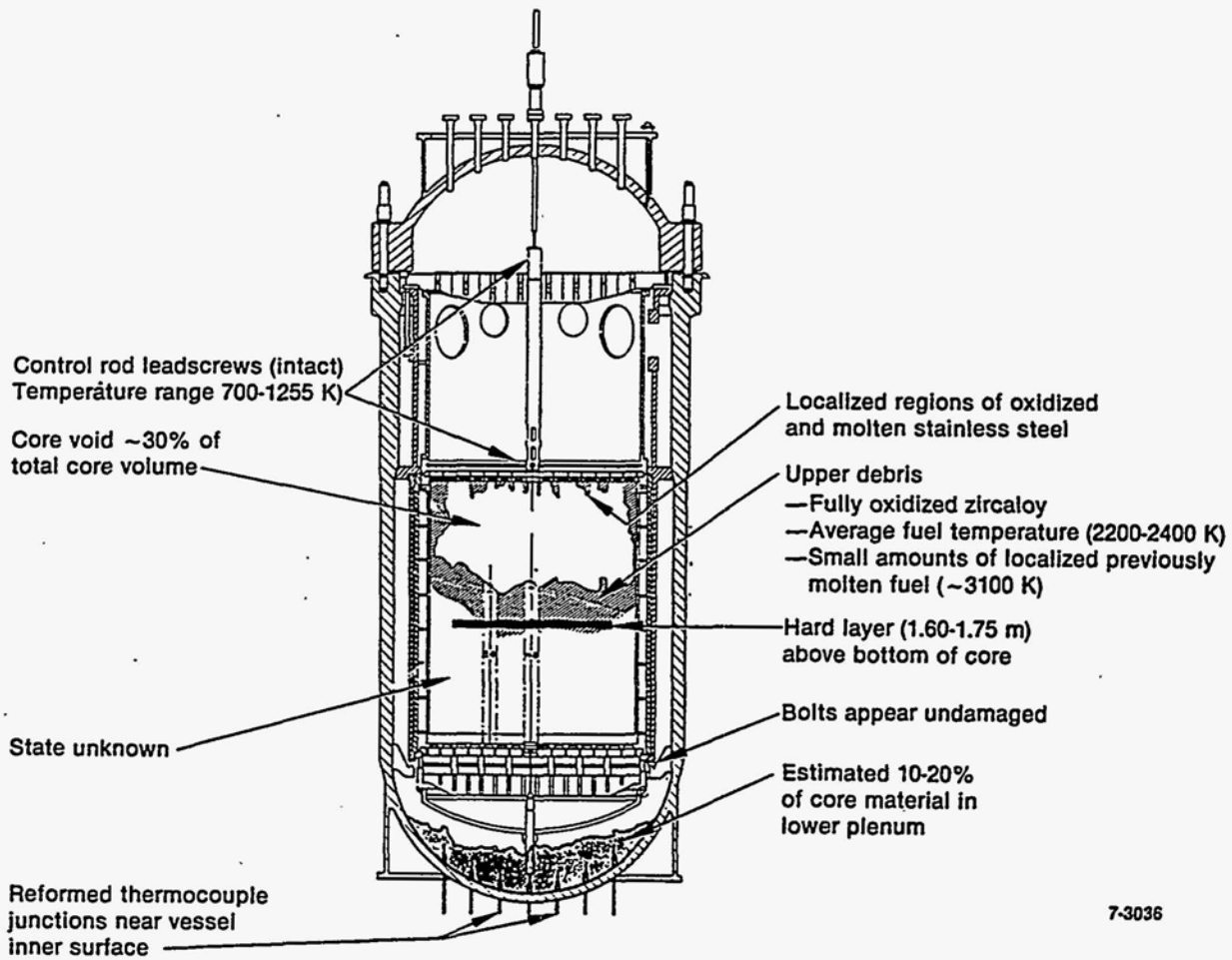

Figure 4. Known core and reactor vessel conditions prior to core bore acquisition.

Video data from the interior of the core bore holes revealed two distinct regions between the hard crust and the fuel assembly lower endfitting. These were: (a) a region of previously molten material directly below and including the hard crust; and (b) a region of intact standing fuel rods extending from the bottom of the previously molten region to the bottom of the core.

The previously molten region was further divided into two types; namely, (a) previously molten ceramic material appearing to have a uniform, homogeneous structure, and (b) previously molten ceramic material surrounding generally degraded but intact fuel pellets and/or fuel rods. Type (b) is hereinafter referred to as "agglomerate" material. In some regions of agglomerate material, the fuel pellets were axially stacked together as in the original fuel rods; and, in other regions of agglomerate material, the fuel pellets appeared to have random orientations. In general, the agglomerate material containing stacked pellets was observed in the peripheral core bore holes and at the bottom of the centrally located core bore holes (G8, K9, and K6). The agglomerate material containing random fuel pellets was observed at the top of core bore holes G8 and G12.

A summary of the observations from a central core location (K9) is shown in Figure 5. As shown in the sketch, homogeneous previously molten ceramic material extends from the top of the core bore hole down to near the top of the second spacer grid, a distance of almost 50 in. Compared with other core bore locations, the previously molten homogeneous material extended to its greatest depth at location K9. The previously molten homogeneous ceramic material was about 40-in. thick at position G8 and about 30-in. thick at position K6. A 4- to 6-in.-thick region of agglomerate material separates the previously molten homogeneous material from standing fuel rods that extend to the bottom of the core in core bore location K9. A metallic-appearing structure that has been partially or perhaps fully molten was observed near the top few inches of the drill hole. A possible metallic form embedded in the homogeneous ceramic material 30 in. above the bottom of the core is shown in Figure 6, and what

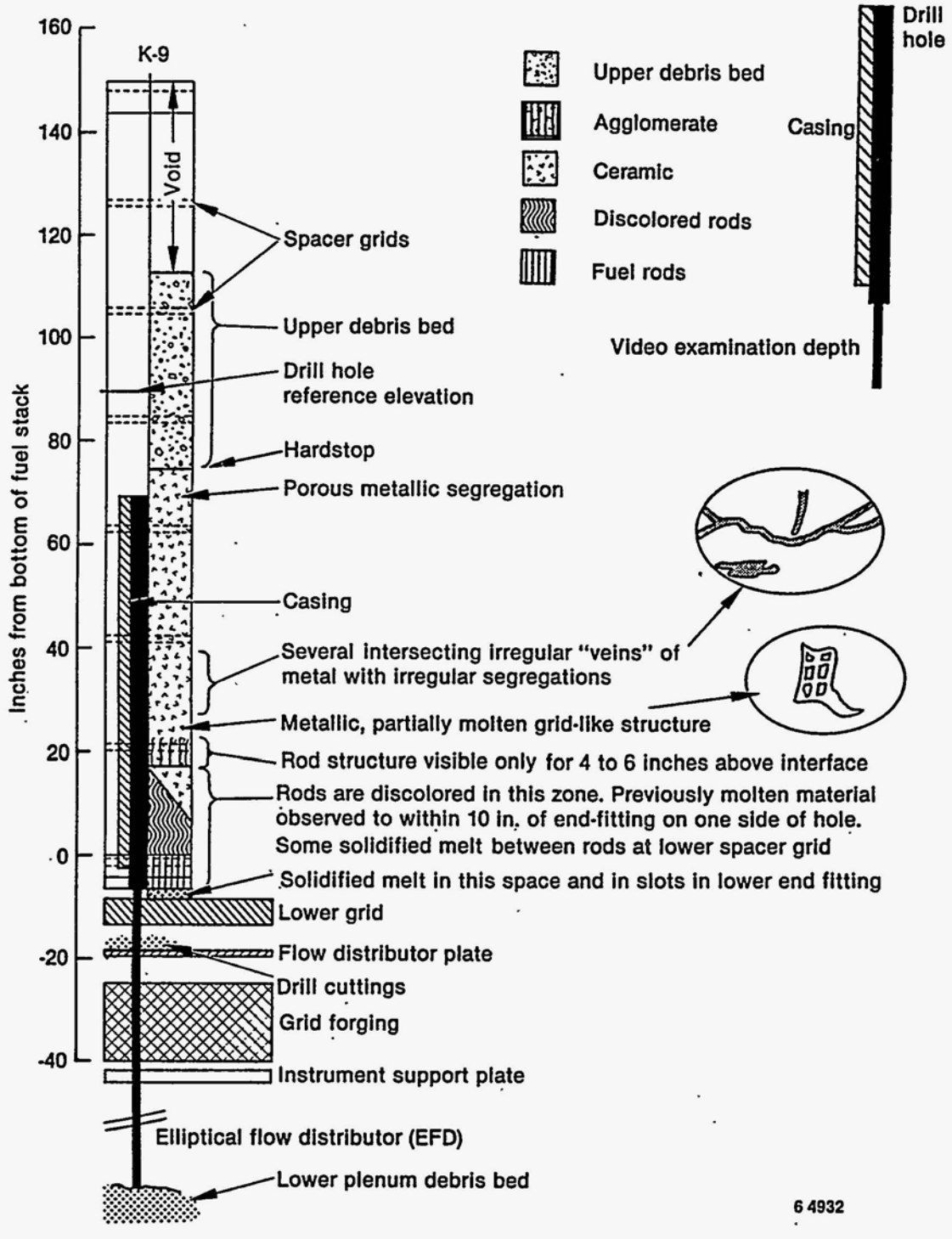

Figure 5. Observation summary from central core bore location (K9).

appears to be a partially melted spacer grid in the homogeneous ceramic material 26 in. above the bottom of the core is shown in Figure 7. The agglomerate material just below the homogeneous ceramic material in core bore hole K9 is shown in Figure 8. Previously molten material was observed between fuel rods as low as 4 in. above core bottom, as illustrated in Figure 9.

A summary of observations from a peripheral core bore location (N12) is shown in Figure 10. Previously molten homogeneous ceramic material was not observed in any of the peripheral core bore holes (D4, D8, N5, N12, O7, O9). Agglomerate material with vertical fuel rod structure extends from the top of the core bore hole to the transition region between agglomerate material and standing fuel rods. The agglomerate material is only about 14 in. thick, and standing fuel rods extend 48 in. above core bottom. The transition zone between the lower intact fuel rods and the agglomerate region in core bore hole N12 is shown in Figure 11, and standing fuel rods about 16 in. above the core bottom are shown in Figure 12.

At location G12, a thin region of previously molten homogeneous ceramic material is bounded by a region of agglomerate material with randomly oriented fuel pellets on top and a zone of agglomerate material with vertical fuel rods on the bottom. The standing fuel rods extend about 42 in. above core bottom, as illustrated in the sketch shown in Figure 13. The top of the rod stubs at 42 in. in the G12 core bore hole are shown in Figure 14.

In core bore hole D4, there are axial regions of alternating agglomerate and relatively undamaged fuel rods with solidified melt droplets attached. One interpretation of the axial variability in material structure is that molten material flowed laterally into this region, rather than axially from above.

The previously molten homogeneous ceramic region, the agglomerate region, the standing fuel rod region, and the upper core debris bed were spatially defined by contour mapping of the interfaces between the various

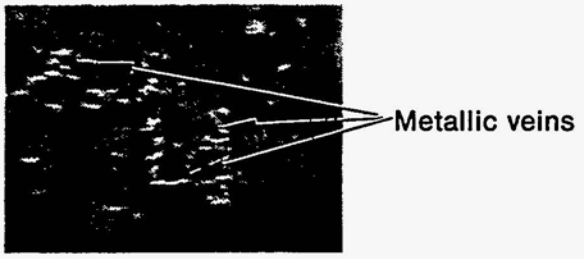

Figure 6. Possible spacer grid remnant at approximately 26 in. above core bottom at core position K9.

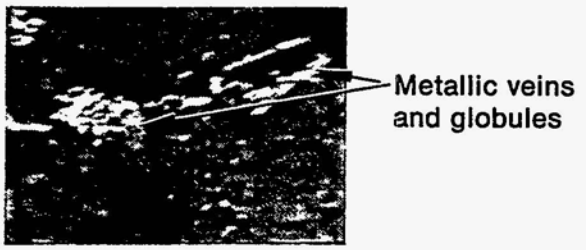

Figure 7. Possible metallic form in agglomerated material approximately 30 in. above core bottom at core position K9.

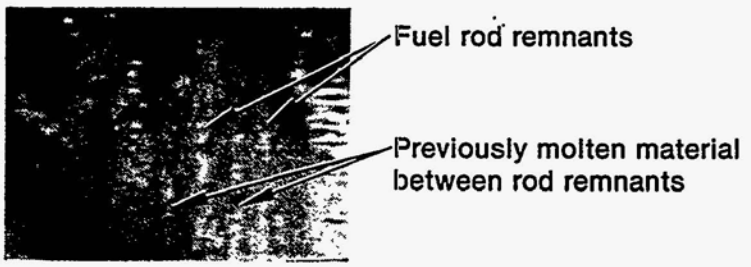

Figure 8. Individual rod decomposition approximately 18 in. above core bottom at core position K9.

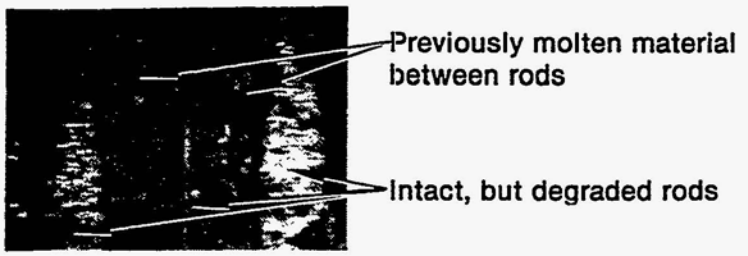

Figure 9. Possible previously molten core material behind fuel rods just above core position K9 fuel assembly lower spacer grid (approximately 4 in. above core bottom).

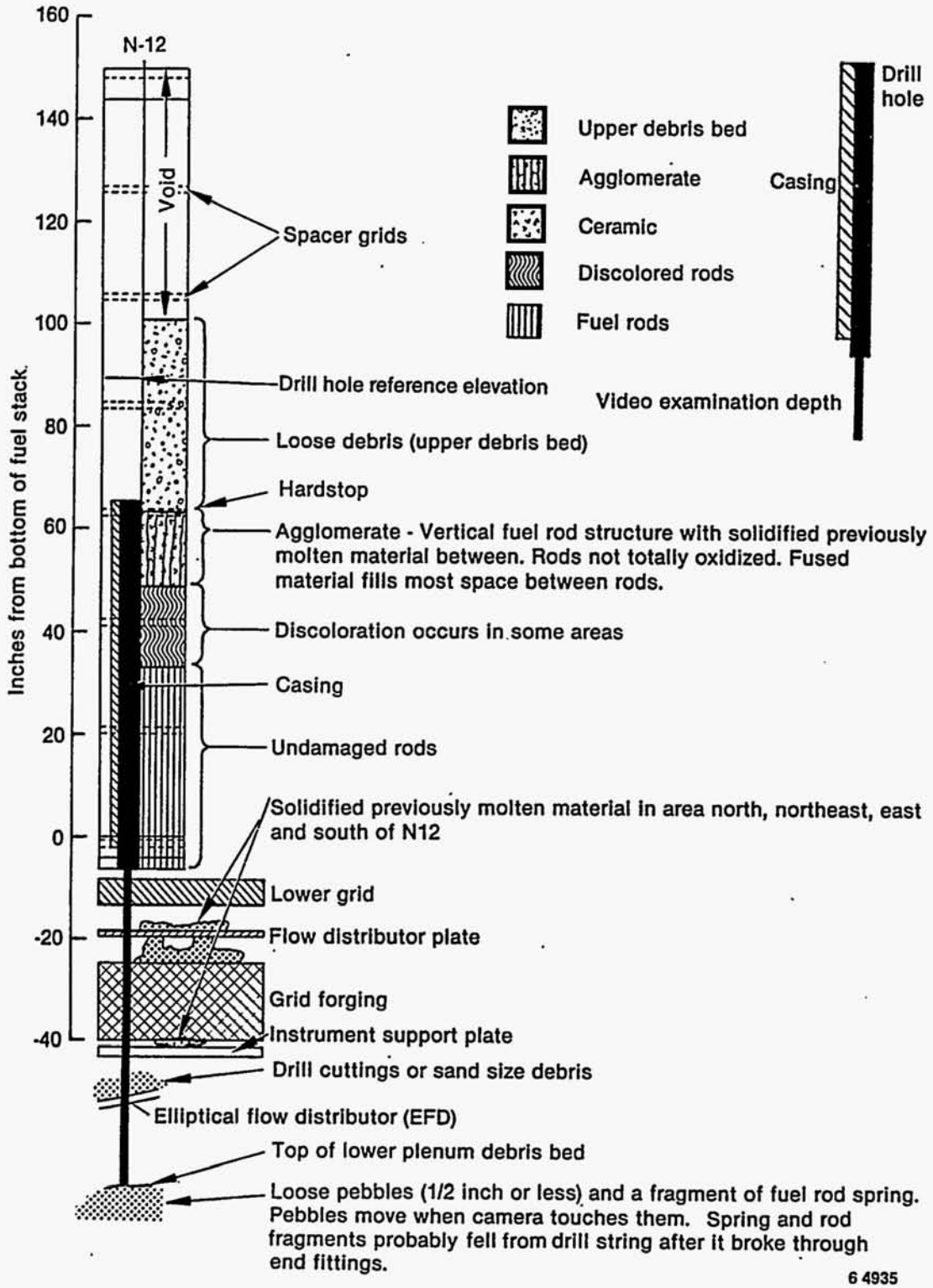

Figure 10. Observation summary from peripheral core bore location (N12).

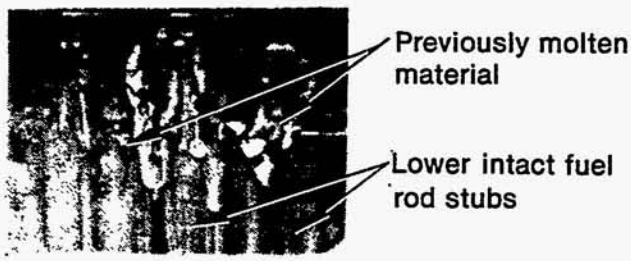

Figure 11. Transition between intact rod bundle and agglomerated core material at top of third spacer grid (approximately 49 in. from fuel rod bottom) at core position N12.

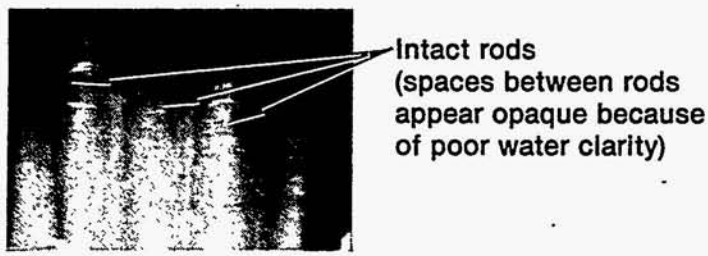

Figure 12. Intact rod bundle between first and second spacer grids (approximately 16 in. above fuel rod bottom) at core position N12.

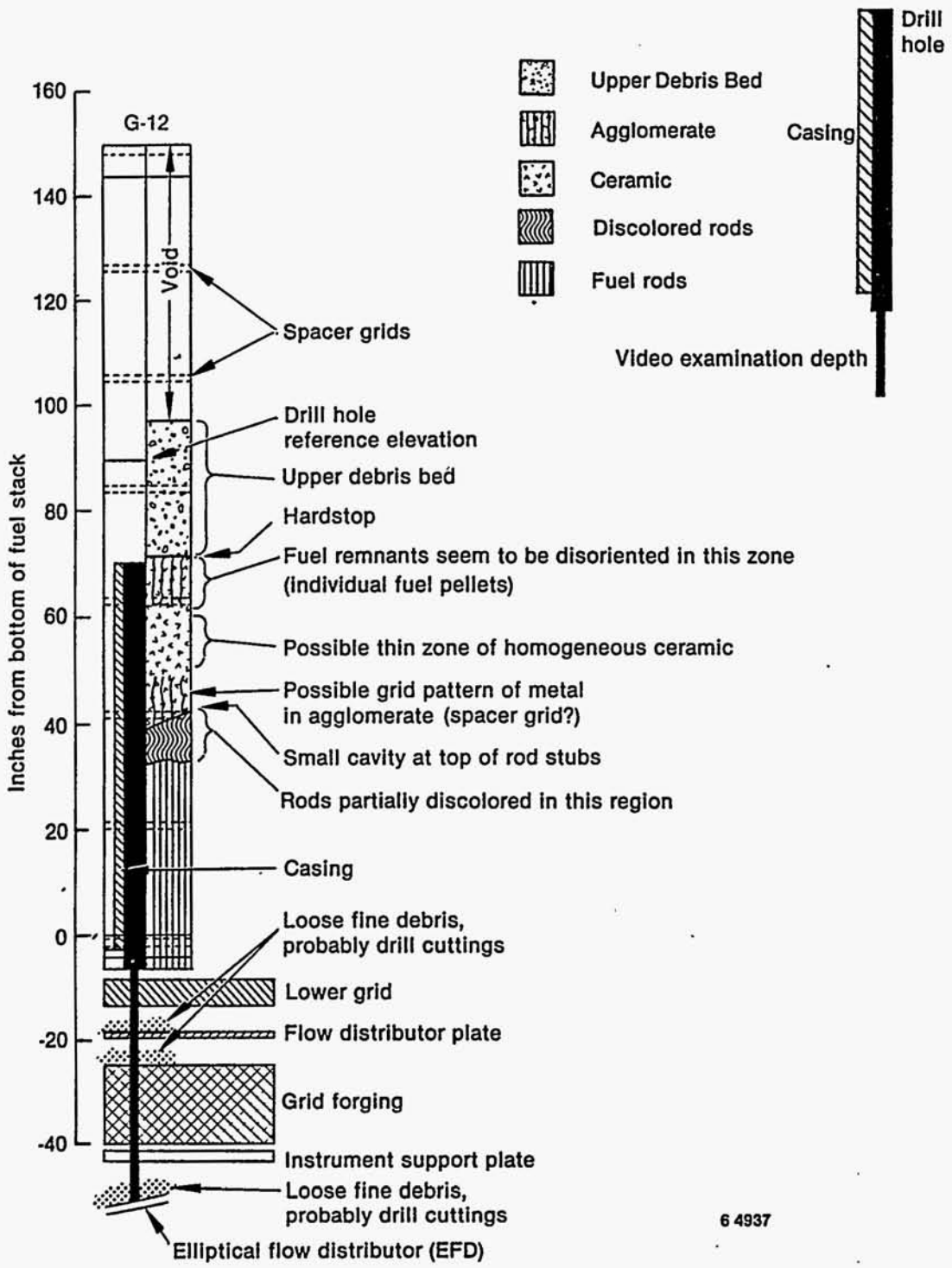

Figure 13. Observation summary from core bore location G12.

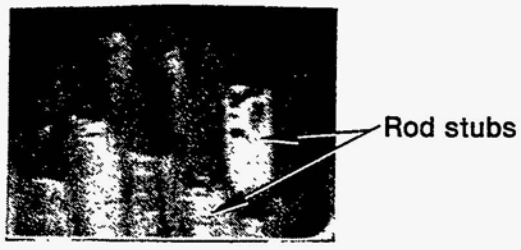

Figure 14. View of rod stub tops at core position G12 approximately 42 in. above fuel rod bottom.

regions. The contour map of the transition region between the standing fuel rod stubs and the agglomerate material (as determined from the core bore visual data) is shown in Figure 15, which illustrates that the height of standing fuel rods above the bottom of the core varies from about 30 in. at the core center to between 50 and 60 in. at the core periphery. In addition to the rod/agglomerate contour data, data from References 5 (core probe data) and 6 (acoustic topography data) were used to construct contour maps defining the lower supporting surface of the debris bed (upper surface of the molten core region) and the upper surface of the debris bed. These contour data are included in Appendixes C and D, respectively. Using these three contour maps, regions defining the lower standing fuel rods, the previously molten core zone, and the upper debris bed can be estimated through any row of core fuel assemblies.

Figure 16 shows these regions as they extend across the G row of fuel assemblies. The standing fuel rod stubs support the agglomerate and molten ceramic regions. The agglomerate region forms a shell around the periphery of the previously molten homogeneous ceramic core region and surrounds the central zone of previously molten ceramic material. The shell is relatively thin under the previously molten ceramic in the central core region but increases in thickness towards the outer regions and forms all of the degraded core material above the standing fuel rods in the outer fuel assemblies As noted earlier, the agglomerate in the lower central region of the core appears to be comprised of previously molten material surrounding intact vertical rod stubs. The rod pellet boundaries are discernible inside the rods (axial interfaces between pellets) but not generally well defined at the outer radial surfaces of the rods which are in contact with the interstitial, solidified melt material.

Additional core cross-section maps across fuel assembly rows B through P are included in Appendix E. These core cross sections define the overall degraded core configuration.

During preparation for the core bore drilling, remnants or large pieces of primarily agglomerate material were observed at the core

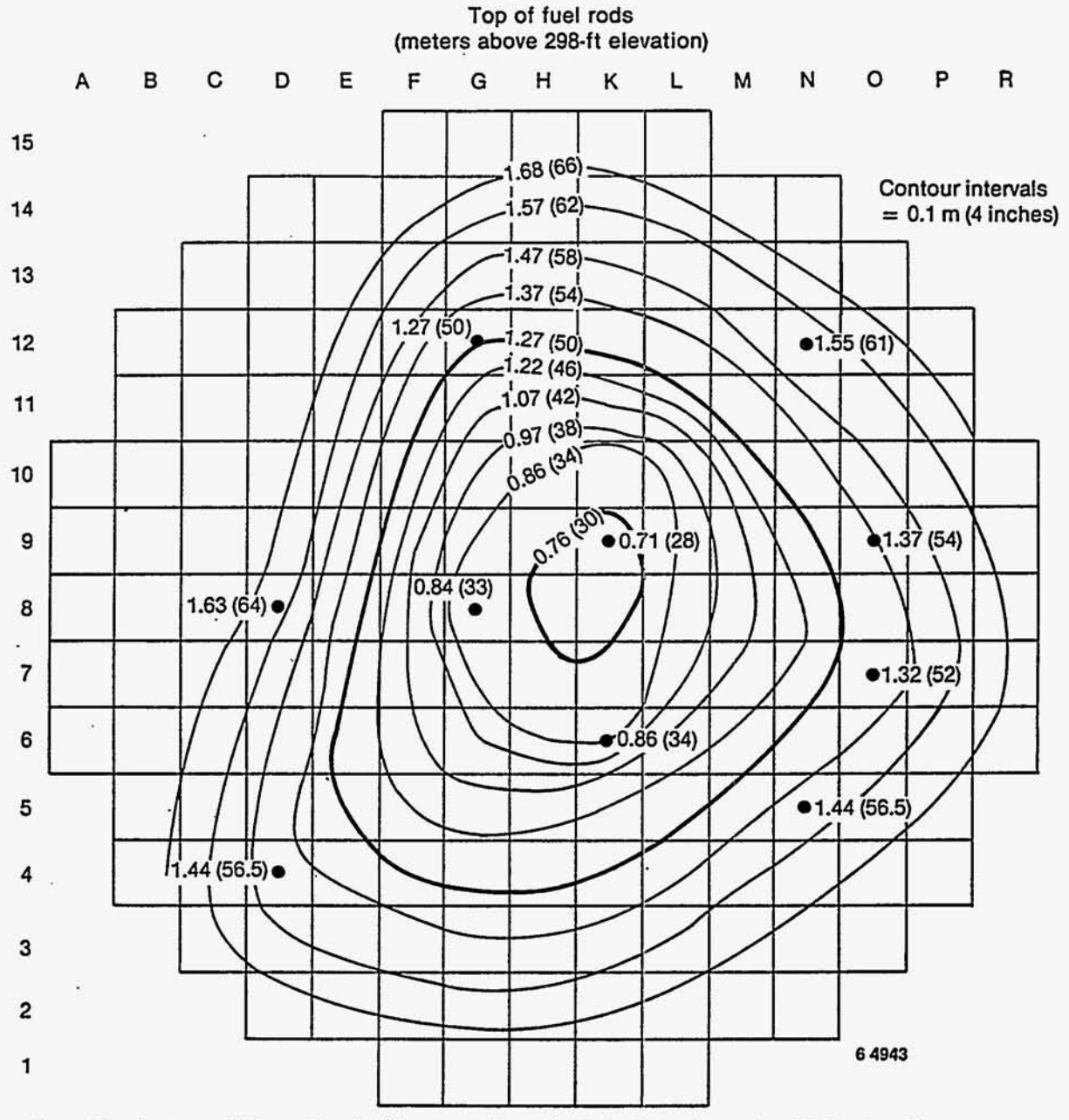

Note: The bottom of the active fuel is approximately 12 inches above the 298-ft elevation.

Figure 15. Contour map of the lower, intact fuel rods and molten core interface.

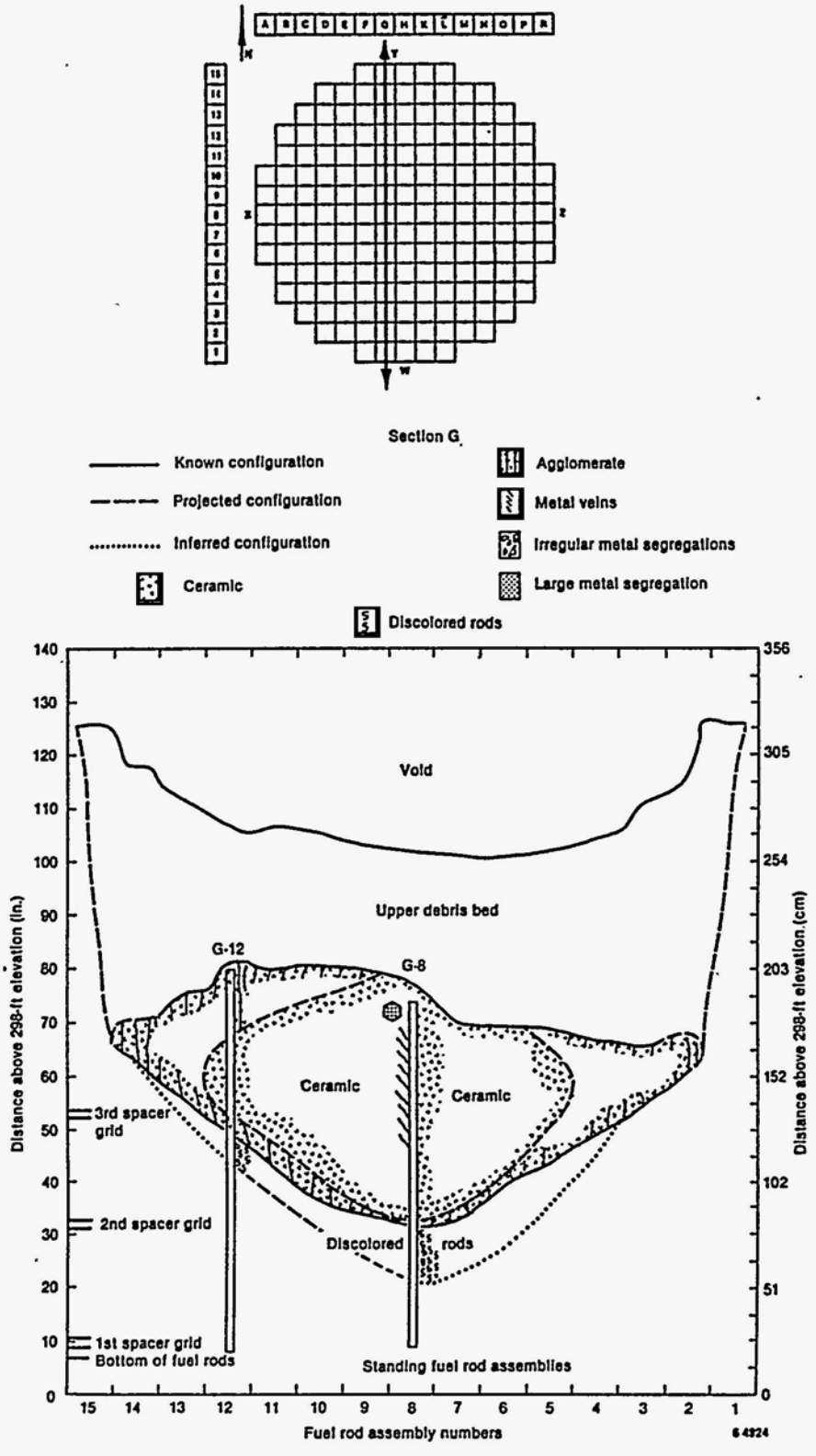

Figure 16. Core cross section across G row of fuel assemblies.

periphery and above the hard surface that had supported the upper debris bed. The exact configuration of this material is not yet well characterized because of limited video data but is roughly approximated in Figure 17. This configuration roughly forms a rim at the periphery of the core and may represent the top of the solid structure prior to relocation of molten material into the lower plenum at 224 min. The top center of the crust may have collapsed as the molten material relocated, forming what appears now to be a "sinkhole" in the solid, previously molten structure. Fuel pellets within the rim of agglomerate material are generally in the original, vertically stacked orientation.

CSA Region

Video inspection of the CSA at each core bore location allowed evaluation of CSA damage and identification of the locations where the core material flowed out of the bottom of the core assemblies and into the lower plenum. The detailed CSA observations are summarized at each drill location in Appendix B. (For details of the CSA configuration, see Appendix F) Figure 18 summarizes the regions of the CSA that were discernible from the visual inspections and indicates that approximately half of the CSA regions were characterized.

Based on the video inspection data, no significant structural damage to the CSA occurred; although some damage to localized support posts and evidence of high temperature is seen. Visual inspection also confirms that no damage to the CSA occurred below the central region of the core. Some fine, sandy material, most likely drilling debris, was observed at each of the central drill locations. The only locations that indicated significant core material relocation into the CSA were N5, N12, 07, and 09, all of which are located on the east side of the core near the periphery. The approximate locations in which significant molten, relocated core material was observed in the CSA are shown in Figure 19. The material resembles the molten ceramic material observed in the core region and looks like it froze in the CSA regions as it flowed downward, thus resembling a "cascade," or "curtain." Cascading previously molten material to the north of core bore

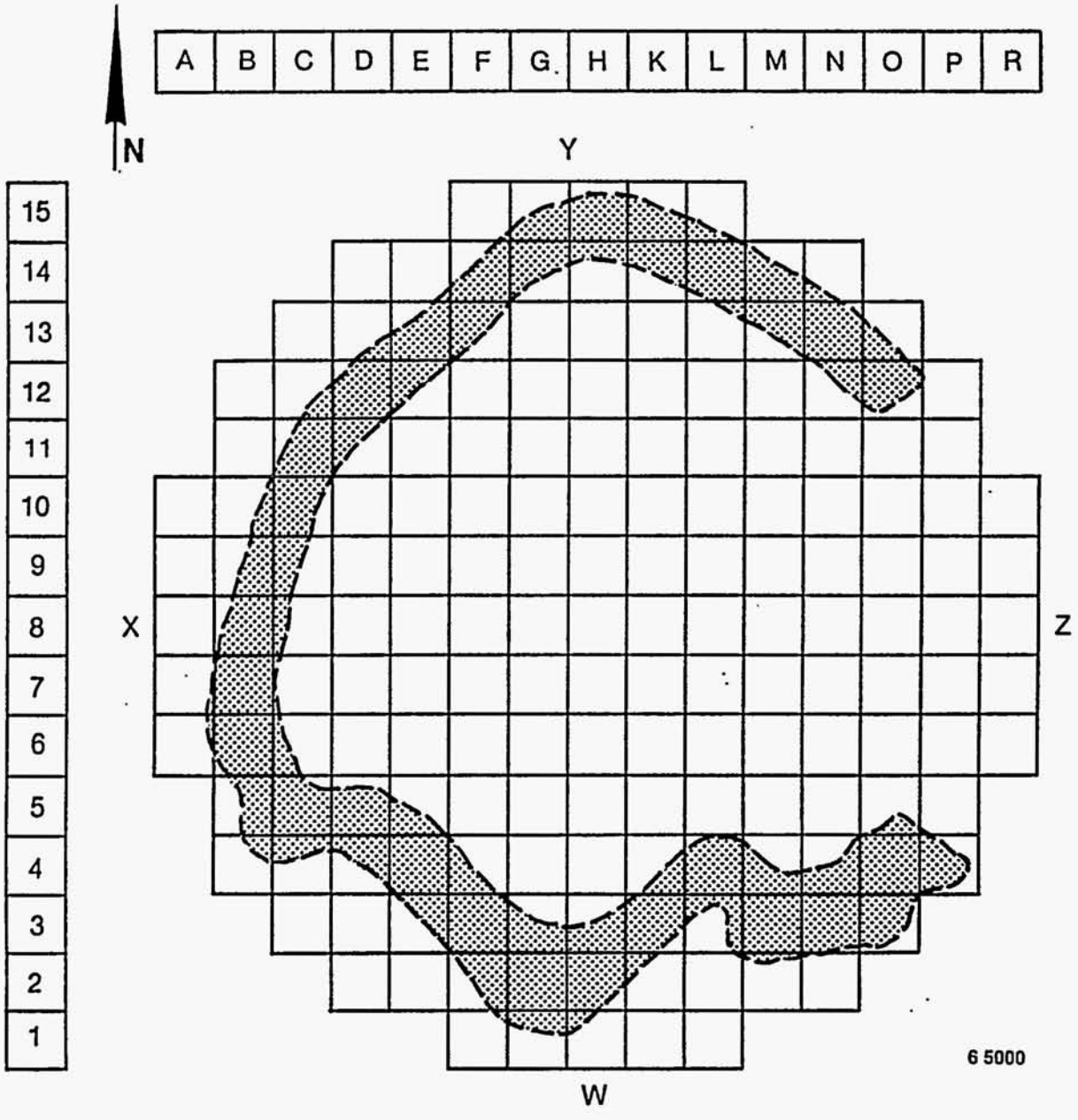

Figure 17. Estimated radial configuration of the upper ridge of agglomerate core material.

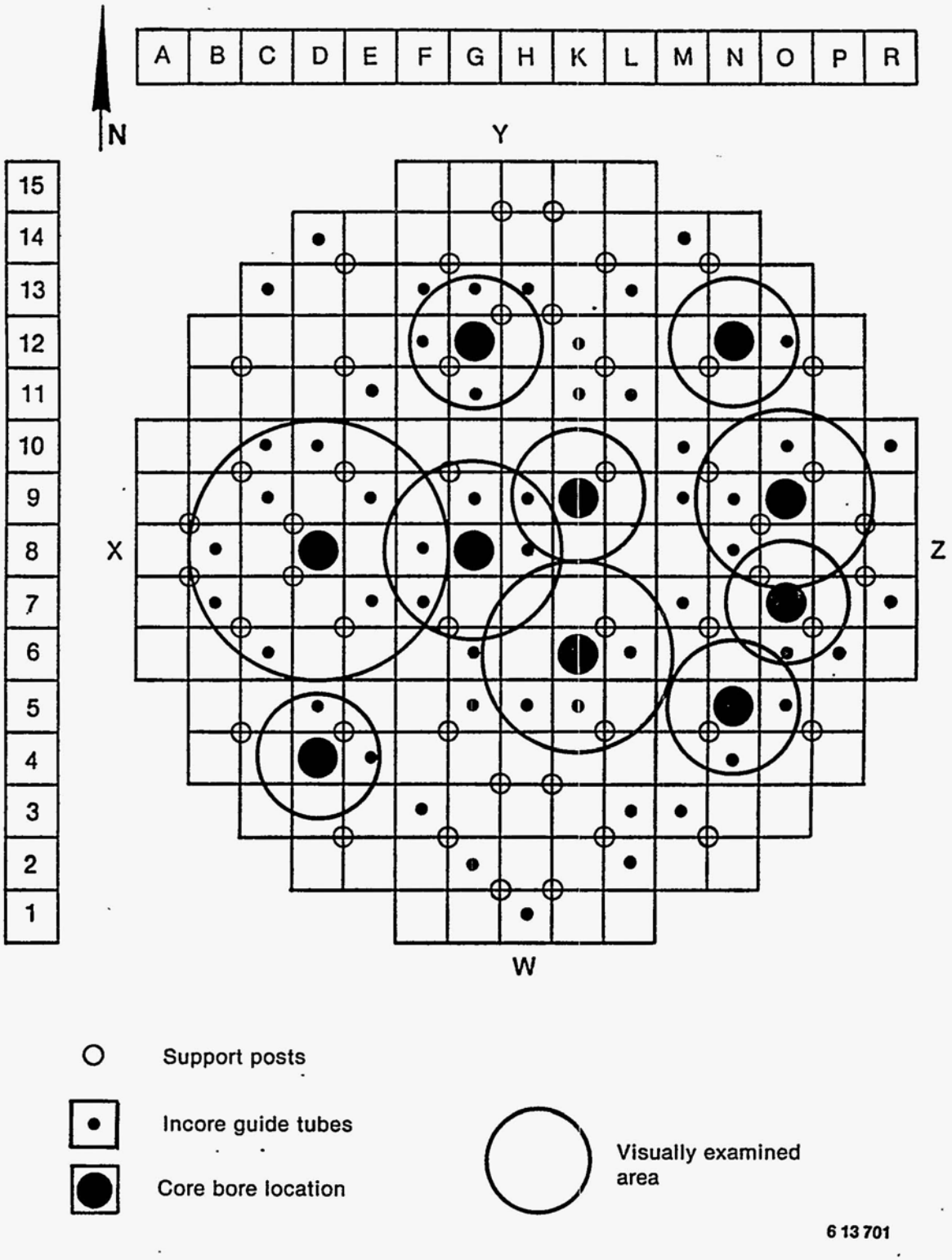

Figure 18. Approximate CSA regions discernible in video data.

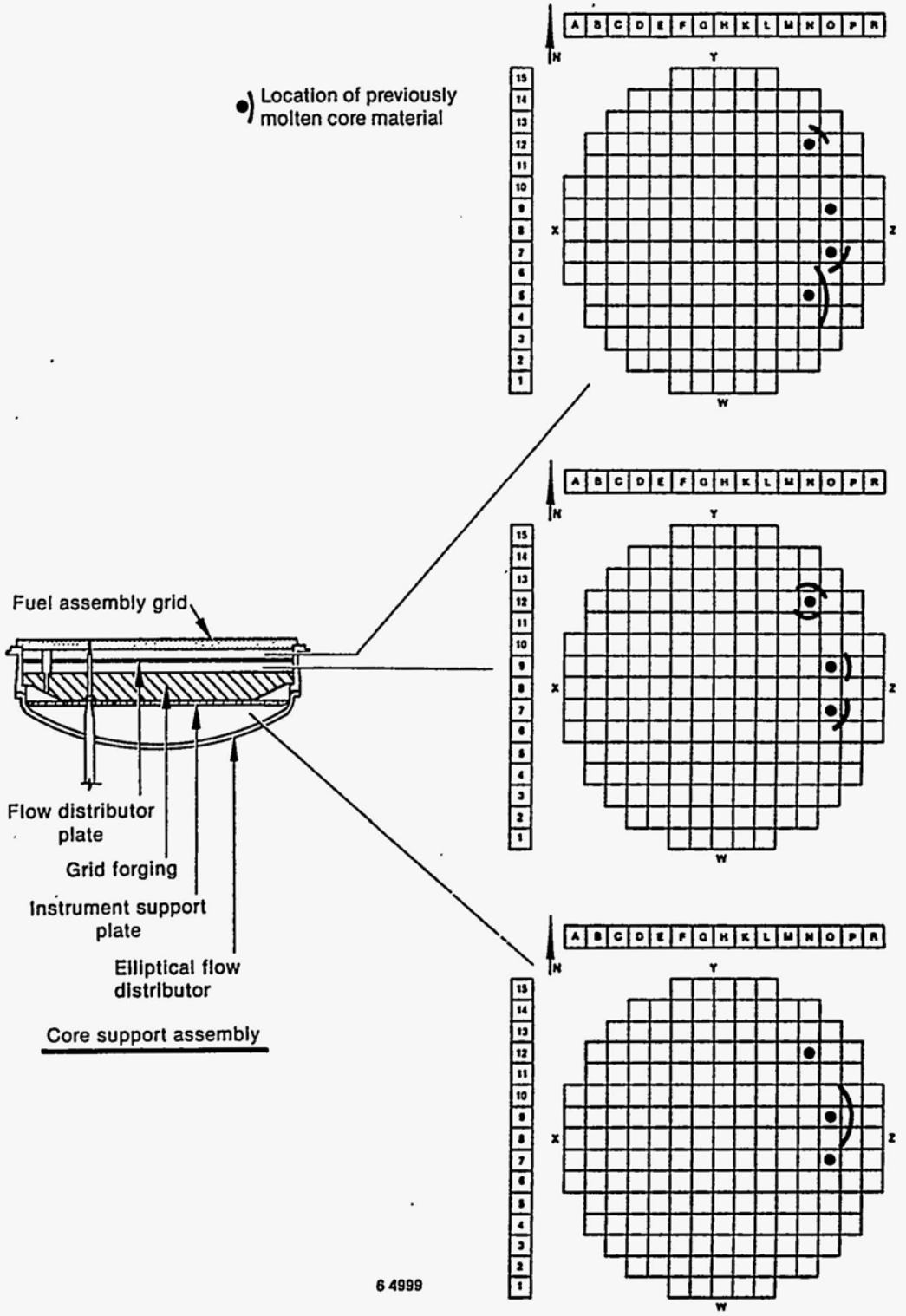

Figure 19. Regions (approximate) of significant fuel relocation in the CSA.

location N12 is shown in Figure 20. The previously molten material in the photo is between the lower flow distributor plate and the grid forging. A fuel rod shard produced by the drilling operation appears in the foreground in Figure 20.

Lower Plenum Region

The core bore inspection provided the first close-up visual inspection of the debris bed surface in the center of the lower plenum, beneath the K9 assembly. Inspection of the lower plenum was also completed beneath the N12 and D4 assemblies. The debris material was basically similar at all locations and appeared like loose gravel having particle diameters less than half an inch. At location 04, some larger debris particles were also observed. Core bore video still images of the lower plenum debris below assemblies K9 and N12 are shown in Figures 21 and 22, respectively.

Sampling of the debris material was attempted at locations K9 and D4 by drilling into the debris bed to within approximately 8 in. of the RV lower head. After removal of the sample casing, the debris appeared to have collapsed into the drill hole. Because the debris was relatively fine, it is doubtful that a significant sample was obtained from either drill location, The estimated heights of the debris bed at each inspection location are illustrated in Figure 23.

Previous inspections of the lower plenum debris have produced a wide range of debris particle sizes and textures, ranging from rather uniform pea-sized gravel to larger, irregular-shaped pieces up to 6 in. in diameter. The core bore inspections have indicated that a significant fraction of the debris is likely to consist of relatively fine particles. However, a wall of very large pieces of previously molten material was observed on the north side of the lower plenum during earlier lower plenum video inspections.

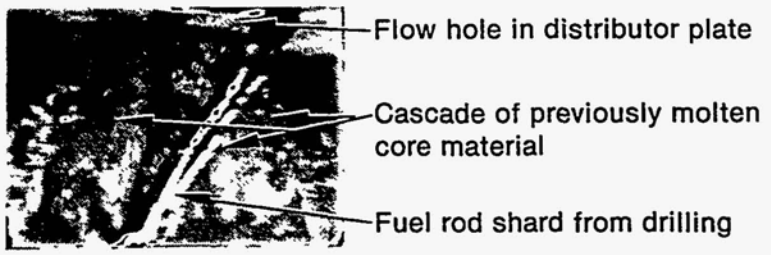

Figure 20. Looking north from core position N12 at previously molten core material underneath the lower grid flow distributor below core position N13 with core-boring-produced fuel shard in foreground.

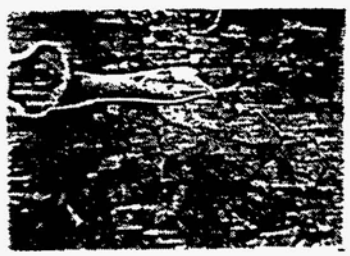

Figure 21. Reactor vessel lower head loose debris below the elliptical flow distributor below core position K9.

Figure 22. Reactor vessel lower head loose debris with possible core-bore-cutter-generated debris below the elliptical flow distributor below core position N12.

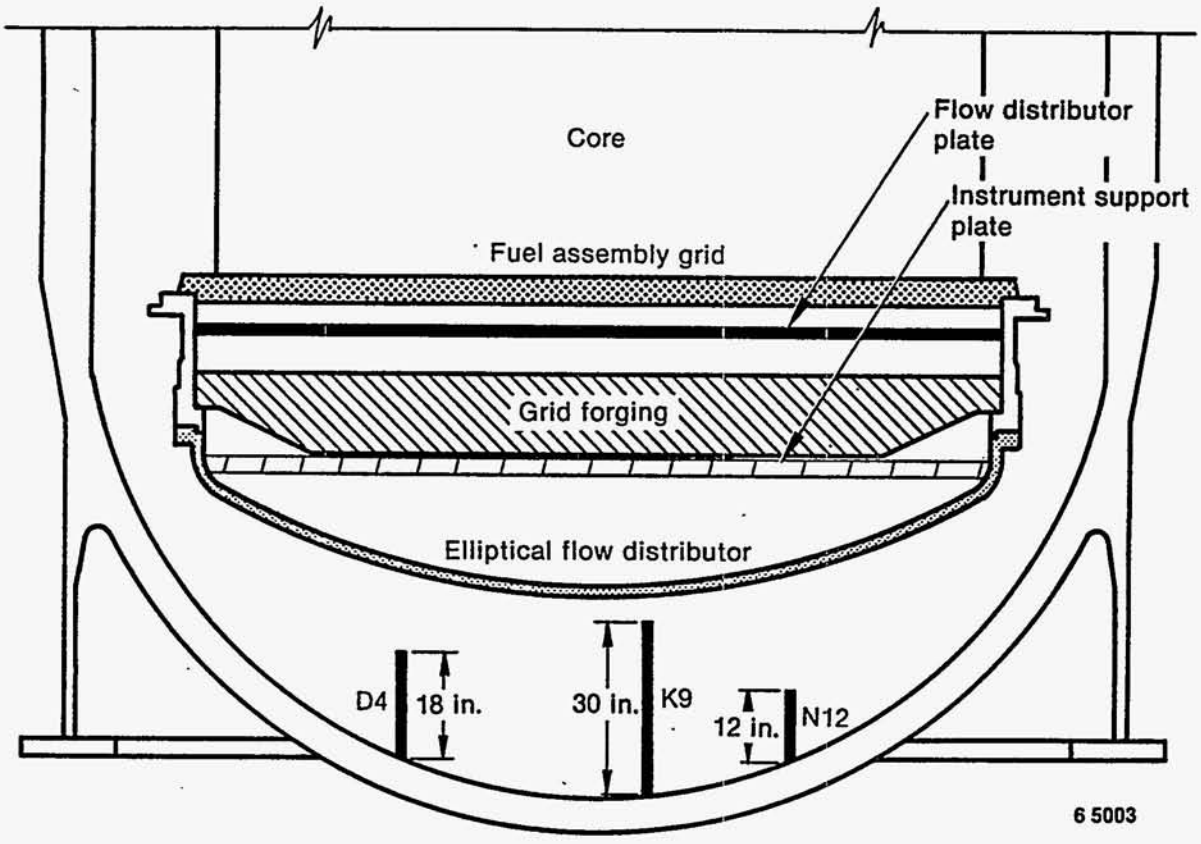

Figure 23. Estimated debris bed heights.

Estimated Volumes and Masses of the Degraded Core Regions

Estimates have been made for the volumes and masses of the various core regions using the core cross sections presented in Appendix E, estimated densities of the degraded core material, and known densities of the intact fuel rods. The density of the degraded (molten) core material is not known precisely; however, it was assumed that the density of the material in the molten core region was identical to the TMI-2 lower plenum particles recently examined. Details of these end-state volume and mass calculations are presented in Appendix G, and the results are presented in Table 2. Based on the estimated mass remaining in the core region, approximately 17 tons of core material are estimated to be in the lower plenum region.

The core configuration just prior to the breakout was estimated by assuming that the lower plenum debris was part of the upper molten ceramic zone prior to the breakout and relocation. Adding the volume of the lower plenum debris to the volume of the ceramic melt region (see Appendix G) resulted in an increased height of from 1 to 2 ft to the upper surface of the degraded core region. This adjusted elevation for the upper surface of the core structure aligns rather well with the axial elevation of the ridge of agglomerate material observed at the core periphery discussed previously and shown in Figure 17.

Updated End-State Core Condition

A revised end-state condition of the TMI-2 core immediately following the accident is shown in Figure 24. This figure was constructed using the cross sections of the upper debris bed region, molten core region (agglomerate and previously molten, homogeneous ceramic), and standing fuel rods for the B through P assembly rows described previously. The upper debris bed surface is approximated in the cutaway view in Figure 24; note the low point of the debris bed near the "B outlet" (east quadrant of the core). The different material structures which currently exist within the core are illustrated approximately to scale. These results are utilized in the following section to update the accident scenario.

TABLE 2. ESTIMATED CORE REGION VOLUMES AND MASSES

Region	Estimated Volume (ft^3)	Estimated Mass (lbm)
Upper core debris	236 ± 47	66,080 ± 20,000
Molten zone	122 ± 24	53,190 ± 13,000
Standing rods	499 ± 50	120,259 ± 12,300
Lower plenum debris	105 ± 64	41,000 ± 27,000

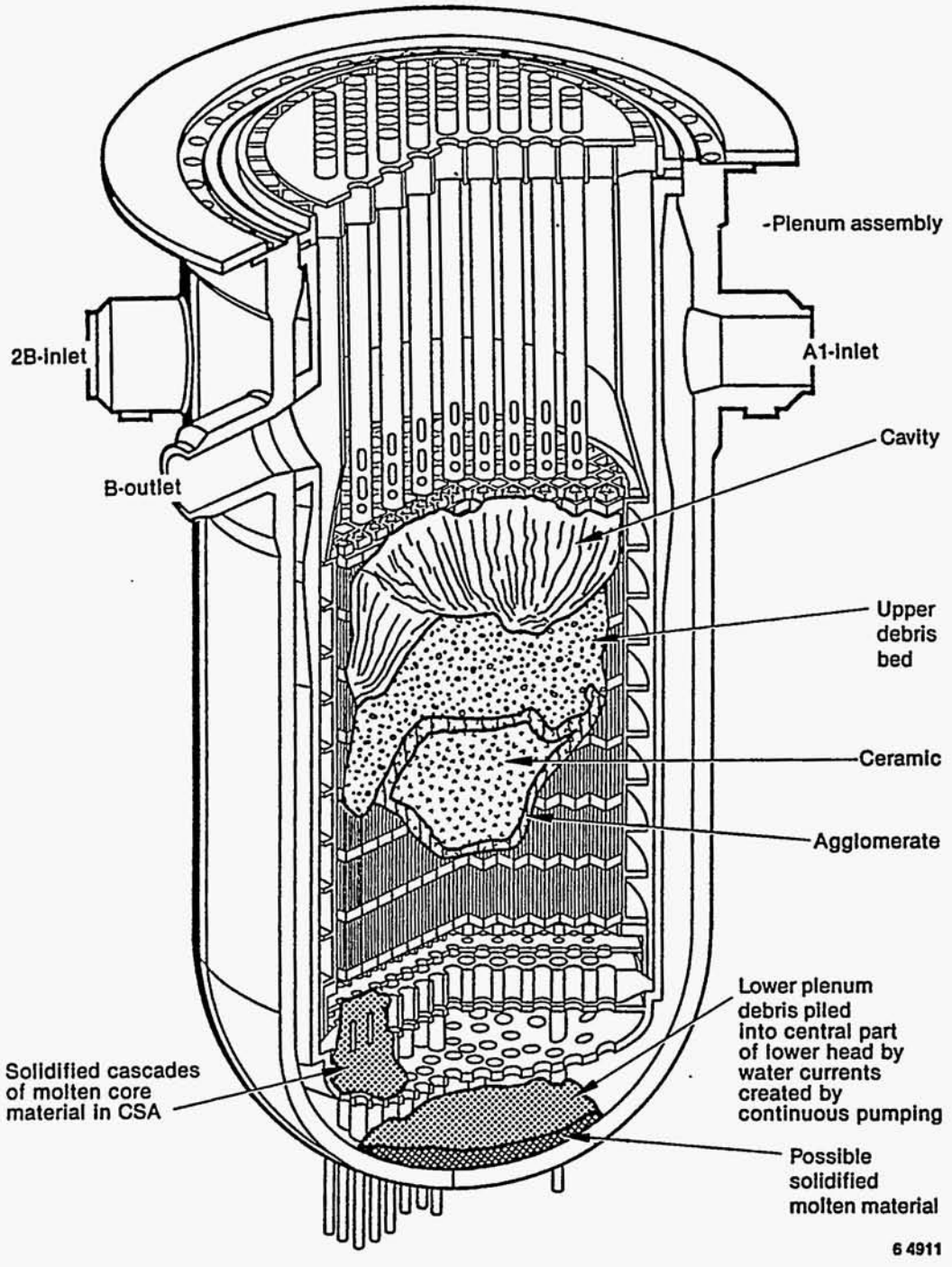

Figure 24. Updated end-state core conditions.

UPDATED ACCIDENT SCENARIO BASED ON CORE BORE DATA

An accident scenario has been hypothesized based upon the known end-state conditions of the core and reactor vessel, data from plant instrumentation recorded during the accident, best-estimate analyses of the accident, and the results from in-pile severe fuel damage experiments.[2] Data from the core boring operation have substantially expanded the known end-state conditions of the core and reactor vessel internals. These data basically substantiate the original accident scenario and provide much information to elaborate on that synopsis. The scenario presented below reflects this new information.

Core uncovery started between 100 and 113 min after turbine trip, which is considered the beginning of the core damage phase of the accident. This is substantiated by the measurement of superheated steam in the hot legs at 113 min. Best-estimate predictions indicate that core temperatures were high enough to balloon and rupture the fuel rod cladding by about 140 min, releasing the noble gases and other more volatile fission products, such as iodine and cesium, which had accumulated in the gap between the fuel pellets and the cladding. These predictions[7] also indicate that cladding temperatures rapidly increased at about 150 min, due to cladding oxidation, and quickly exceeded the zircaloy cladding melting point. The molten zircaloy dissolved some fuel; this molten U-Zr-O ternary mixture flowed down and solidified in the lower, cooler regions of the core probably at the reactor coolant liquid-vapor interface. At 150 min, the best-estimate of core liquid level is approximately 0.7 m, which is consistent with the lower limit of previously molten core materials in the center of the core. At this time, the high-temperature zone and most of the core damage was probably confined to the central region of the core. A schematic of this hypothesized configuration at 150 min is shown in Figure 25.

By 174 min (just prior to the primary coolant pump transient), some of the fuel had been dissolved by molten cladding or melted in the central, highest-temperature regions of the core. This relocation of fuel material

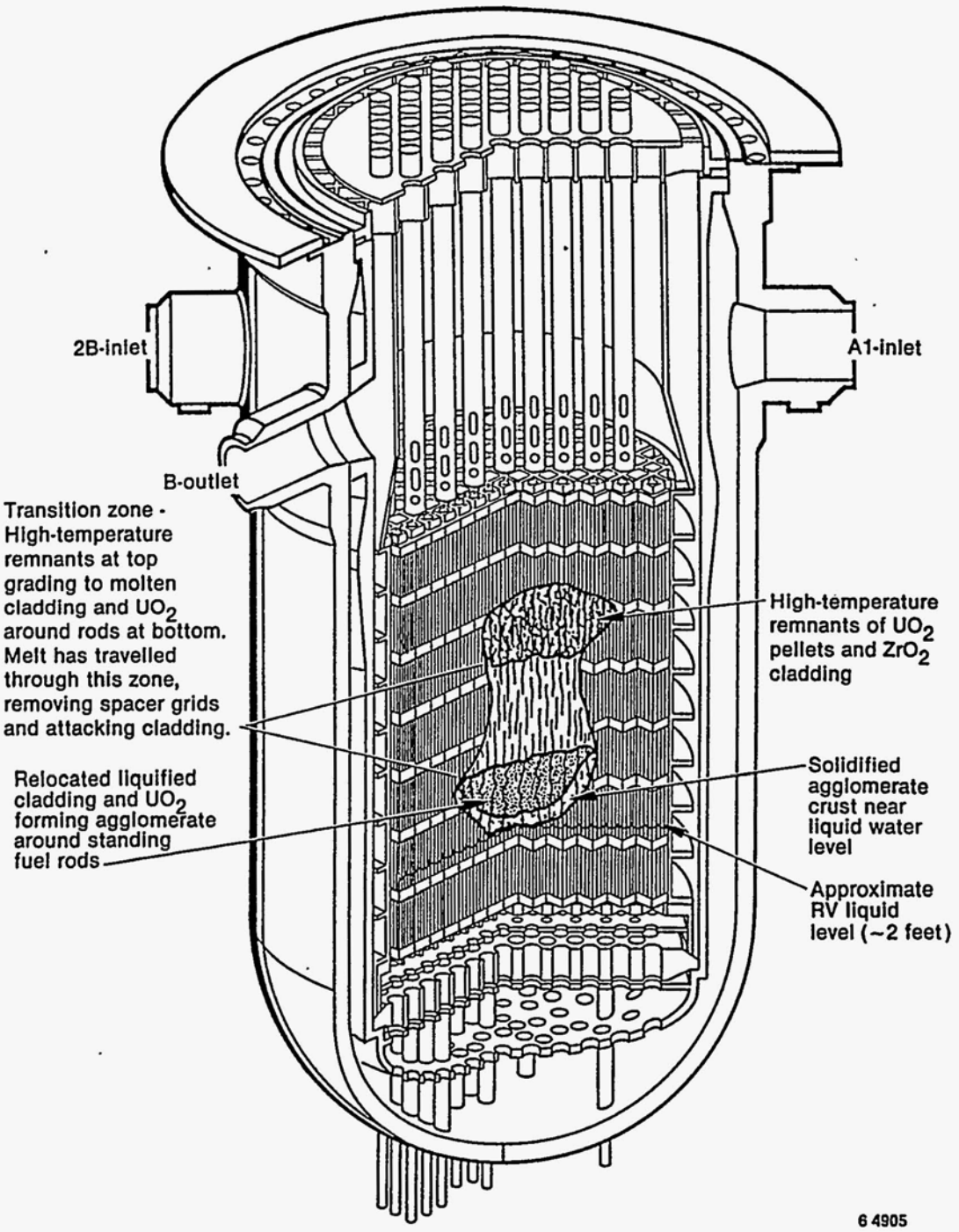

Figure 25. Hypothesized core damage configuration at 150 min.

into the lower regions of the core probably resulted in the funnel-shaped, end-state configuration as determined from the core boring operation. The hypothesized conditions at 174 min are illustrated in Figure 26. Fuel rod remnants composed of oxidized cladding and the undissolved UO_2 fuel remained standing above the solid structure of relocated material. Relatively undamaged fuel assemblies existed around most of the core periphery and beneath the bottom crust of ceramic fuel rod materials. The funnel-like shape of the bottom crust was probably caused by the initial blockage of flow in the center of the core and diversion of coolant flow to the core periphery. This flow diversion enhanced the heat transfer and prevented the relocating molten core materials from flowing down to the same elevation as that at the core center.

The primary coolant pump transient at 174 min injected some coolant, possibly as much as 1000 ft^3 in less than 15 s, into the core. The intact fuel rods near the core bottom substantiate that core cooling was maintained in the bottom of the core. However, the extent of core cooling is not known, because of the flow blockage resulting from the solid structure of relocated molten core materials in the bottom of the core. The oxidized (and embrittled) fuel rod remnants above the solid structure were probably fragmented by thermal and mechanical shock due to the injected water, as shown in Figure 27. The extent of fuel rod fragmentation and mixing of the debris bed at this time is uncertain. It is difficult to envision a mixing process that would mix the debris bed to the extent that currently exists in such a short time. Examination of debris from the core indicates that many of the particles are agglomerates composed of oxidized cladding, unrestructured fuel pellet fragments, and previously molten fuel rod materials These agglomerates have not been found in the PBF Severe Fuel Damage Test SFD-ST[8] which was subjected to similar conditions of heatup and reflood as the TMI-2 core experienced.

At 200 min, the high-pressure injection system (HPIS) was turned on; and some coolant was injected in the primary cooling system. The amount of coolant injected is highly uncertain; however, the best estimate of the injection rate and the water injected by the primary cooling pump

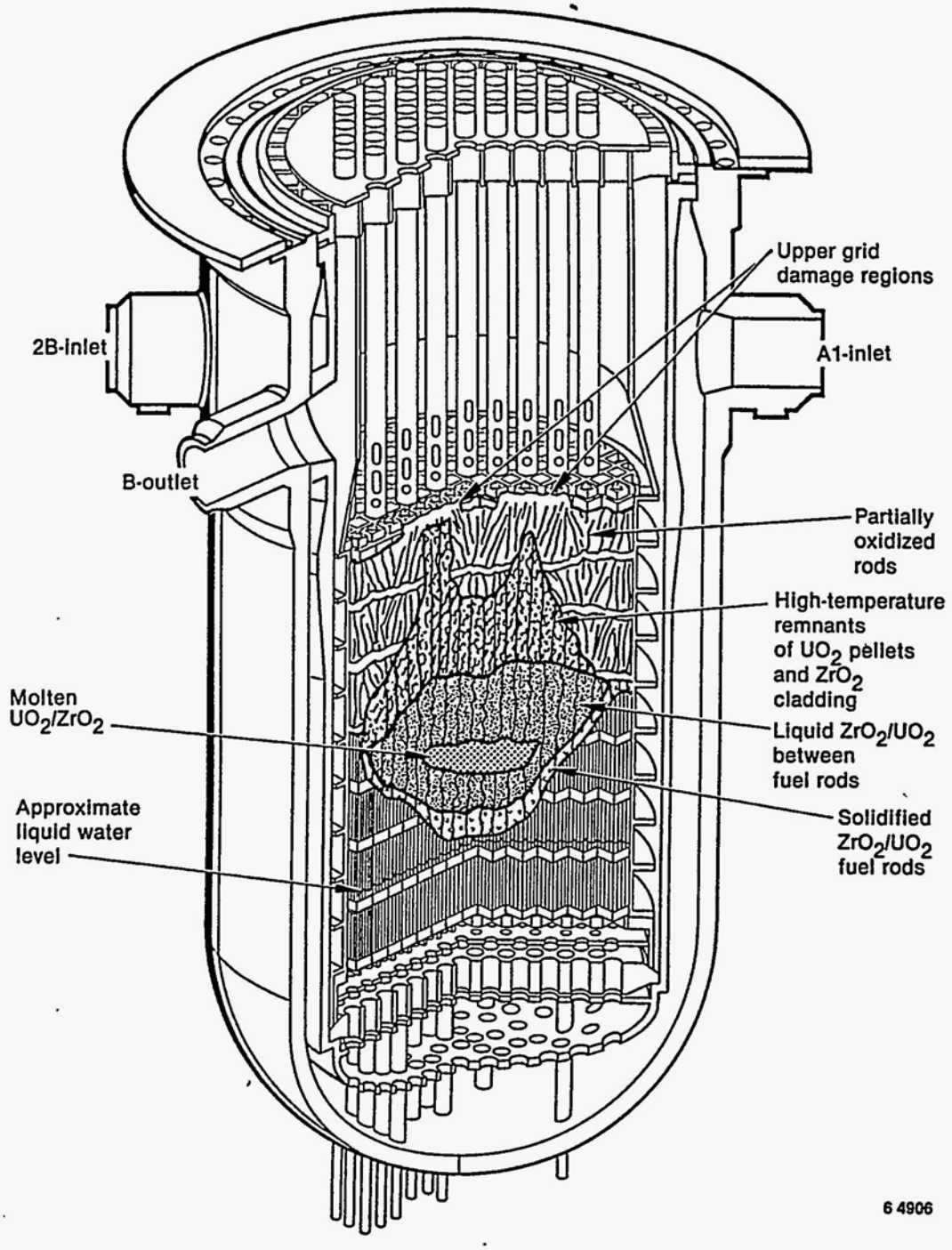

Figure 26. Hypothesized core damage configuration at 174 min (just prior to B-pump transient).

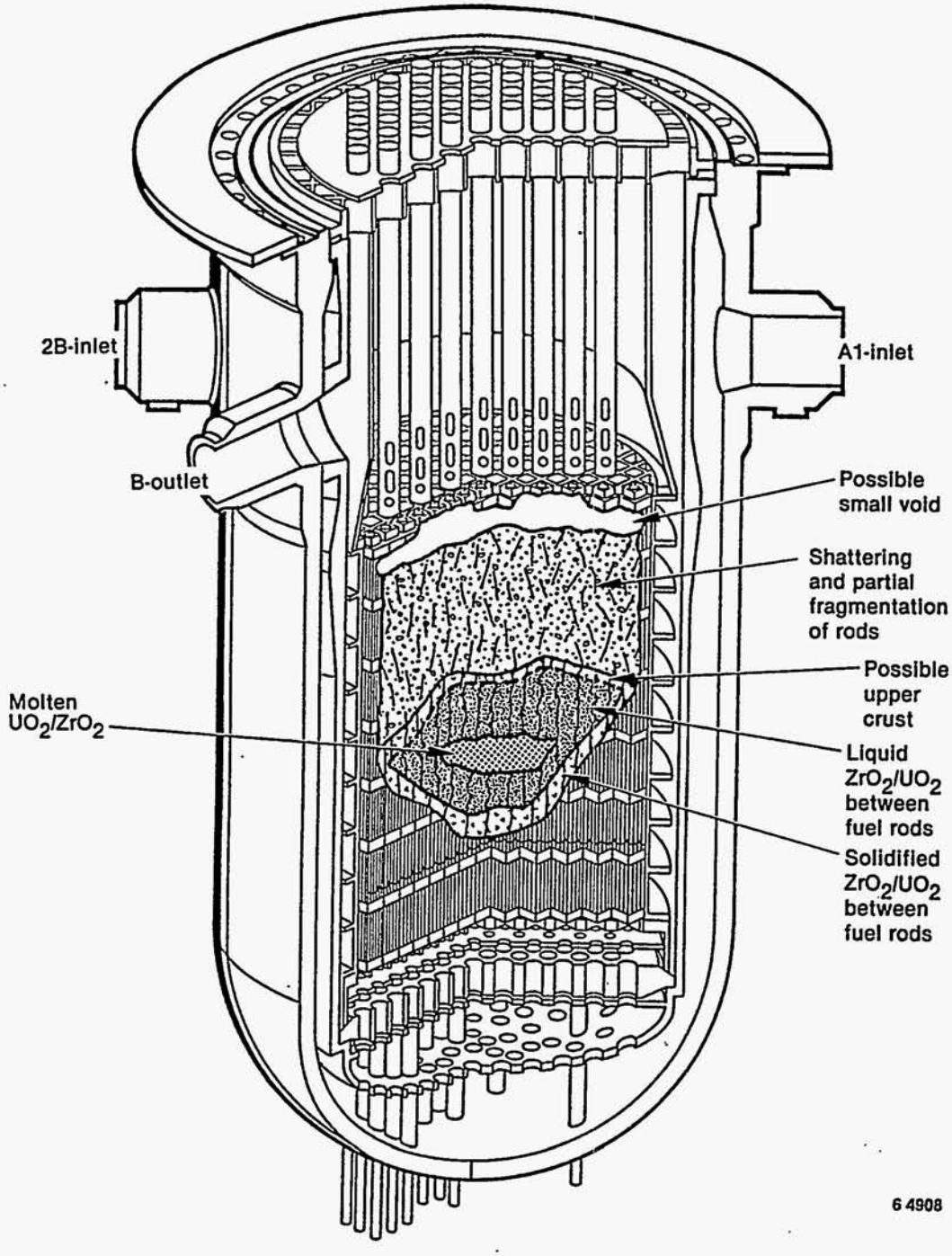

Figure 27. Hypothesized core damage configuration at 175-180 min (just after B-pump transient).

transients at 174 min, if directed entirely into the reactor vessel, would result in a covered core sometime after 200 min. This would provide continuous cooling to the surface of the solid structure of relocated core materials and coolant which would eventually quench the debris bed. Quenching of the debris bed may have been a relatively long-term and rather violent process, with water gradually penetrating the interior of the debris bed from the core periphery. The resultant steam and hydrogen (byproduct of the steam/metal oxidation process) would rapidly flow from the core into the upper plenum. This process of intermittent water ingress followed by the flow of high-velocity gases out the top of the core could vigorously mix the debris bed as well as bring molten ceramic material from the top of the solid structure up into the debris bed where the agglomerated particles were formed. Cooling at the outside surface of the solid structure would have been insufficient to prevent continued heating from decay heat and remelting of ceramic material within the interior as shown. The high-velocity steam and hydrogen flowing from the core would cause the melting and oxidation which has been observed on the underside of the core upper-grid structure, as shown in Figure 28. An alternate explanation for the end-state conditions observed is that the damage to the upper grid occurred prior to 174 min during core heatup and that the debris bed was mixed by the primary coolant pump after core cooling was reestablished at about 16 h into the accident. These processes must be evaluated to ascertain the most probable scenario.

Most, if not all, of the core materials found in the lower plenum probably relocated at approximately 224 min and were molten. This relocation was indicated by anomalous output from the Levels 1 and 2 self-powered neutron detectors (SPNDs), by a very rapid increase of approximately 2 MPa in the primary cooling system pressure, and by a rapid increase in the source range monitors. The results of analysis of the core boring data as well as data from the debris bed probing operation conducted by GPU in December 1985 indicated that this relocation of molten core materials into the lower plenum occurred primarily in the southeast quadrant of the core near the periphery through assemblies P5 and P6, as depicted in Figure 29. Since there is no voided region in the previously

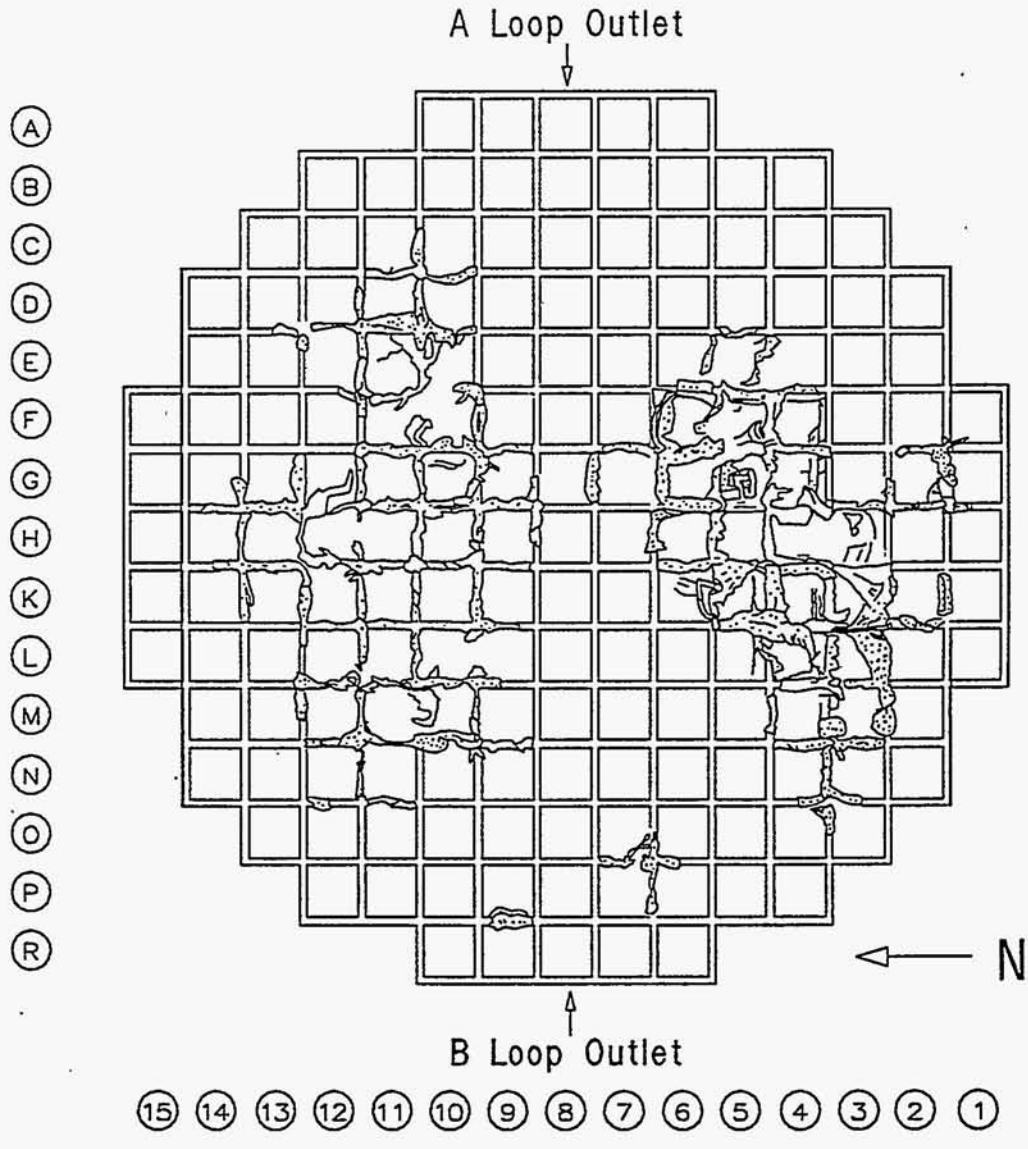

Figure 28. Damage map of the TMI-2 core upper grid structure as viewed from its underside.

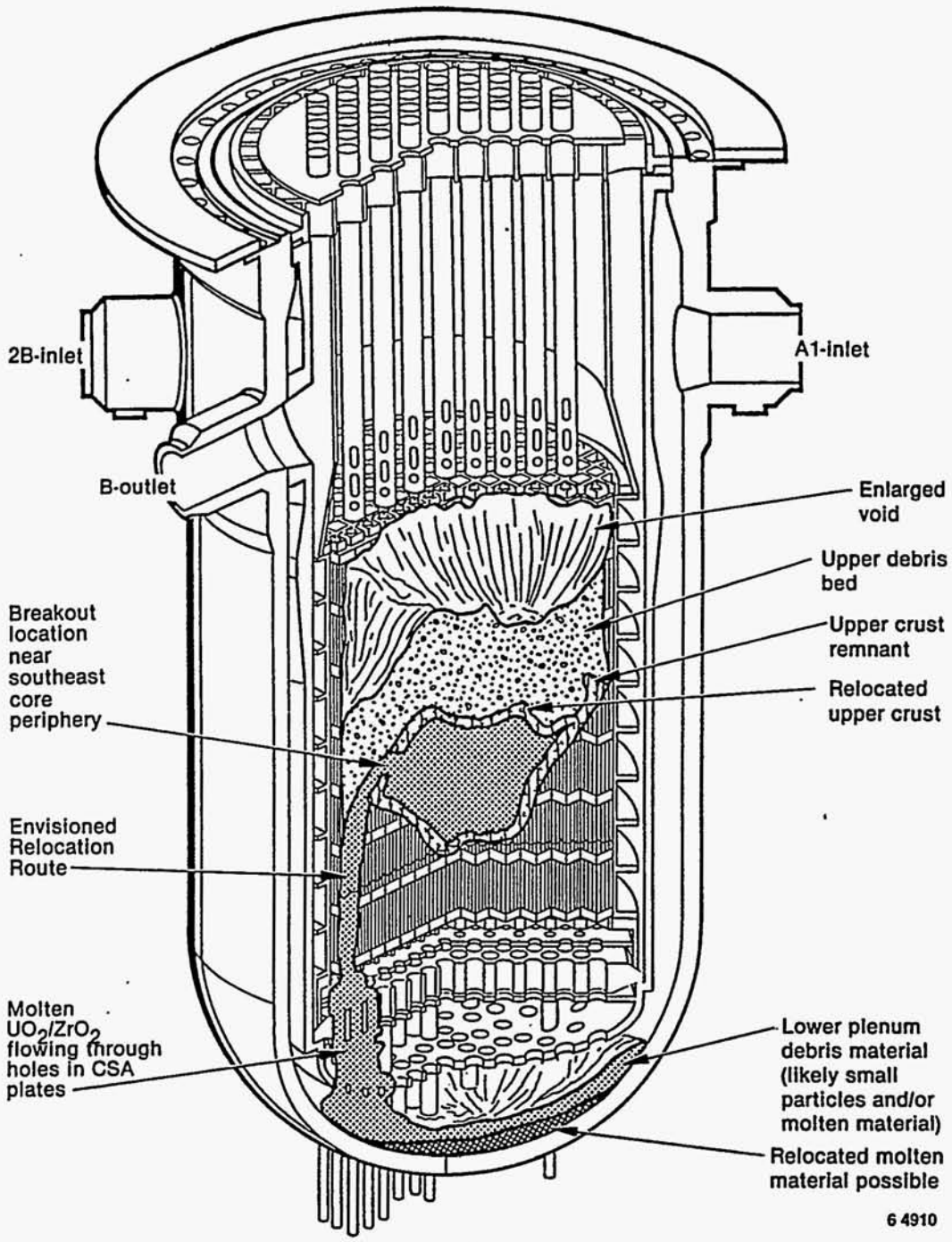

Figure 29. Hypothesized core damage configuration at 224 min (lower plenum relocation).

molten core zone, the central portion of the top crust apparently collapsed as the material flowed into the lower plenum, leaving behind a ridge of material at the core periphery. The top of this ridge indicates the top of the crust or solid structure prior to relocation. The volume of this "sinkhole" formed by the existing ridge identified from video examinations of the core debris bed periphery and core boring at assemblies D4 and D8 and the current top of the crust is approximately 80 ft^3. This volume is essentially the same as the volume of material estimated to be in the lower plenum from the video exams and also the same as the estimated volume of fuel rod materials currently missing from the core as determined from the mass balance presented previously.

Failure of the crust near the core periphery or at least relocation of molten materials downward at the periphery was not originally anticipated. Material structures identified from the core boring operation indicate that the highest-temperature material was probably in the central part of the core near the bottom of the solid structure. This is consistent with the original scenario in which it was postulated that the material relocation was through the bottom crust near core center. Crust failure mechanisms that could explain a peripheral failure location include:

1. A thermal melt-through of the upper crust caused by the preferential convective heat transfer of decay heat from the interior to the top crust and the limited cooling of the upper surface by the debris bed.

2. A thermal/mechanical stress failure of the upper crust near the periphery, due primarily to pressure differences between the melting interior (at this time contained by a solid crust of frozen core material) and the exterior reactor system pressure. The failure time of 224 min coincides with a system depressurization of approximately 400 psi. A mechanical stress could also have been induced by the melting of ceramic material and the resultant volume expansion.

3. A eutectic interaction between the ceramic crust material and the stainless steel core former wall. It is known that zircaloy significantly dissolves stainless steel at temperatures exceeding ~1570 K.

Water in the lower plenum probably prevented significant damage to the CSA or the lower head and was also instrumental in the formation of a coolable configuration in the lower head. The expanding steam probably fragmented the molten material as it relocated into the lower plenum. Fragmentation of the molten material would result in a very large increase in available surface area for cooling the molten core materials; and, therefore, a coolable configuration for the lower debris bed could result. The postulated final configuration of the core and reactor vessel as noted in the previous section is shown in Figure 24. The layer of non-fissile metallic material shown on the lower head would have separated from the molten material after relocation, because the metallic materials have a slightly greater density than do the ceramic materials which have been examined.

As noted above, some details of the core damage progression are not yet sufficiently understood; therefore, definition of the accident scenario is not yet complete. The most important questions remaining to be answered regarding core damage and potential failure of the RV lower head during the accident include:

1. What was the thermal response of the solid degraded core structure, and did the core former wall interact thermally or chemically with the supporting crust of ceramic material to induce failure of the crust?

2. What was the impact of the coolant and RCS pressure changes on the formation and mechanical stability of the ceramic crust?

3. What are the effects of control rods and burnable poison rods on core damage progression?

4. What were the heat transfer characteristics of the upper core debris bed and to what extent were the debris bed and the solid structure thermally and mechanically coupled?

5. What were the controlling thermal-hydraulic mechanisms that resulted in the formation and current state of the upper core debris bed?

6. What was the extent of thermal and chemical interaction between the molten core materials and the CSA, the RV lower head, and instrument penetration nozzles and guide tubes?

7. What was the long-term thermal response (coolability) of the solid structure of core materials contained within the core region and the core debris in the lower plenum?

Detailed metallographic and chemical examinations of the core bore samples, as well as first-principle calculations that focus on the controlling mechanisms, are crucial in resolving these questions. These examinations and engineering analysis are currently in progress.

REFERENCES

1. E. Tolman et.al, TMI-2 Accident Evaluation Program, EGG-TMI-7048, February 1986.

2. J. Broughton, "Core Condition and Accident Scenario," Proceedings of the First International Information Meeting on the TMI-2 Accident, Conf-8510166, October 1985.

3. M. Russell et.at, TMI-2 Accident Evaluation Program Sample Acquisition and Examination Plan, EGG-TMI-7132, January 1986.

4. M. R Martin and D. A. Lopez, TMI-2 Core Stratification Sampling Project System Design Description, EGG-TMI-6824, Vols. 1 and 2, May 1985.

5. GPU Memorandum No. 4730-86-0037, from D. M. Lake to R. H. Fillnow, "Debris Bed Topography," March 31, 1986.

6. L. Beller, H. Brown, Design and Operation of the Core Topography Data Acquisition System for TMI-2, GEND-INF-012, May 1984.

7. C. Allison et al., SCDAP/MOD1 Analysis of the Progression of Core Damage During the TMI-2 Accident, EG&G Idaho, Inc. Report SE-CMD-84, 009.

8. A. Knipe et al, PBF Severe Fuel Damage Scoping Test - Test Results Report, NUREG/CR-4683, August 1986.

APPENDIX A

DESCRIPTION OF DRILLING UNIT

APPENDIX A

DESCRIPTION OF DRILLING UNIT

The TMI-2 Core Stratification Sampling (CSS) System is a complex assembly of mechanical, electrical, and electronic hardware. Utilizing this machine, the custom computer programs, and the operating procedures especially developed for these operations, a series of stratigraphically intact samples has been removed from the TMI-2 reactor core. In general, the system was developed to meet the requirements outlined below.

1. Utilize the GPU shielded work platform for support over the reactor.

2. Access any position within a 4-ft radius of the center of the core.

3. Meet stringent positioning and targeting limits (planar location within ± 0.125 in. at reactor vessel flange, plumb within ± 3 arc min, intersect the center of the lower endfitting 50 ft away within ± 0.375 in.), all without usable in-vessel referents.

4. Cut and extract a sample approximately 2.5 in. in diameter and up to 8 ft long.

5. Utilize the GPU defueling canisters for removal of the samples from the reactor.

6. Consist of modules sized to pass through the containment building personnel airlock (39 in. wide by 74 in. high).

7. Minimize the number of operating personnel and the required sample acquisition time.

8. Provide data during operations to characterize the material being drilled against four general categories--standing fuel arrays, loose debris, resolidified material, and void space.

Drill Unit Configuration

Drill Unit

The CSS drill rig is based on a compact, self-contained machine commercially known as a Longyear 38-EHS drill unit. Functionally, it consists of a hydrostatically driven spindle (which applies torque to the drill string), a hydraulic chuck (which clamps the drill string in the spindle), and hydraulic ram cylinders (which apply upward and downward force). The CSS drill rig is equipped with a non-standard spindle assembly called the Megalo head, which is manufactured by the Japanese subsidiary of Longyear Corp. The spindle and chuck of the Megalo head are large enough to permit passage of the large-diameter drill string and casing. Different sizes of pipe are accommodated by changing the clamping jaws in the chuck.

Spindle rotation is powered by a 50-hp electric motor driving a hydrostatic pump/motor combination. The high-pressure, low-flow hydrostatic motor provides power to the spindle via a four-speed transmission with a two-speed differential. The net result provides a wide variation in available rotational speeds and torque capacities, with overlapping gear ranges allowing rotation up to 500 rpm and torque up to 3,000 ft-lb. A separate hydraulic pump, driven by the same electric motor, provides power to the feed cylinders, spindle chuck, and two separately mounted clamps used in handling the drill and casing strings. Downward and upward force capacities are limited to 10,000 lb. (The load limit was due to design load considerations for the GPU shielded work platform.)

Controls for all operations are located within easy reach of an operator standing alongside the drill unit, as is instrumentation to provide readout of rotational speed, spindle torque, and the load applied by the head. The original instruments were supplemented with

computer-compatible electronic monitoring systems developed specifically for this application. These additional systems culminate in digital (LED) displays activated by the system control computer. Located on the operator's control panel, the calibrated displays show spindle rotation speed (rpm) and torque (ft-lb), weight on bit (lb) applied by the head, depth (in.), and coolant flow (gpm).

Computer Control and Data Acquisition Systems

The "high-tech" portion of the CSS drill rig is its brain--the process control and data acquisition systems (DAS). The standard Longyear unit, like virtually all such rigs, utilizes direct hydraulic controls manipulated by a skilled and knowledgeable operator. To meet the requirements presented above, i.e., drilling in a previously unknown medium, the sample acquisition operations had to be executed with precision using unskilled operators and with safety for both plant and personnel. In addition, drilling parameters had to be logged in order to provide qualitative data to characterize the materials being drilled.

The process control instrumentation, centered around an Allen-Bradley microprocessor, provides a number of operating functions to resolve these problems. All operator interface is via the computer, permitting automatic control of rotational speed, torque, weight on bit, and an adjustable torque setpoint (for making and breaking drill string and casing joints). In addition, the computer manages all system safety interlocks. The operating program includes: primary load-related limits (positive and negative weight on bit, redundantly backed with non-electronic limiters); prohibited-operations interlocks (clamp actuation and interaction logic) with annunciators to alert the operator to procedural errors; special-case overrides with auxiliary interlocks to permit required limited-use operations that would otherwise be precluded (e.g., spindle rotation with all clamps closed only during drill string make/break); and system-protection functions (fluid levels, temperatures, flow rates and/or pressures, rpm, torque, and rate-of-penetration limits).

The DAS, using a Compaq computer and a Tallgrass recording system, serves to provide information for post-drilling data reduction. The intent was to provide sufficient data to determine stratification of the core region by monitoring its relative "drillability" as a function of elevation (relative to reactor vessel internals). This information was obtained from a database developed during thorough testing of the drilling system prior to delivery to TMI-2. During operations, nearly every function provided by the drill unit is monitored and the data stored on a hard disk within the computer cabinet. The data are subsequently transferred to tape for removal from containment. Data reduction and manipulation are performed to develop qualitative information from the monitored parameters. Those parameters, which are updated once per second, include: a time reference (in seconds); weight-on-bit (lb); torque applied by the spindle (ft-lb); elevation of the bit (1000ths of an inch); bit coolant pressure and flow rate (psi and gpm, respectively); and sixteen status functions (clamps open or closed, switches enabled or disabled, etc.).

Supporting and Auxiliary Equipment

Bits, Drill String and Casing. Best estimates of the conditions in the core region indicated that the sample materials would include loose gravel-like debris, resolidified fuel-bearing material ("liquified fuel"), standing fuel rods, intact spacer grids, and the lower endfitting. This imposed a requirement that the drill bit be capable of cutting both extremely hard ceramics (i.e., the fuel and fuel-bearing materials) and the relatively soft ductile metallics. A series of tests were performed to evaluate various types of cutting tools. The drilling mockup included composite test samples consisting of zircaloy-clad quartz rods, Inconel spacer grids, 300-series stainless steel endfittings, concrete blocks, ungraded 3/8-in. gravel, and hard-fired alumina plates.

Of the eleven bits tested, only the Norton-Christensen "Chrisdril" bit was successful in cutting all of the anticipated materials. The bit has a sintered tungsten-carbide matrix crown set with industrial diamonds on the outer and inner surfaces and has toothed inserts made of "Stratapax"

material set into the crown with silver solder. "Stratapax", manufactured by the General Electric Corp., is a composite material consisting of synthetic diamond bonded to a tungsten carbide backing. The resulting tooth has the hardness of diamond and the high modulus of carbide.

The core barrel assembly, which is a standard commercial design, carries the drill bit, transmits the drilling forces, contains and protects the sample, and channels flush (coolant) water through the bit. A double-tube core barrel was used to permit the inner tube to remain stationary around the sample while the outside tube rotates the bit. The space above the 8-ft inner tube contains a swivel mechanism, a vent with a check valve to allow water to escape as it is displaced by the sample, coolant/flush water channels, and an anti-jam mechanism to counteract wedging of the inner tube by laterally compressed intact fuel rods. The overall length of the core barrels, including the bit, was less than 11 ft to ensure compatibility with the defueling canister.

The drill string consists of a core barrel assembly and the hollow tubular extensions necessary to reach between the core barrel and the drill rig. The casing is also a hollow tubular extension, carrying a modified drill bit called a casing shoe. The casing is used (on the CSS drill rig) to provide stability to the drill string during drilling operations and to maintain a clear hole for subsequent CCTV inspection.

During drilling operations, borated water at flow rates up to 6 gpm is required to provide cooling to the bit and to flush cutting fines. This water was provided by a standard positive displacement pump, with the suction taken directly from the reactor vessel. Clean borated water, used for rinsing the drill string during removal, was drawn from stainless steel 55-gal flush water supply tanks.

Drill Unit Support Structures. The support structures for the CSS drill unit consist of a straight forward superstructure secured to the GPU shielded work platform by an interface plate. Figure A-1 shows an elevation view of the system as it is installed on the reactor vessel. The

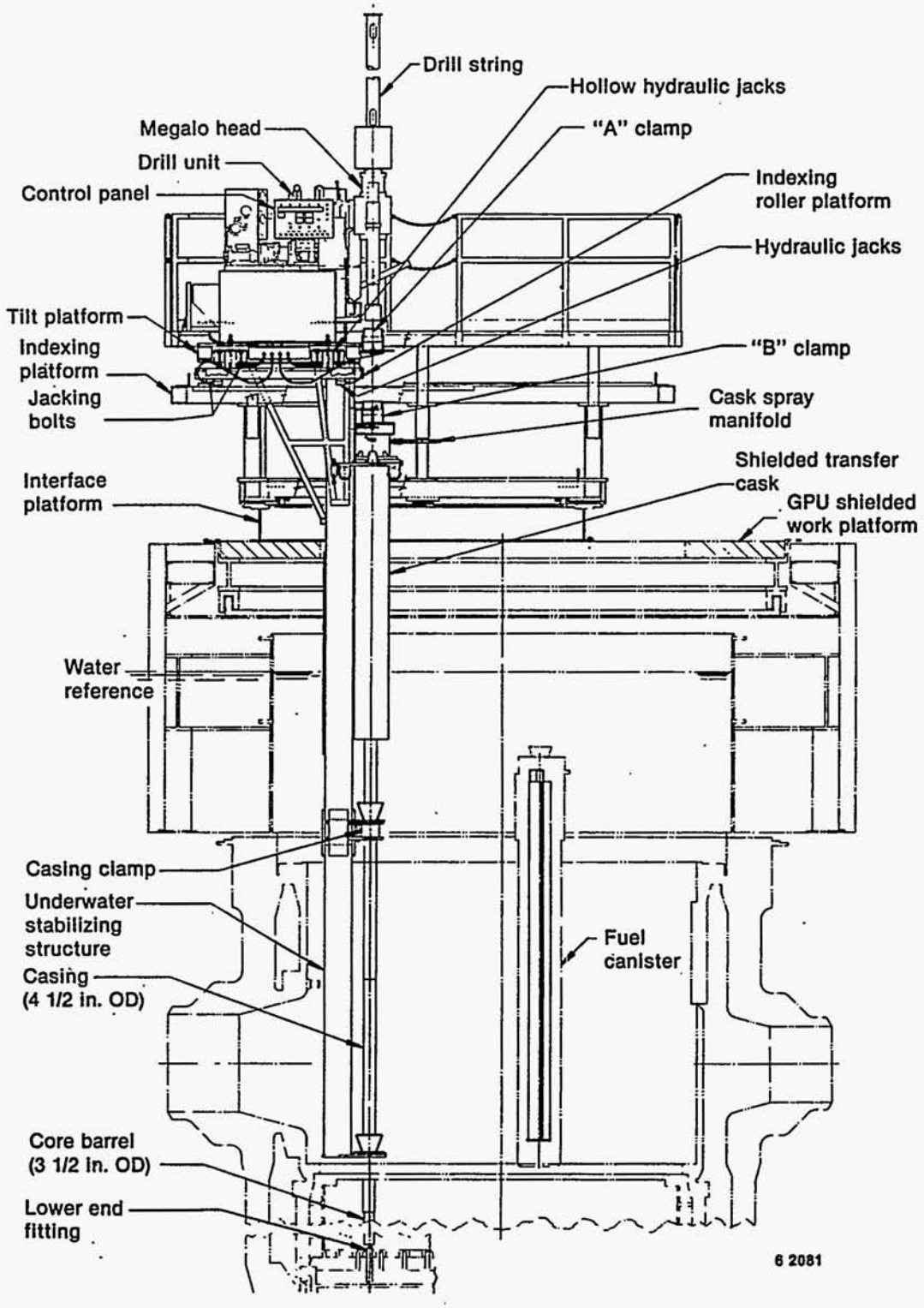

Figure A-1. Elevation view of the drill unit with its supporting structures and equipment.

components of the superstructure are: the main support frame (indexing platform); the indexing roller platform; the tilt platform; and the underwater stabilizing structure. The shielded work platform is a "lazy Susan" style structure mounted on the reactor vessel flange. It has a horizontal circular platform capable of rotation through 360 degrees about the reactor's vertical centerline. A diametral slot 18 in. wide provides access to the reactor internals for defueling.

The superstructure, in conjunction with the rotating work platform, permits the centerline of the drill string to be positioned anywhere within a 4-ft radius of the reactor vessel centerline. Positioning references for accurately locating the drill rig within the required tolerances was provided by a commercially available computer-aided theodolite (CAT) system. Using the CAT system, in-vessel core positions were established by surveying control rod positions in the plenum assembly prior to its removal. By referencing these data to fixed targets on the containment building wall, new core locations can be selected at any time; and their positions in three-dimensional space can be calculated with a high degree of precision by the CAT system. Helium-neon lasers attached to the eyepieces of the theodolites then provide a fixed point directly over the center of the desired fuel assembly position. Using the work platform and the adjustment motions available on the superstructure, the entire CSS system can be easily and repeatability located at the required position within less than ± 1/16-in. Inclinometers attached to the underwater stabilizing structure are used in conjunction with the planar positioning procedure to establish vertical alignment (plumb). In addition, strain gage arrays with associated alarm circuitry are used during drilling to indicate excessive lateral deflection of the drill strings.

A transfer cask and cask roller platform are supported by the indexing platform. The cask can be moved both radially and tangentially, independent of the drill unit and superstructure, to position it over the defueling canister for core barrel insertion. To help contamination control, the cask incorporates a water manifold to spray rinse water on the drill string and casing as they are withdrawn from the reactor.

Drilling Procedure

A typical sampling operation proceeds as follows:

1. The drill unit is positioned (using the CAT system) over the desired sampling location.

2. Casing is installed with the casing shoe just above the surface of the drill target, and the upper end is supported in the "B" clamp. Casing sections above the "B" clamp are removed.

3. The core barrel and associated drill string are installed, and drilling is initiated.

4. Drilling is stopped when the drill bit has penetrated the lower fuel assembly endfitting.

5. The drill string is allowed to rest on the lower grid distributor plate, and the upper end is temporarily plugged.

6. The upper casing sections are reinstalled, and the casing is drilled down around the drill string to the upper surface of the endfitting.

7. The casing is clamped in the underwater clamp, and the sections above that clamp are removed.

8. The upper sections of the drill string are removed, raising the core barrel. The core barrel is secured inside the transfer cask, with the upper end clamped in "B" clamp.

9. The cask is rolled into position over the defueling canister, and the core barrel is lowered into the canister using a crane.

10. A CCTV camera is lowered into the open casing to inspect the lower core support spaces.

11. If required, a smaller core barrel is installed and a sample is taken from the relocated core material in the spaces below the endfitting. The core barrel is transferred to the canister in a manner similar to that used for the large core barrel.

12. The casing is recovered from the reactor, with the lower 11-ft section transferred to the canister for disposal. Video inspection of the normal core space accompanies gradual casing removal.

Reference Drilling Data

Core drilling mockups were used at INEL in conjunction with equipment and procedure development. Employing the same hardware, drill bits, and distances required for TMI-2, the operations teams were trained by drilling into these mockups. In addition to training, the intent was to present the range of material conditions anticipated in the reactor. Because of radiological and economic considerations, material "simulators" were used for some portions of the mockup targets. While broad variations were used in assembly sequences, a typical mockup included (from the bottom up):

1. A cast 300-series stainless steel lower endfitting.

2. A 2- to 2-1/2-ft "bundle" of standing zircaloy tubes filled with quartz rod "fuel" or aluminum rod "control" materials, held in an appropriate array by Inconel spacer grids.

3. A 4-ft stack made up of cement blocks, hard-fired alumina plates, and void spaces of varying heights.

Drilling samples in the normal core space and subsequent inspection of the spaces below the core require cutting through the lower endfitting. Hence, a stainless steel endfitting of the type used in TMI-2 was needed in the mockup. The simulation of the surviving fuel bundles was an accurate representation except for avoiding the use of UO_2 or Ag-In-Cd. The

simulation of the liquified fuel region was more difficult. Sand and ungraded gravel were used in early tests, but the only noticeable effects were a tendency to wedge the large components in place (making them easier to cut) and increased difficulty in disassembly and cleanup. The loose materials were dispensed with early in the testing series.

Work performed in West Germany and at INEL indicated that the maximum hardness of liquified fuel material could, for our purposes, be simulated by hard-fired alumina. (Fully-fired alumina is actually harder than the U-Zr-O ceramic; both are harder than tungsten carbide.) The mix of void spaces, relatively "soft" cement block, and extremely hard alumina provided an adequate range of variables to test the DAS and to train the operators.

Operation of the drill rig is set up with the following functional limitations and control parameters:

1. Rotation speed (rpm) is basically constant, although some response lag is noticeable.

2. The operator inputs the torque value, and the microprocessor attempts to achieve and maintain this value by varying the weight on bit.

3. Penetration rate is artificially constrained to a maximum of 3 in./min; insertion rates approaching this value will cause the weight on bit to be decreased (limiting downfeed even without drilling resistance) independent of torque.

4. The spindle has a maximum vertical travel of 23.9 in., necessitating an operational shutdown (i.e., zero rotation, weight on bit, and rate of penetration) at the limit of travel.

5. Torque, as measured and recorded, includes more than just the resistance to bit rotation under load; the value also includes mechanical losses in the head and transmission, the drag of the

drill string inside the lateral supports (fairly constant and <25 ft-lb), and the drag of the walls of the bore hole on the drill string.

6. All parameters and status indicators are logged by the DAS once a second. (In retrospect, this was too often for some data and too infrequent for other data.)

7. Exceeding the preset torque value by 50 ft-lb or weight-on-bit loads exceeding ± 9,000 lb will result in an operational shutdown.

Drilling operations using the mockups, along with the reduction of the data logged by DAS, led to the following conclusions:

1. In relatively homogeneous materials, the sensitivity of the data system is such that even the boundaries between concrete blocks is detectible. (However, the chemical and physical heterogeneities expected in the relocated core material are such that the sensitivity is "swamped" with uninterpretable detail.)

2. Large-scale behavior is such that an experienced operator can distinguish ceramics from metallics from rod arrays by observing the machine during the drilling operation. In addition, transitions or discontinuities between media (i.e, reaching standing fuel rods, an intact spacer grid, or a void) are also apparent.

3. Because the control parameters and limitations are sometimes at odds with one another (e.g., simultaneously low torque and weight-on-bit), more than one form of data output is necessary to provide usable information.

4. The data are only meaningful if the machine is operated in the automatic mode; manual control of drilling adds too many variables.

5. In the automatic mode, the machine is powerful enough to penetrate the hardest ceramics at nearly maximum rate (3 ips); stainless steel, on the other hand, is work-hardened and chipped away at roughly 1 in./h.

With this general information in mind, the technique for interpreting the DAS output can be illustrated using the attached figures. Figure A-2 shows a representation of the mockup drilling target used for this sample exercise. Figures A-3 through A-6 show various parameters plotted as a function of drill bit penetration. All of the graphs have been corrected for time and for elevation, with zero distance representing the top of the mockup. Even a cursory look shows a pattern of behavior, common on all four graphs, where the parameter drops to null at approximately 18, 42, and 66 in. This is indicative of the operational shutdown required at roughly 24-in. intervals to accommodate rechucking. Fourth and fifth null points are also noticeable at approximately 76 and 78.5 in., respectively, on all four graphs. The fourth is the result of a shutdown created by over-torque as the bit makes the transition from dummy fuel rods to the face of the endfitting. The fifth is the cessation of operations after the endfitting has been penetrated.

Figure A-6, which shows rotation speed as a function of penetration, is included solely for reference. Except to document or verify shutdowns, its comparatively uniform behavior makes it nearly useless. The other graphs, however, illustrate varying sensitivities to the types of materials and transitions present in the mockup.

Figure A-3, which displays the changes in penetration rate, clearly shows the slowdown as the drill bit made the transition from the cement block to the hard-fired alumina plate. Also apparent is the relatively abrupt decline as the bit chews up the short remnants of the fuel rods just above the endfitting (~73 to 76 in.). The graph also shows that the alumina plate fractured at a point where the drill bit was only halfway through, but only allowed limited displacement before reestablishing the cutting resistance typical of such hard ceramics. (The decreasing

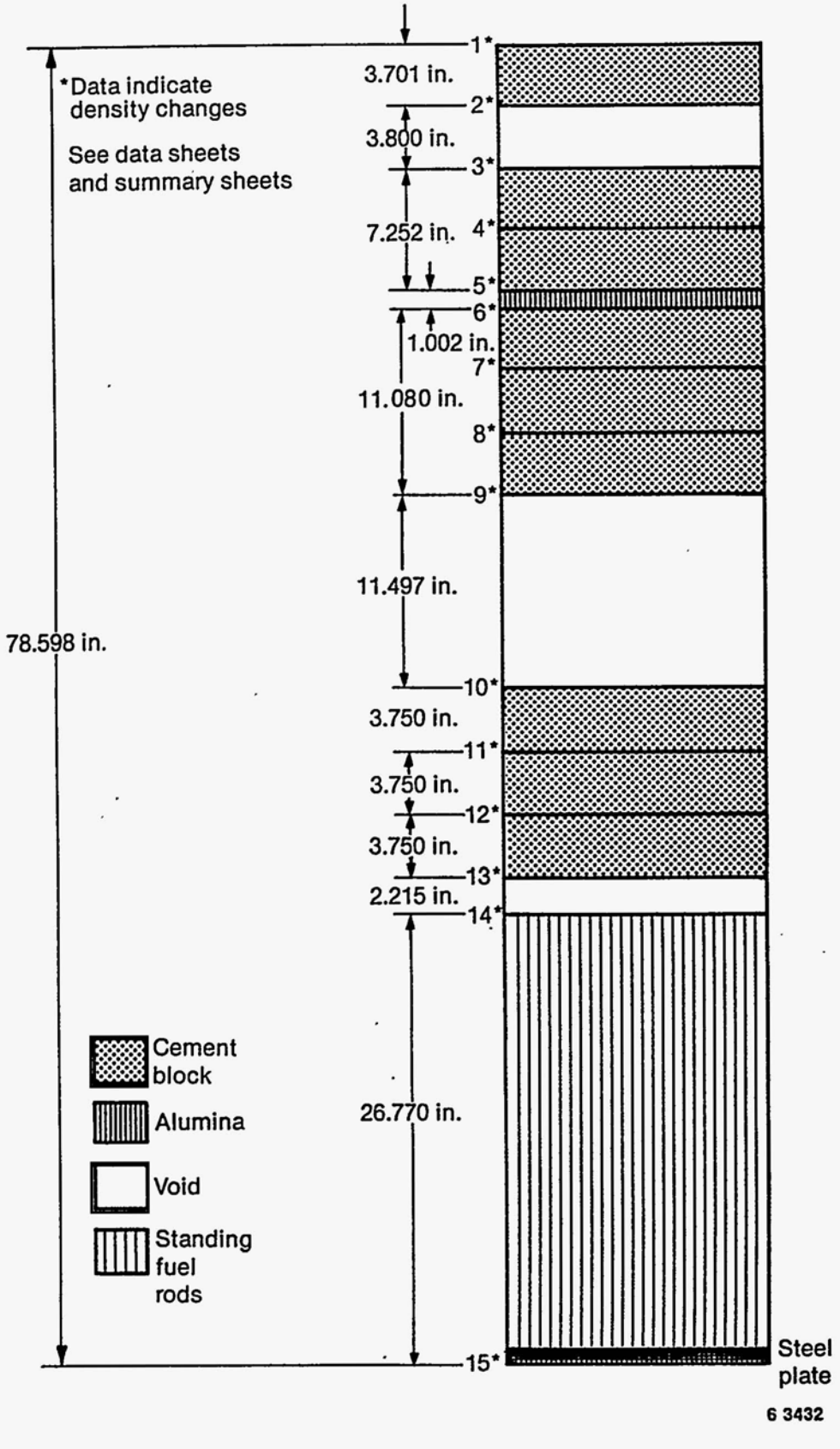

Figure A-2. Simulated drilling target for TMI-2 core bore machine.

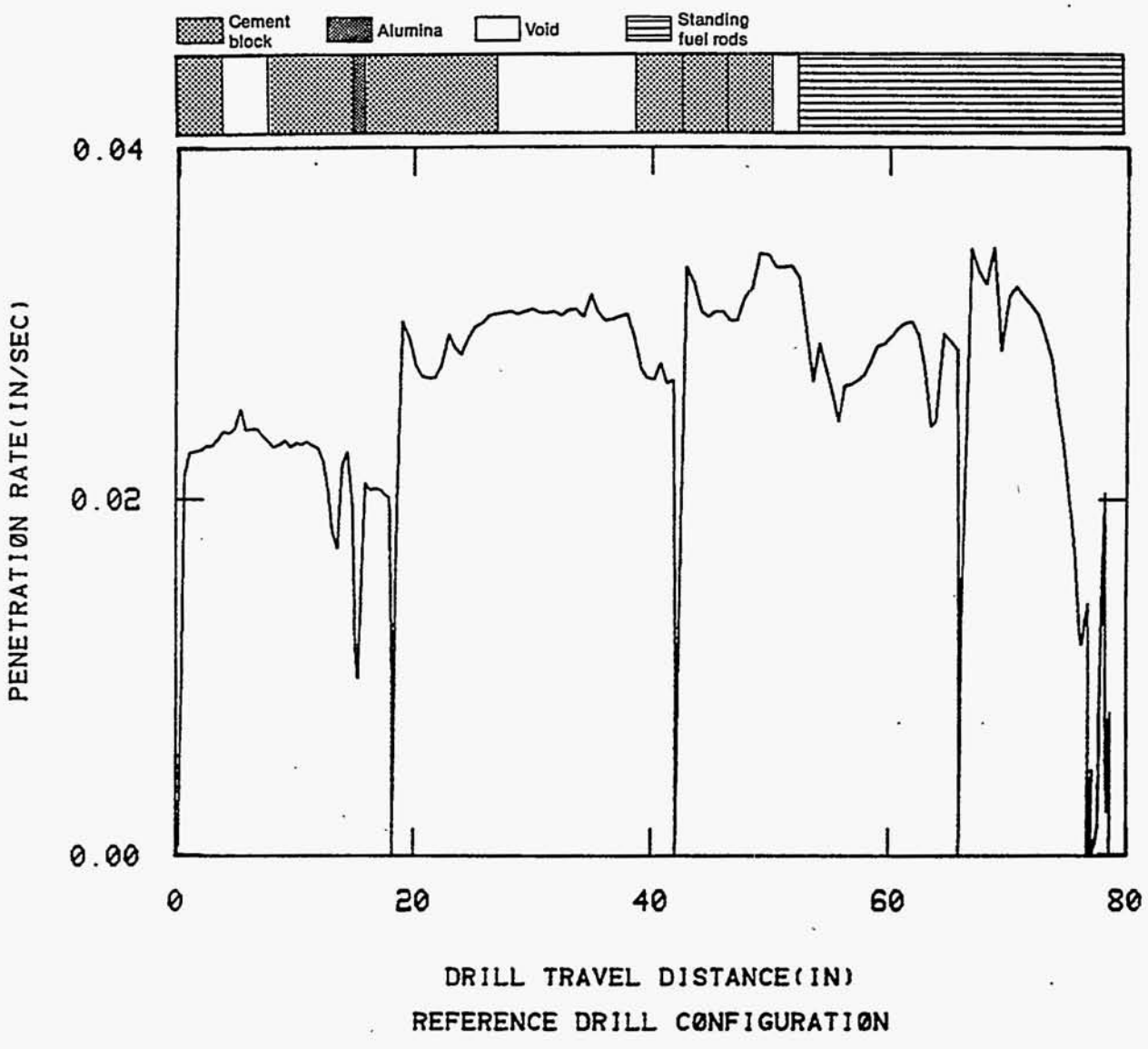

Figure A-3. Reference core bore drilling data, penetration rate vs. drill travel distance.

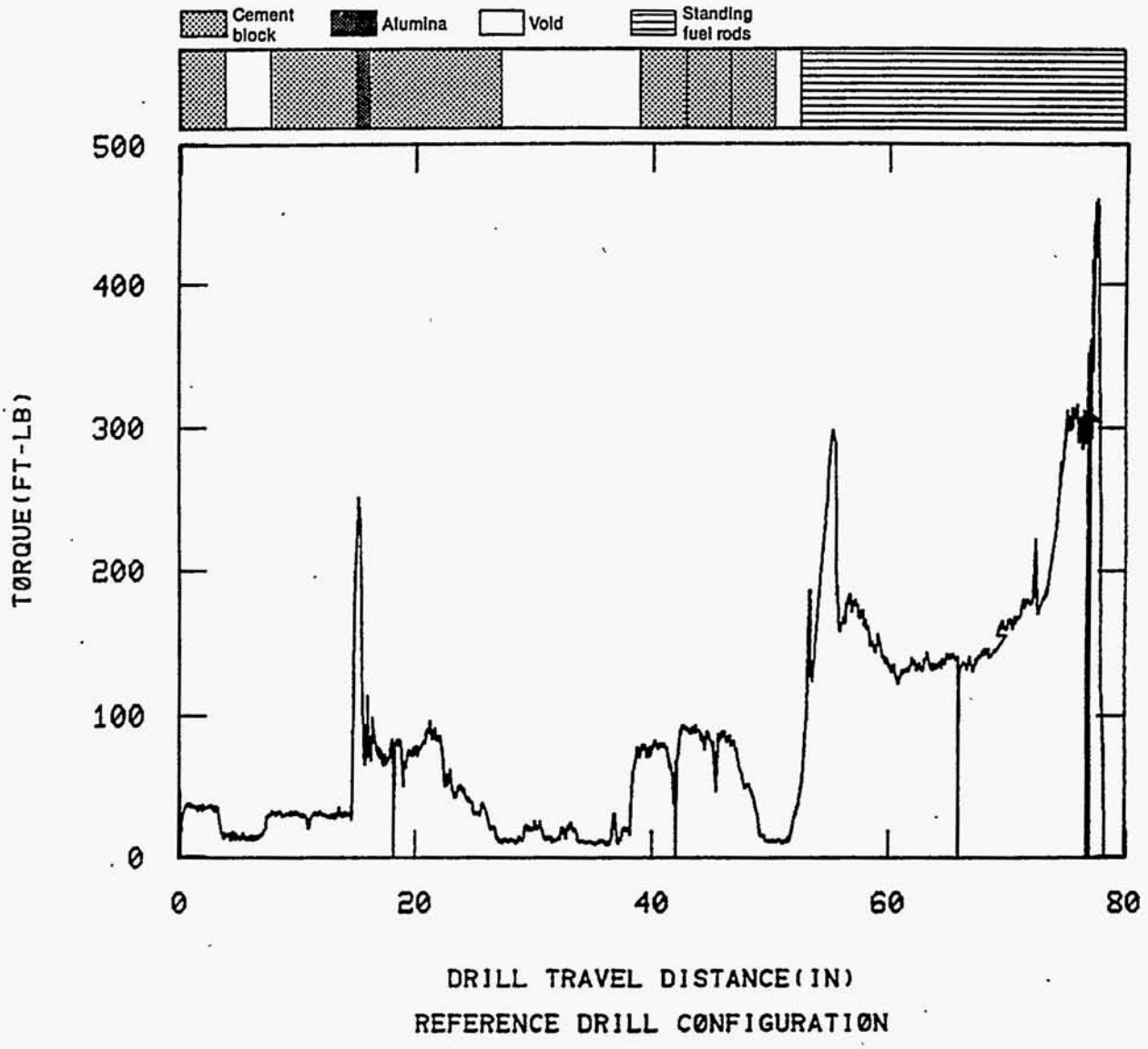

Figure A-4. Reference core bore drilling data, torque vs. drill travel distance.

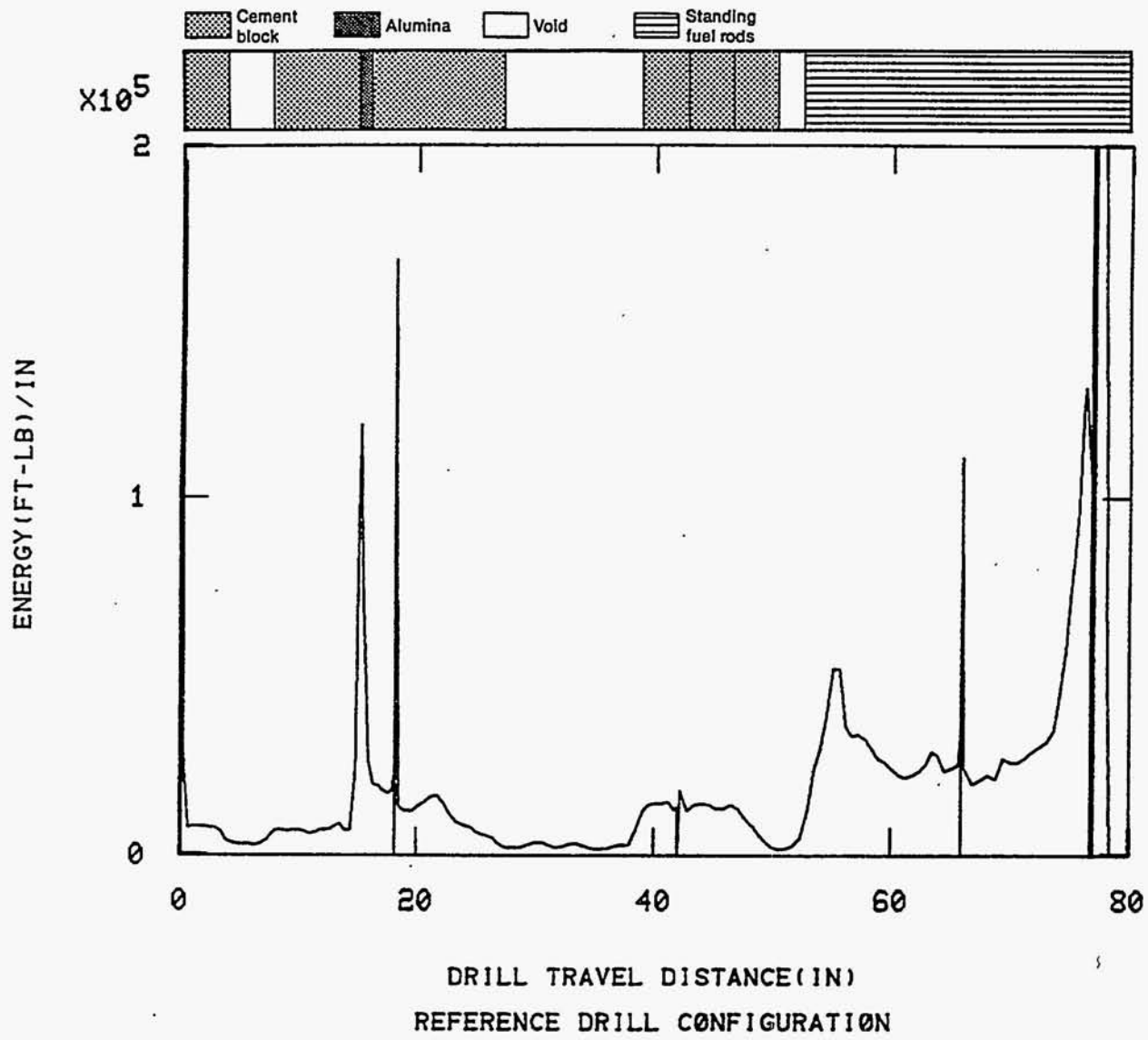

Figure A-5. Reference core bore drilling data, energy per inch vs. drill travel distance.

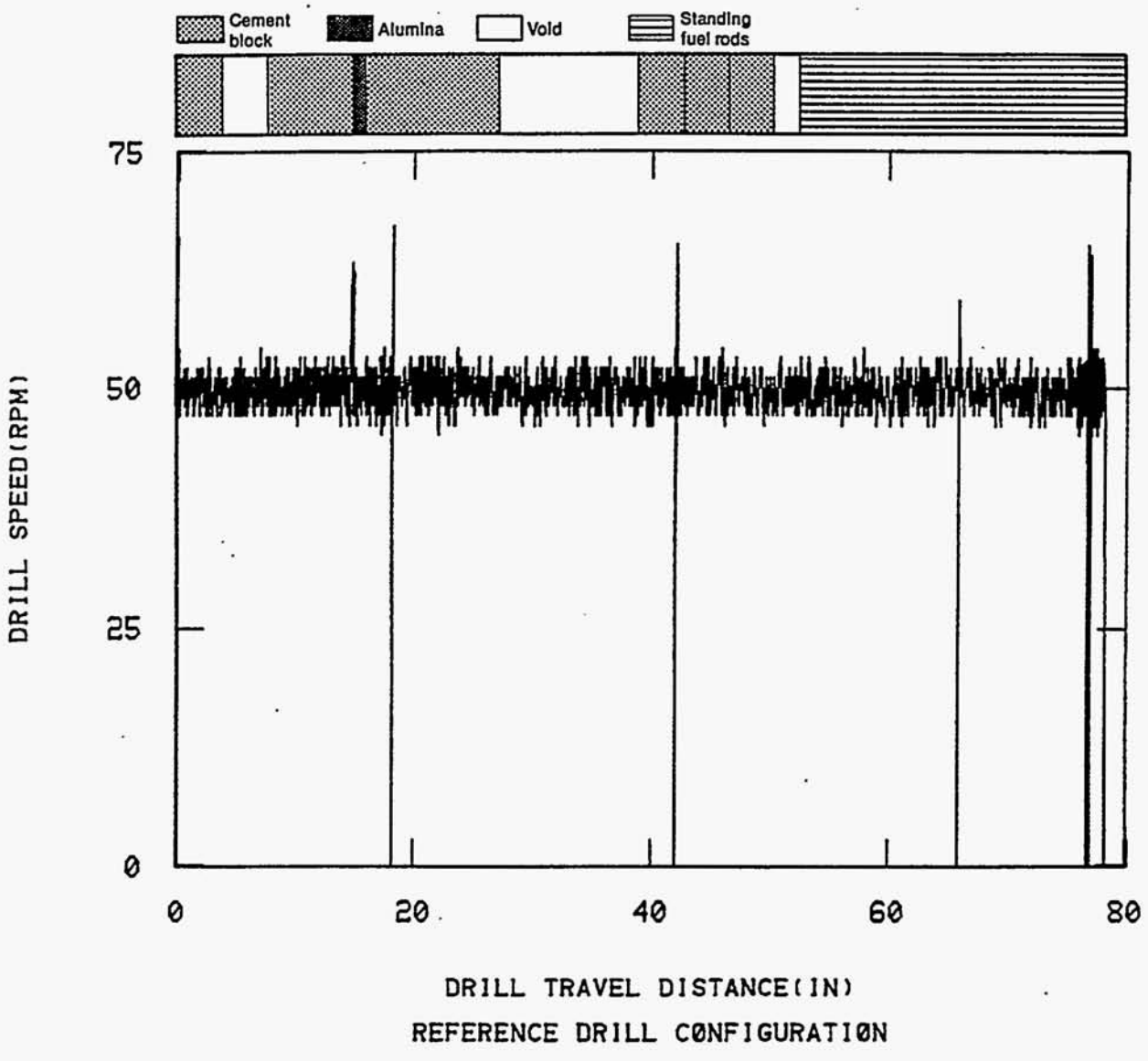

Figure A-6. Reference core bore drilling data, drill speed vs. drill travel distance.

penetration rate jumps up, then abruptly slows down again as the fractured pieces are ground away.) Much less evident are the effects of standing fuel rods, spacer grids, or void spaces. Only the spacer grids slow the penetration rate, and then the data are easily overlooked in the general variations.

Figure A-4, which plots torque, shows several of the same phenomena, namely, the initial resistance of the alumina plate and the extended effort required to penetrate the endfitting. More importantly, the torque curve shows conditions that penetration rate does not. (Remember that the unit limits maximum penetration rate.) All three voids in the mockup are immediately apparent by the significant lowering of torque (in spite of the computer's attempts to maintain torque at the preset level). The transition to fuel rods and the effects of the spacer grids at the top and bottom of the rod arrays are also noticeable. Less obvious, but present even in the averaged graphical data, are the transitions between cement blocks (regularly spaced small declines in torque as the drill bit cuts into the very small void created at the discontinuity).

Figure A-5 shows energy delivered per inch as a function of penetration. Aside from the step increases which accompany the restart of the drill rig after rechucking, this representation is more responsive to the high-energy consumers that are cut through. The alumina block, the spacer grids at the top and bottom of the rod array, and the endfitting stand out. The low resistance media (cement block, unrestrained rods, void spaces) are nearly lost in the data, in much the same manner as occurs in Figures A-3 and A-4.

APPENDIX B

DETAILED OBSERVATIONS AND DRILLING DATA FOR EACH CORE BORE

APPENDIX B

DETAILED OBSERVATIONS AND DRILLING DATA FOR EACH CORE BORE

This Appendix presents a more detailed summary of the video and on-line drilling data for each core bore location. Figures are presented for each drill location, highlighting the regions of the core and CSA drilled and the major observations. Selected enhanced video images of the core and CSA region are also presented. The accompanying discussion describes the major observations and relates these observations to other drill location observations. The on-line drilling data are presented and briefly discussed.

The CSA configuration and nomenclature to describe the CSA components are presented in Appendix F.

N5 Data Summary

Figure B-1 summarizes the N5 drilling and inspection regions and major observations. Figure B-2 presents selected video images from the core and CSA regions.

Core Region Observations

Standing rods extend from the lower fuel assembly end fitting to the third spacer grid (located about 47 in. from the bottom of the fuel rod. The upper 6 in. of the fuel rods appear to have localized regions of discoloration. However, the rods do not appear distorted. The third spacer grid (in contact with the agglomerate) appears to have undergone some melting on one side but appears to be intact on the opposite side.

The agglomerate above the third spacer grid extends to at least 50 in. and includes previously molten material. Above about 50 in., no useful video data were recorded. The previously molten material fills most of the spaces between fuel rods. Since some vertical fuel rod structure is

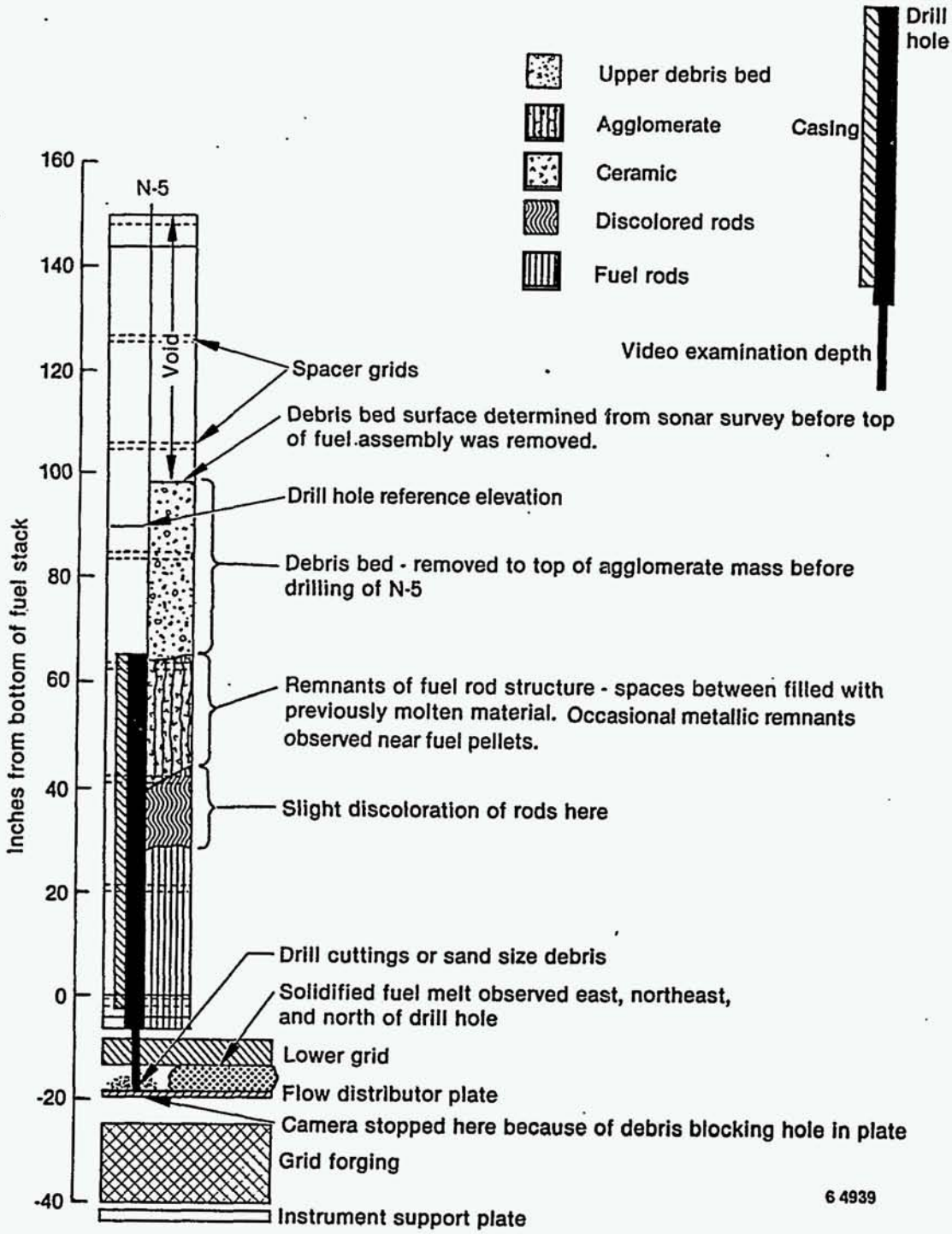

Figure B-1. N5 drill configuration and inspection summary.

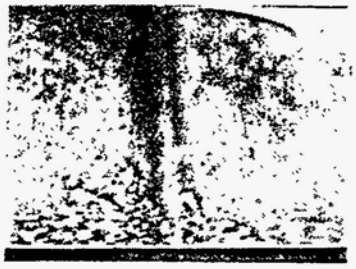

View from core position N5 of previously molten core material below the lower grid underneath core position 05 (86-417-1-6)

View from core position N5 of previously molten core material below the lower grid underneath core position 04 (86-417-1-5)

View from core position N5 of previously molten core material below the lower grid underneath core position 04 (86-417-1-3)

View from core position N5 of previously molten core material and wrinkled and deformed core instrument guide tube (right side of photo) below the lower grid underneath core position N4 (86-417-1-1)

Possible previously molten core material at edge of core position N5 lower endfitting tie plate bottom (86-417-1-8)

Figure B-2. Enhanced video images about N5.

Intact rod bundle between casing and lower endfitting at core position N5 (86-417-1-10)

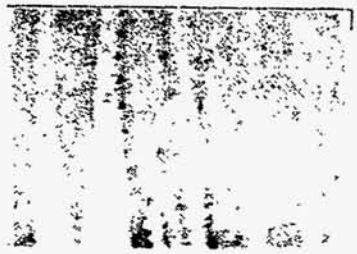

Intact rod bundle between second and third (approximately 36 in. above core bottom) spacer grids at core position N5 (86-417-1-11)

Transition between intact rod bundle and agglomerated core material at third spacer grid (approximately 48 in. above core bottom) at core position N5 (86-417-1-12)

Agglomerated core material at third spacer grid (approximately 48 in. above core bottom) at core position N5 (86-417-2-1)

Agglomerated core material with fuel rod remnants at approximately 58 in. above core bottom at core position N5 (86-417-2-2)

Figure B-2. (continued)

discernible, it appears that the relocated core material did not completely melt the original fuel rods. The cladding material surrounding the intact rods in many cases is indistinguishable from the surrounding previously molten material. Occasional metallic (shiny) pieces are observed next to the fuel pellets in the original cladding region. Fuel pellet boundaries are commonly discernible where the drill bit cut into the fuel rods.

Core Support Assembly Observations

The video camera was lowered into the CSA region but was blocked by loose debris at the flow distributor plate. The debris, most likely from the drilling operation, consists of irregular size drill cuttings, broken and split fuel rods, and a solid cylinder about the size of the core bore sample that is most likely a piece of the lower grid.

The smaller diameter drilling hardware was used to drill through the debris above the flow distributor plate in an attempt to obtain a sample of any previously molten material above the elliptical flow distributor. The drilling parameters indicated no significant drilling resistance below the distributor plate. After CSA drilling, the drill hole was still blocked with drill cuttings, thus preventing visual characterization of the CSA below the distributor plate.

Solidified previously molten material nearly fills the space between the lower grid and the flow distributor plate. The material is located to the north, east, and northeast of the drill hole (in the regions of 04, 05, 06, and N6).[B-1] An observable instrument guide tube appears to have some surface damage.

On-line Drilling Data

The on-line (automatic mode) drilling data are shown in Figure B-3. The automatic drilling started in the lower agglomerate region just above the third spacer grid. The torque and RPM data are uniform below the third spacer grid (until the lower fuel assembly endfittings are encountered).

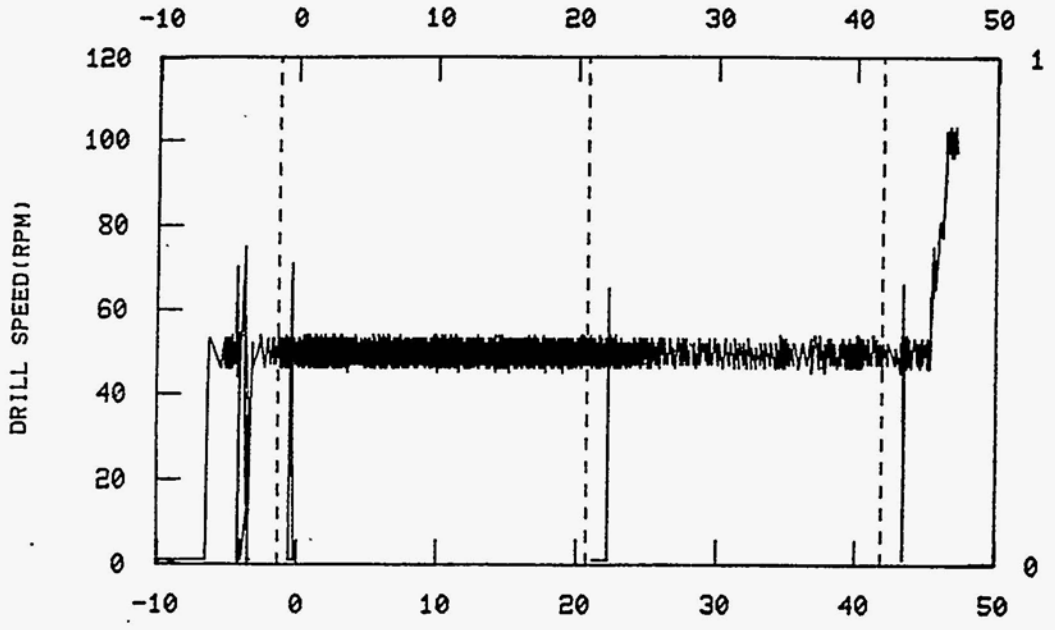

DISTANCE FROM BOTTOM OF FUEL STACK
BORE HOLE N5
DASHED LINES INDICATE MIDPOINT
OF SPACER GRIDS

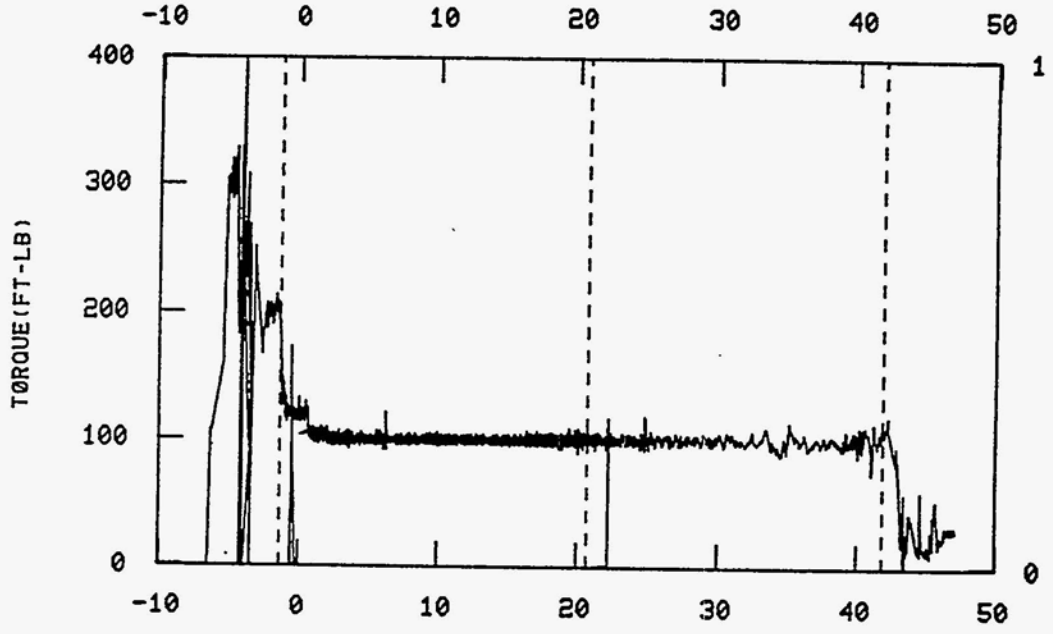

DISTANCE FROM BOTTOM OF FUEL STACK
BORE HOLE N5
DASHED LINES INDICATE MIDPOINT
OF SPACER GRIDS

Figure B-3. On-line drilling data for N5.

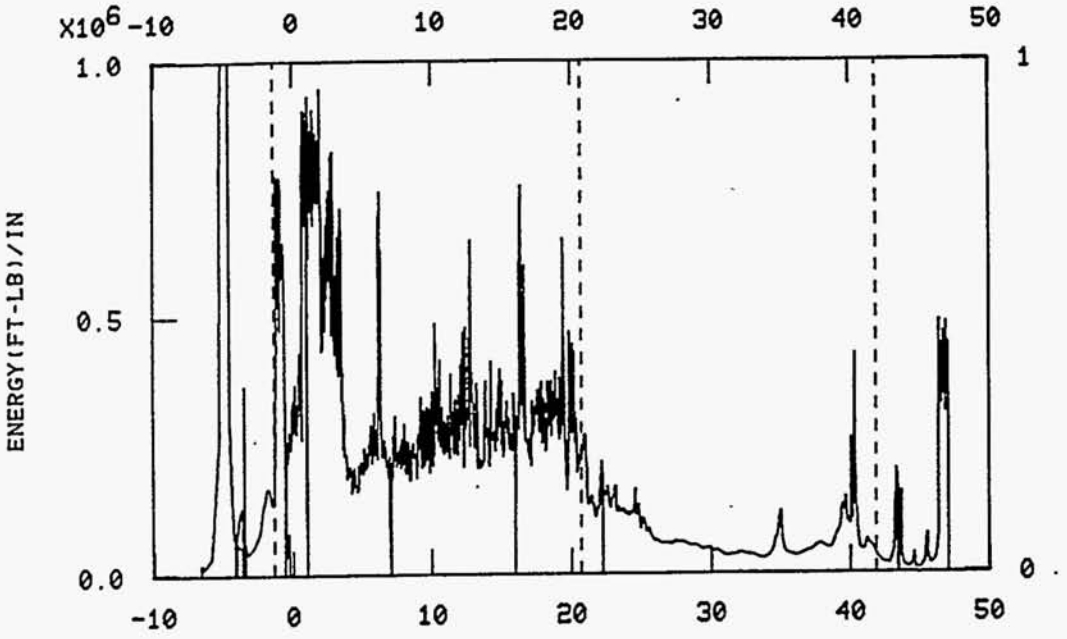

DISTANCE FROM BOTTOM OF FUEL STACK
BORE HOLE N5
DASHED LINES INDICATE MIDPOINT
OF SPACER GRIDS

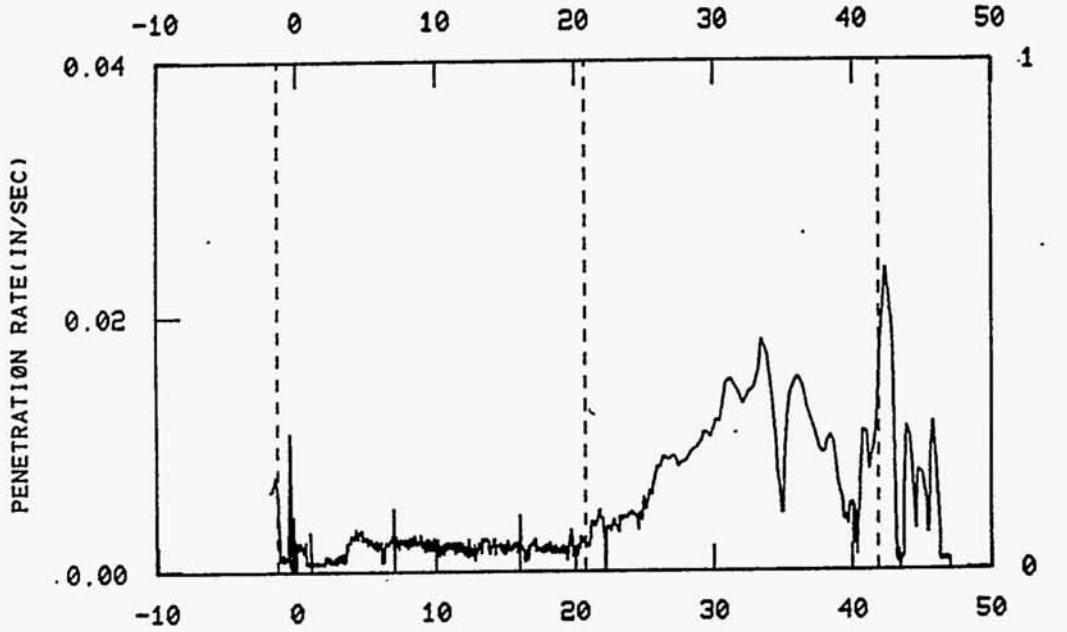

DISTANCE FROM BOTTOM OF FUEL STACK
BORE HOLE N5
DASHED LINES INDICATE MIDPOINT
OF SPACER GRIDS

Figure B-3. (continued)

The penetration rate and energy data show that the material between the second and third spacer grids has significantly lower drilling resistance than the material between the first and second spacer grids. This data trend suggests that the materials between the two spacer grids may be different. One source of this difference may be oxidation of the rods between the second and third spacer grid.

A localized change in drilling resistance is seen at approximately 34-36 in. (between the second and third spacer grid), suggesting a change in material composition at this location.

Relationship to Other Drill Holes

The agglomerate structure with vertical fuel rod remnants surrounded by resolidified material is similar to that observed at other drill holes near the core periphery, e.g., 07, N12, 09 and D4.

N12 Data Summary

Figure B-4 summarizes the N12 drilling and inspection regions and the major observations. Figure B-5 presents selected video images from the core and CSA regions.

Core Region Observations

Intact standing fuel rods are observed from the fuel assembly lower endfitting to slightly above the third spacer grid. Discoloration of the standing fuel rods is observed from below the third spacer grid to the rod/agglomerate interface. The discoloration appears to become more pronounced toward the agglomerate interface.

An agglomerate region of previously molten material surrounding fuel rod remnants is observed starting above the third spacer grid and extending to the top of the drill hole. The cladding is generally non-discernible from the surrounding previously molten material. There were a few metallic

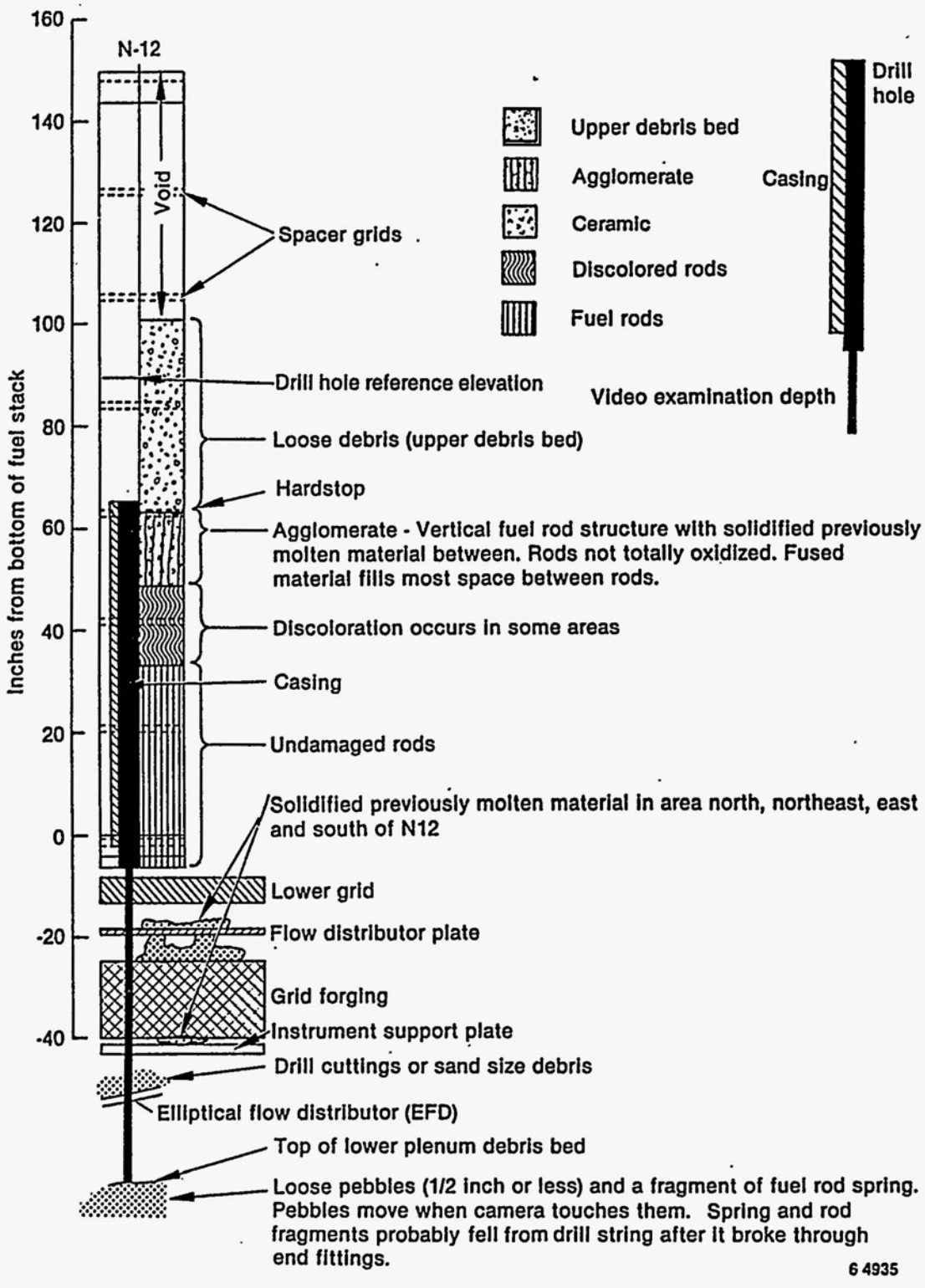

Figure B-4. N12 drill configuration and inspection summary.

Reactor vessel lower head loose debris with possible core-bore-cutter-generated debris below the elliptical flow distributor below core position N12 (86-417-4-5)

Looking northwest from core position N12 at bottom of elliptical flow distributor (86-417-6-1)

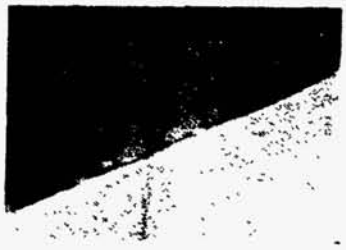

Looking northwest from core position N12 at top of elliptical flow distributor (86-417-5-12)

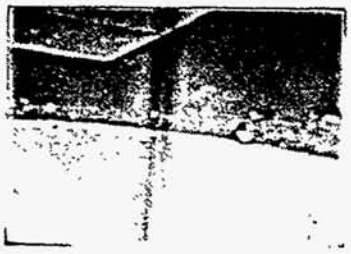

Looking northwest from core position N12 at space between the in-core instrument support plate and lower grid forging (86-417-5-11)

Looking southeast from core position N12 at previously molten core material between the in-core instrument support plate and lower grid forging (86-417-3-4)

Figure B-5. Enhanced video images about N12.

Previously molten material at top of lower grid forging below core position N12 (typical all around) (86-417-3-1)

Looking northwest from core position N12 at previously molten core material underneath the lower grid flow distributor below core position M13 (86-417-6-3)

Looking north from core position N12 at previously molten core material underneath the lower grid flow distributor below core position N13 with core-boring-produced fuel rod shard in foreground (86-417-5-9)

Looking northeast from core position N12 at previously molten core material underneath the lower grid flow distributor below core position O13 (86-417-6-4)

Possible previously molten core material at edge of core position N12 lower endfitting tie plate bottom (86-417-4-7)

Figure B-5. (continued)

Intact rod bundle between first and second spacer grids (approximately 16 in. above fuel rod bottom) at core position N12 (86-417-3-7)

Transition between intact rod bundle and agglomerated core material at bottom of third spacer grid (approximately 47 in. from fuel rod bottom) at core position N12 (86-417-3-9)

Transition between intact rod bundle and agglomerated core material at top of third spacer grid (approximately 49 in. from fuel rod bottom) at core position N12 (86-417-3-10)

Figure B-5. (continued)

remnants observed in the region of the cladding (adjacent to fuel pellets). The usefulness of the video images was limited above about 48 in. because of poor lighting and focus.

CSA and Lower Plenum Observations

The lower plenum debris appears as a bed of loose pebbles with diameters less than 0.5 in. The upper surface of the debris bed is estimated to be about 18 in. below the elliptical flow distributor. The debris particles appeared to "bounce" away as the camera was lowered and contacted the debris bed.

"Cascades" of solidified, previously molten material were observed in areas to the northeast of N12[B-1] just above and below the lower grid flow distributor plate. The material appears to be similar in texture to the molten ceramic material in the core region and looks like it froze in the CSA regions as it flowed downward, thus resembling a "wall" or "curtain."

On-line Drilling Data

The on-line (automatic mode) drilling data are shown in Figure B-6. Comparison to Figure B-4 shows that the automatic drill data for N12 started above the upper crust hard stop location. The abrupt change in drill resistance about midway between the third and fourth grid spacers likely indicates the lower agglomerate interface and may indicate a metallic rich crust.

Relationship to Other Drill Holes

The agglomerate structure with vertical fuel rod remnants surrounded by resolidified material is similar to that observed at other drill holes near the core periphery, e.g., O7, N5 and O9. The form and pattern of molten material in the CSA is similar to that observed in locations N5, O7 and O9. However, no significant amounts of previously molten material were observed on the upper surface of the elliptical flow distributor, suggesting that this location was not a direct flow path to the lower plenum.

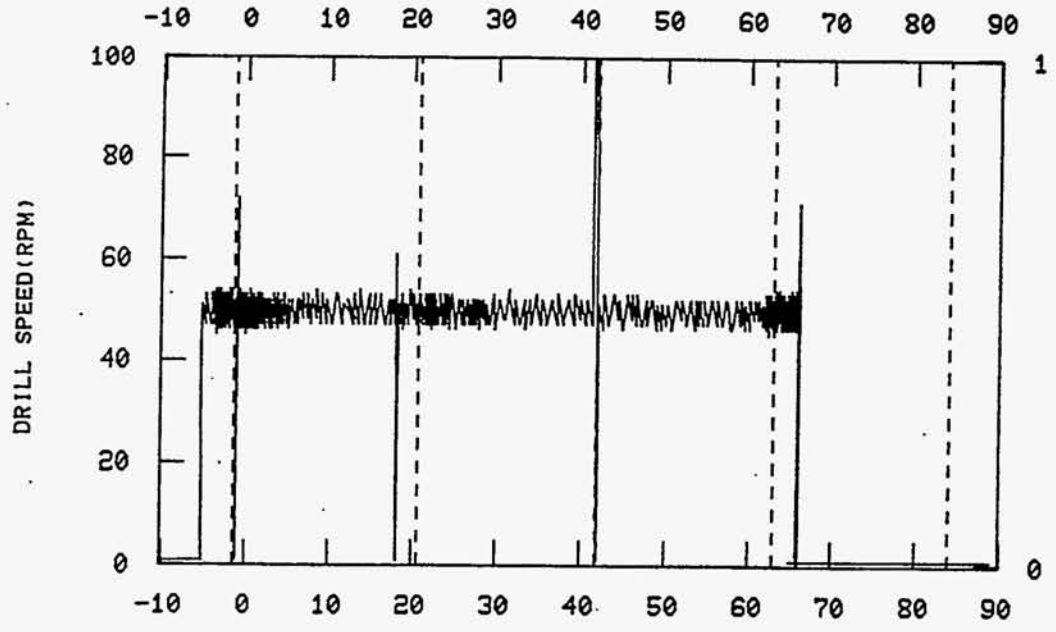

DISTANCE FROM BOTTOM OF FUEL STACK
BORE HOLE N12
DASHED LINES INDICATE MIDPOINT
OF SPACER GRIDS

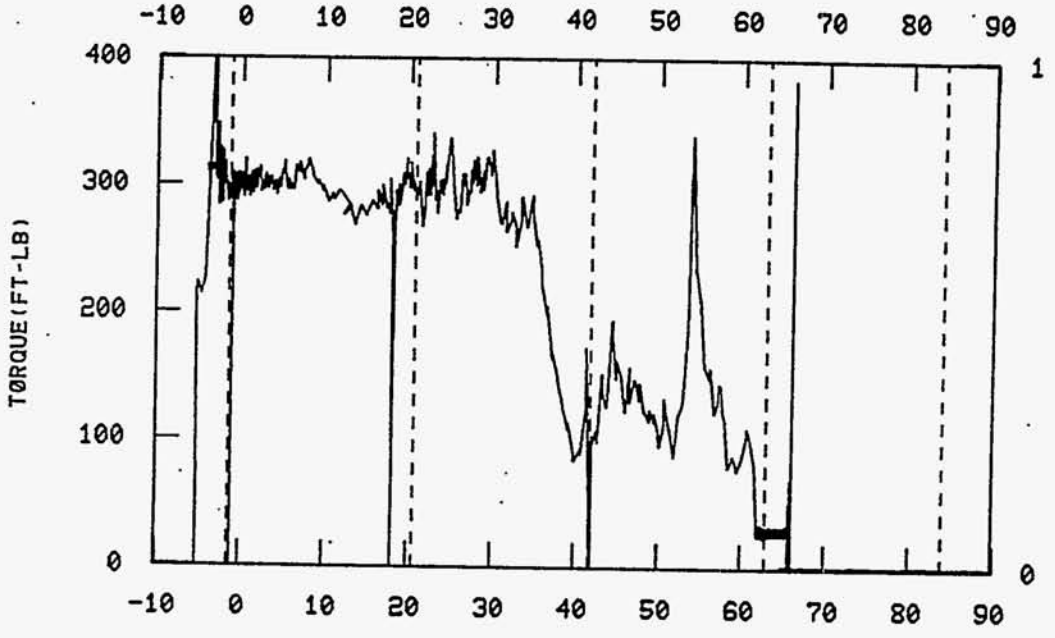

DISTANCE FROM BOTTOM OF FUEL STACK
BORE HOLE N12
DASHED LINES INDICATE MIDPOINT
OF SPACER GRIDS

Figure B-6. On-line drilling data for N12.

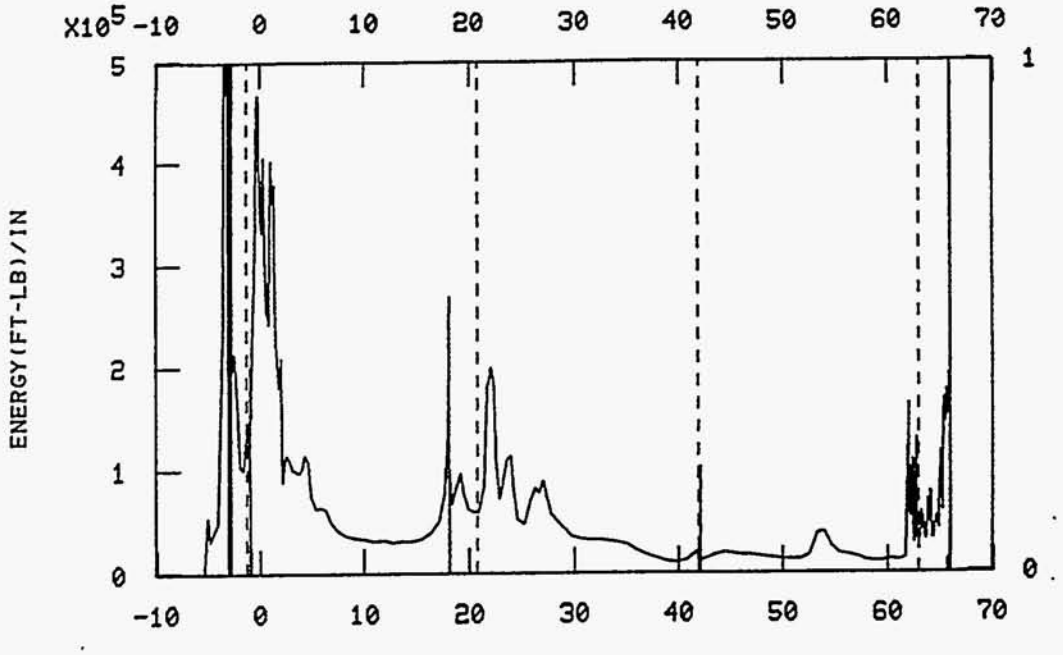

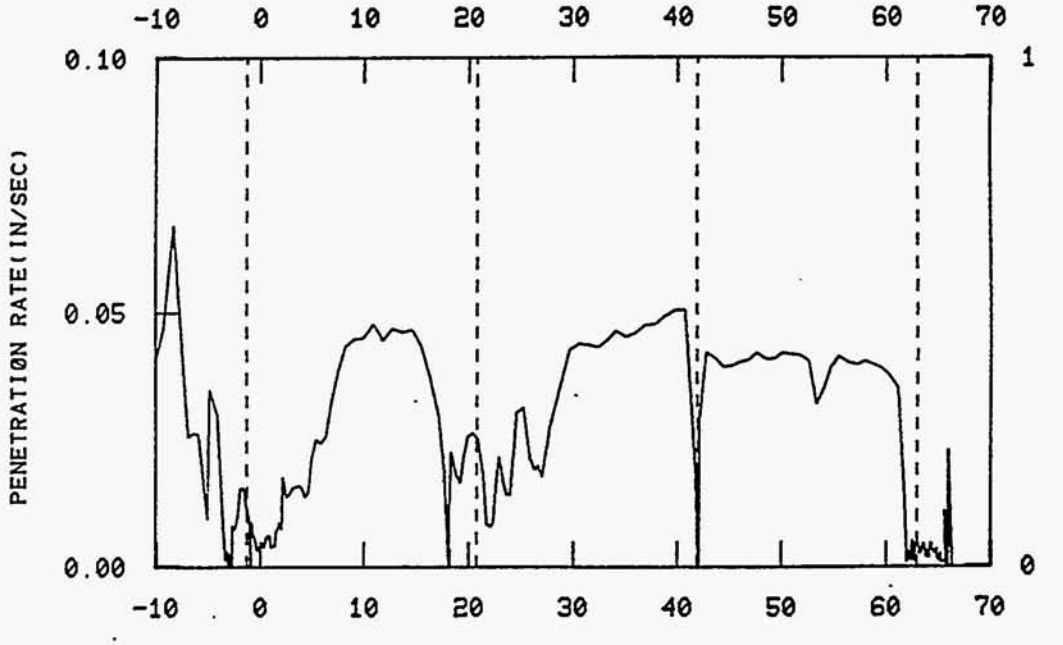

Figure B-6. (continued)

G8 Data Summary

Figure B-7 summarizes the G8 drilling and inspection regions and the major observations. Figure B-8 presents selected video images from the core and CSA regions.

Core Region Observations

Standing intact fuel rods are observed from the lower fuel assembly endfitting up to the second spacer grid and show some discoloration near the agglomerate interface. Also, some solidified, previously molten material is observed between rods in this region.

The agglomerate region (molten core material surrounding fuel rods and/or fuel rod remnants) was only slightly discernible and is limited to the very bottom and possibly the very top of the drill hole.

Most of the material above the standing fuel rods appear to be uniformly molten ceramic. This region appears to be over 40 in. thick and shows the following evidences of thorough melting:

- The only fuel pellet remnant is within an inch or so of the top of fuel rods.
- Most of the observed metal-like structure in the ceramic shows evidence of having been melted; i.e., vein-like structure as if the ceramic solidified and fractured, allowing the molten metal to fill the fractures. The only exceptions are (a) a metallic grid-like structure (possibly a spacer grid remnant) and (b) a large metallic segregation near the top of the hole.
- The bottom 12-14 in. of ceramic is free of metal segregations or veins.

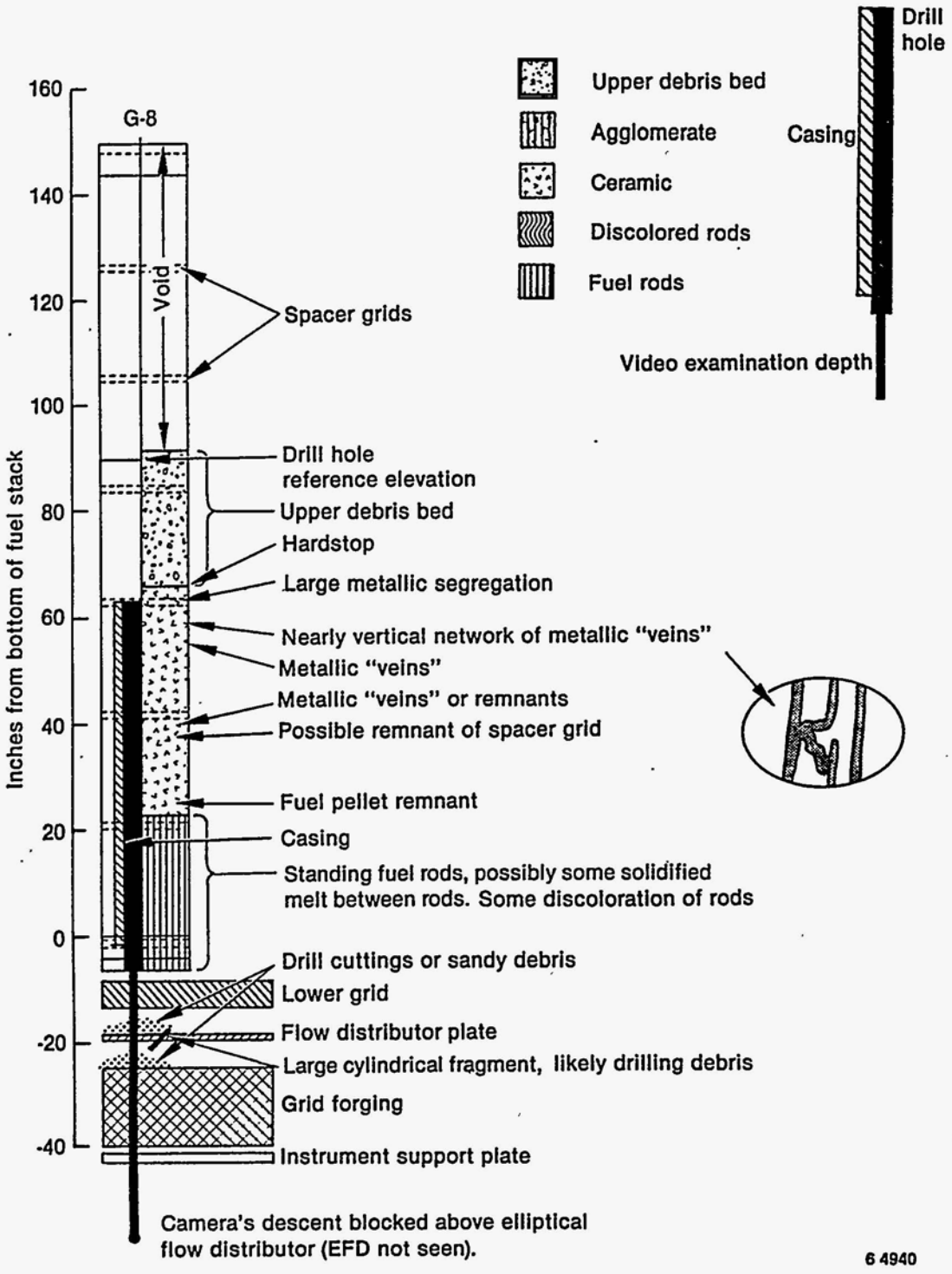

Figure B-7. G8 drill configuration and inspection summary.

View from below core position G8 of possible biological growth stringers hanging from in-core instrument support plate with core instrument guide tubes in background (86-443-2-5)

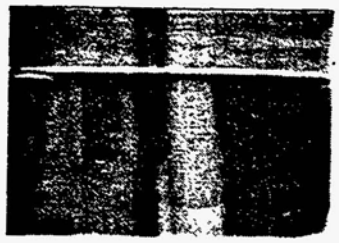

View from below core position G8 of a typical region below the lower grid with a core instrument guide tube and support post in the background (86-443-2-6)

Core position G8 fuel rod bundle at the top of the lowest spacer grid (approximately 4 in. above fuel rod bottom) with a guide tube coolant hole visible (86-443-2-7)

Foggy view of core position G8 fuel rod bundle between lowest spacer grids (approximately 16 in. above fuel rod bottom) with possible previously molten material behind fuel rods in foreground (86-443-2-8)

Core position G8 fuel rod bundle at second spacer grid (approximately 27 in. above fuel rod bottom) with some possible previously molten material toward the top (86-443-2-9)

Figure B-8. Enhanced video images about G8.

Top of small cavern in previously molten core material at core position G8 approximately 34 in. above fuel rod bottom
(86-443-2-11)

Coarse-surfaced, porous, lava-like agglomerated core material at core position G8 approximately 48 in. above fuel rod bottom with bore casing bottom at top (86-443-2-10)

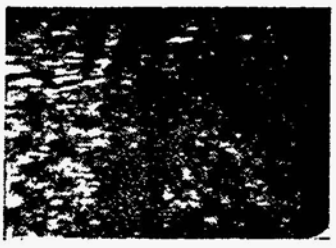

Possible view of finer-grained material in agglomerated core material at core position G8 approximately 53 in. above fuel rod bottom
(86-443-3-1)

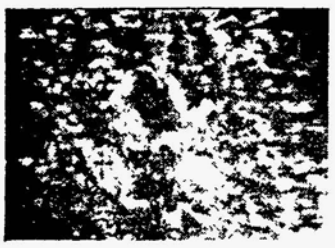

Possible view of metallic material in agglomerated core material at core position G8 approximately 58 in. above fuel rod bottom
(86-443-2-12)

Metallic form in agglomerated material at 70 in. above fuel rod bottom at core position G8
(86-484-10-4)

Figure B-8. (continued)

Closeup of metallic form (possible upper endfitting) in agglomerated material at approximately 70 in. above fuel rod bottom at core position G8
(86-484-10-5)

Closeup of top of metallic form (possible upper endfitting) in agglomerated material at approximately 70 in. above fuel rod bottom at core position G8
(86-484-10-6)

Figure B-8. (continued)

Core Support Assembly Observations

Fine material, probably drill cuttings, was observed on the flow distributor plate, the grid forging, and the instrument support plate. A cylindrical metallic plug was seen lodged in a hole in the grid distributor plate and is likely a piece of the lower grid or fuel assembly endfitting that was previously drilled and had fallen to the CSA region. Previously molten core material was not observed in the CSA at this drill location.

On-line Drilling Data

The core material in the G8 location was difficult to drill and resulted in frequent alignment difficulties. As a result, almost the entire core bore was drilled in the manual drilling mode. Thus, no data plots are presented.

Relationship to Other Drill Holes

The observations in G8 are generally consistent with the other central core locations (K9 and K6) and show the molten ceramic material to fill the region between the second and fourth spacer grids. The ceramic material at all three locations has metallic segregations. G8 showed the most "vein-like" metallic structures of any of the central drill locations. The metallic structures in K6 location were irregular, "glob-like" structures.

G12 Data Summary

Figure B-9 summarizes the G12 drilling and inspection regions and the major observations. Figure B-10 presents selected video images from the core and CSA regions.

Core Region Observations

Standing intact fuel rods are observed from the lower fuel assembly endfitting to the third spacer grid. The rods appeared discolored next to

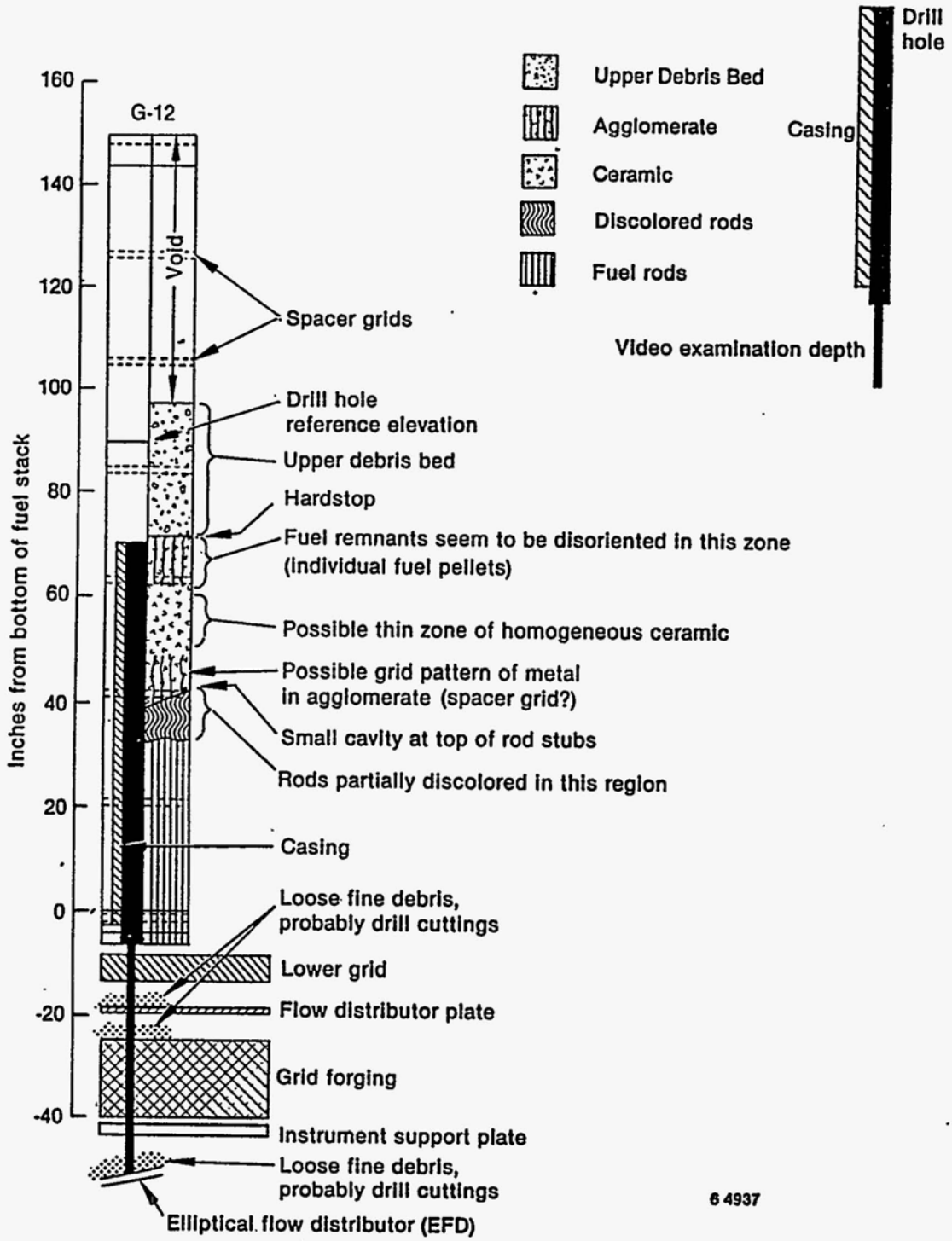

Figure B-9. G12 drill configuration and inspection summary.

Possible top of reactor vessel lower head loose debris below core position G12 with probable core boring debris deposit
(86-443-3-3)

Looking west from below core position G12 at core instrument guide tube intersection with loose debris at top of elliptical flow distributor
(86-443-3-4)

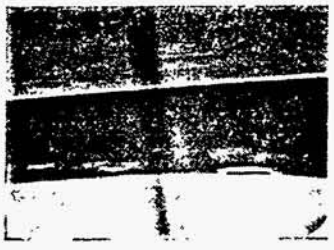

Typical view from below core position G12 of space between in-core instrument support plate and lower grid forging
(86-443-3-5)

Typical view from below core position G12 of probable core boring debris on top of lower grid flow distributor
(86-443-3-6)

Typical view of core position G12 lower endfitting tie plate with guide tube fastener (hex nut) in background at left
(86-443-3-7)

Core position G12 fuel rod bundle between lower spacer grids with probable core-boring-produced fuel rod cladding shard in lower foreground
(86-443-3-8)

Figure B-10. Enhanced video images about G12.

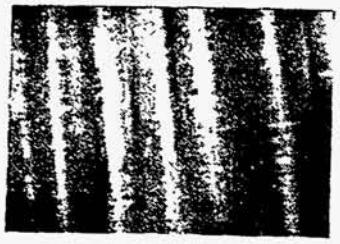

Core position G12 fuel rod bundle approximately 34 in. above fuel rod bottom
(86-443-3-10)

View of rod stub tops at core position G12 approximately 42 in. above fuel rod bottom
(86-443-4-3)

View of rod stub tops at floor of small cavity approximately 45 in. above core position G12 fuel rod bottom
(86-443-4-7)

View of agglomerated core material at core position G12 approximately 45 in. above fuel rod bottom with possible small cavity visible at lower left
(86-443-3-12)

Coarse, porous previously molten core material at core position G12 approximately 48 in. above fuel rod bottom
(86-443-3-11)

Figure B-10. (continued)

the agglomerate/rod interface. A small cavity was observed at the rod/agglomerate interface and may have been caused by the drilling operation.

In the lower agglomerate region, standing rod remnants were observed surrounded by previously molten core material. In the upper region, fuel pellets were also discernible, although they did not show a vertical structure but have a more random orientation. Near the lower regions of the agglomerate, a grid-like metallic pattern was observed.

The video data are inadequate to clearly discern whether or not a molten ceramic region in the middle of the agglomerate region is present.

Core Support Assembly Observations

Loose, fine debris (most likely drill cuttings) was observed on the flow distributor plate, grid forging, and elliptical flow distributor. No solidified previously molten material was observed in the CSA area.

On-line Drilling Data

The on-line (automatic mode) drilling data are shown in Figure B-11. The automatic drilling started at about the rod/agglomerate interface, just above the third spacer grid. As seen in the figure, a significant increase in drilling resistance was encountered for 2-3 in. about mid-way between the second and third spacer grids. However, the change also is coincident with drill start-up; therefore, it is difficult to conclude that the change in drill data is related to a localized change in material structure.

Relationship to Other Drill Holes

This drill location is about mid-core radius, and the thickness of the agglomerate/ceramic region is greater (25-30 in.) than observed at the peripheral locations (15-20 in.). The disoriented nature of fuel pellets in the upper part of the agglomerate in G12 was similar to that observed at D8.

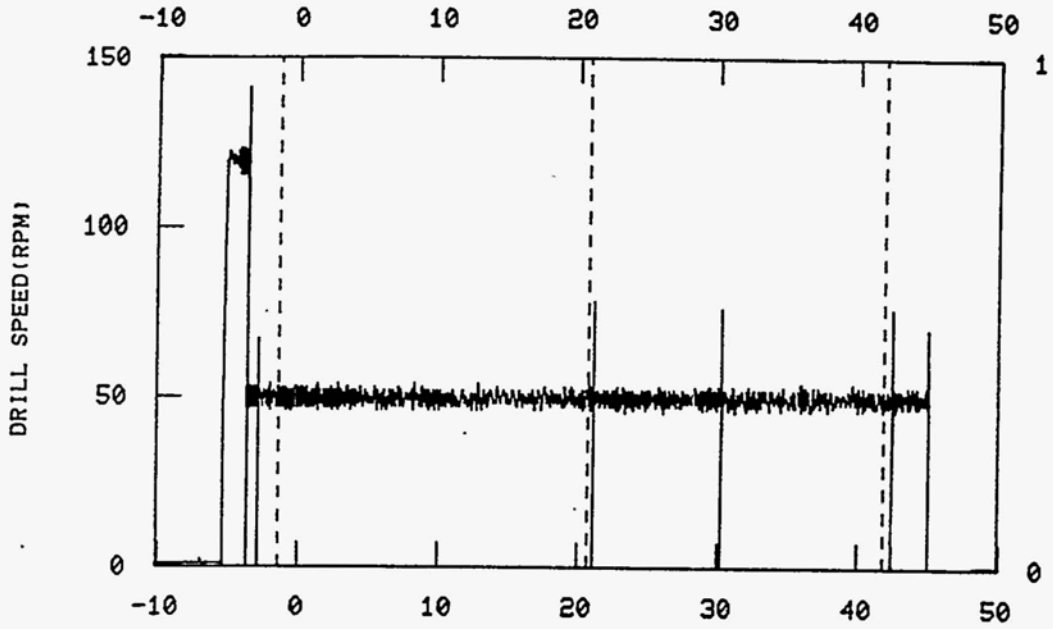

DISTANCE FROM BOTTOM OF FUEL STACK
BORE HOLE G12
DASHED LINES INDICATE MIDPOINT
OF SPACER GRIDS

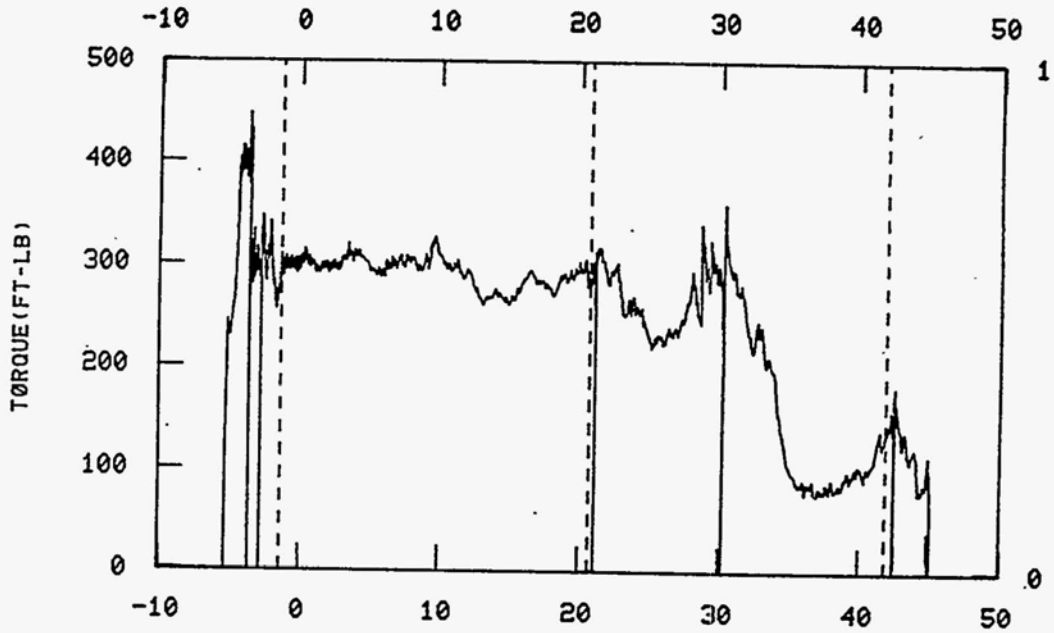

DISTANCE FROM BOTTOM OF FUEL STACK
BORE HOLE G12
DASHED LINES INDICATE MIDPOINT
OF SPACER GRIDS

Figure B-11. On-line drilling data for G12.

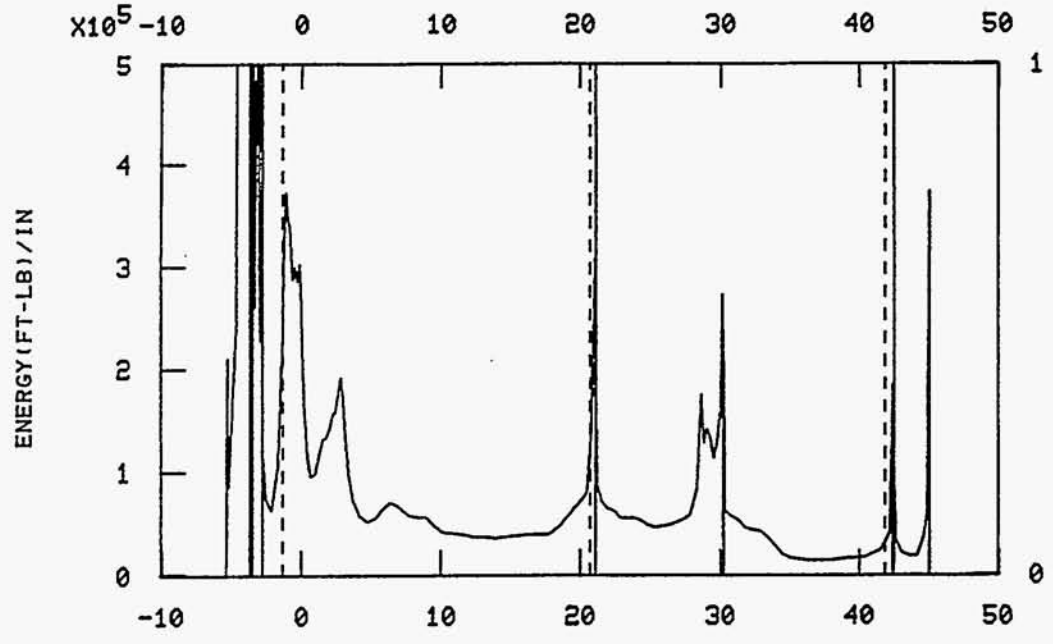

DISTANCE FROM BOTTOM OF FUEL STACK
BORE HOLE G12
DASHED LINES INDICATE MIDPOINT
OF SPACER GRIDS

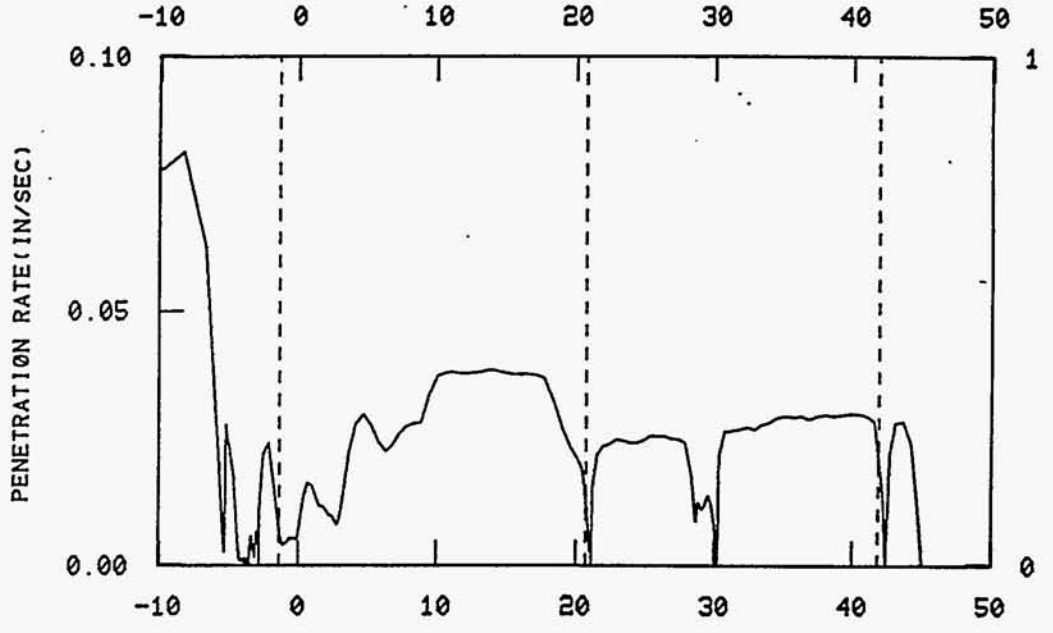

DISTANCE FROM BOTTOM OF FUEL STACK
BORE HOLE G12
DASHED LINES INDICATE MIDPOINT
OF SPACER GRIDS

Figure B-11. (continued)

K9 Data Summary

Figure B-12 summarizes the K9 drilling and inspection regions and the major observations. Figure B-13 presents selected video images from the core and CSA regions.

Core Region Observations

Standing intact fuel rods are observed from the lower fuel assembly endfitting to the second spacer grid. Previously molten material is observed between rods near the first spacer grid and is also observed in the spaces around the lower endfitting.

The lower agglomerate region is relatively thin (approximately 4-6 in.), with observable standing fuel rod remnants surrounded by previously molten core material.

The molten ceramic zone is approximately 50 in. thick and appears for the most part homogeneous. Metal segregations and vein-like structures that appear to be fully or partially previously molten were observed in the lower 20 in. of the ceramic mass. A large metallic-like structure that appeared partially or perhaps fully molten was observed near the top several inches of the drill hole.

Core Support Assembly and Lower Plenum Observations

Fine, loose particles, probably drill cuttings, were observed on the flow distributor plate. No significant quantities of previously molten core material were observed.

The lower plenum debris appears as a bed of loose pebbles with diameters less than 0.5 in., much the same as observed in N12. Based on the inspection data (obtained after the lower plenum core bore was taken), the upper surface of the debris bed is estimated to be about 8 in. below the elliptical flow distributor. Pieces of fuel rods were observed on the surface of the debris and most likely fell during the drilling operation.

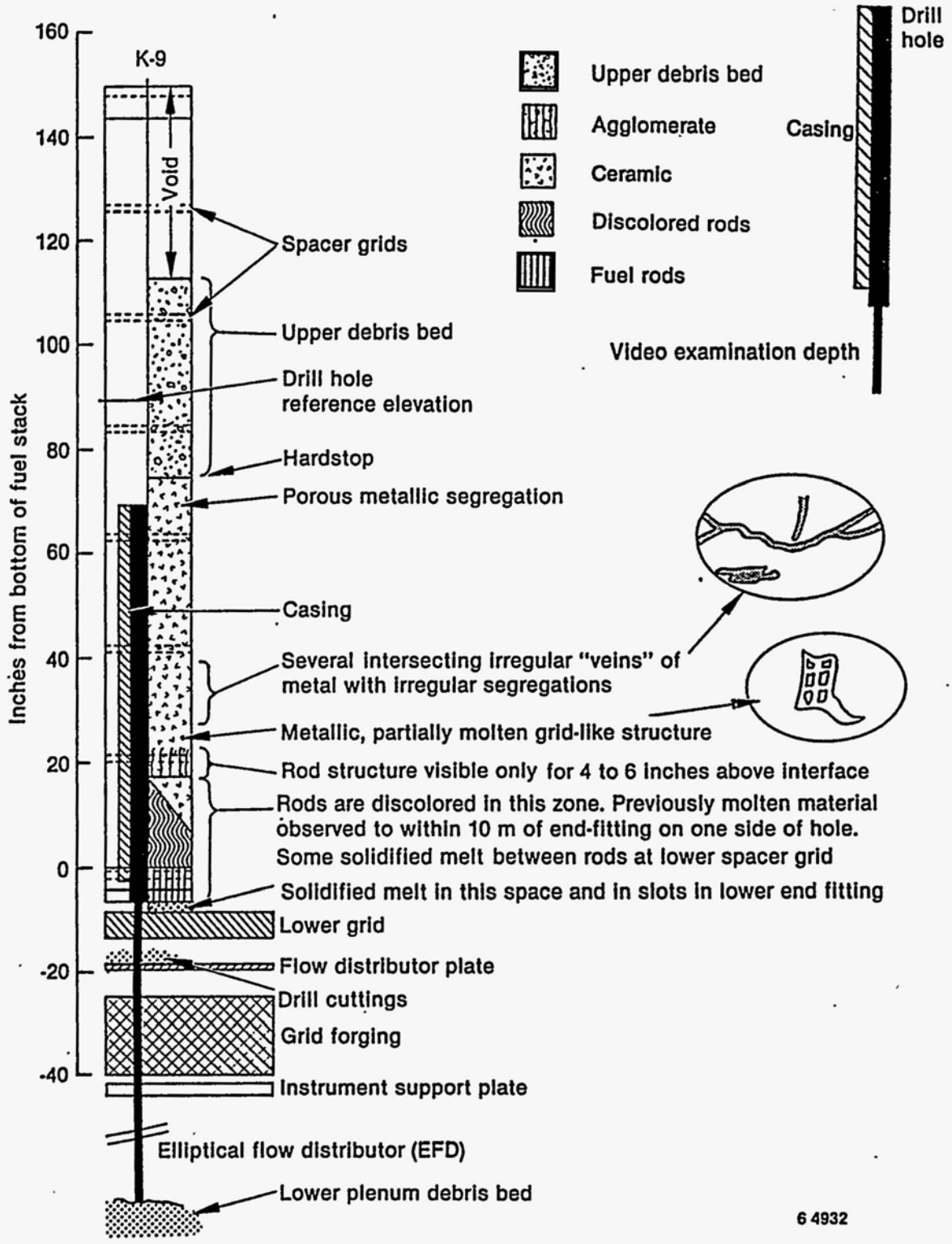

Figure B-12. K9 drill configuration and inspection summary.

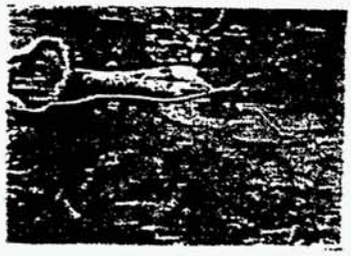

Reactor vessel lower head loose debris below the elliptical flow distributor below core position K9 (86-417-2-4)

Possible previously molten core material at core position K9 fuel assembly lower endfitting corner (86-417-2-8)

Possible previously molten core material behind fuel rods just above core position K9 fuel assembly lower spacer grid (approximately 4 in. above core bottom (86-417-2-9)

Individual rod decomposition approximately 18 in. above core bottom at core position K9 (86-417-2-10)

Possible cutter tool abraided, crystalline-appearing rod surface approximately 20 in. above core bottom at core position K9 (86-417-6-6)

Figure B-13. Enhanced video images about K9.

Possible spacer grid remnant at approximately 26 in. above core bottom at core position K9
(86-417-6-7)

Possible metallic form in agglomerated material at approximately 30 in. above core bottom at core position K9
(86-417-6-9)

Figure B-13. (continued)

On-line Drilling Data

The on-line (automatic mode) drilling data are shown in Figure B-14. The automatic drilling started at about 70 in. from the rod bottom near the top of the molten ceramic region. There appears to be some variability in the material composition, as inferred from the changes in the drilling parameters between the second/third and the third/fourth spacer grids. The localized changes in drill resistance are consistent with observed metallic-like structures interlaced with the ceramic material.

Relationship to Other Drill Holes

The observations in the core region at K9 indicate that the center regions of the core experienced the most severe temperatures and degradation. This is consistent with the observations at the other drill locations near the core center (K6 and G8). The agglomerate/rod interface at K9 was at the lowest axial elevation of any of the core bore locations.

The region of discolored lower fuel rod stubs extends farther downward than in any other drill location, and the quantity of solidified previously molten material between the lower rod stubs is also greater than observed at any other drill location, except perhaps K6. The lower rod stub discoloration suggests that the reactor vessel water level was below the lower fuel assembly endfitting during the initial core heatup. K9 is the only location in which solidified melt was observed in and just below the lower endfitting.

D8 Data Summary

Figure B-15 summarizes the D8 drilling and inspection regions and major observations. Figure B-16 presents selected video images from the core and CSA regions.

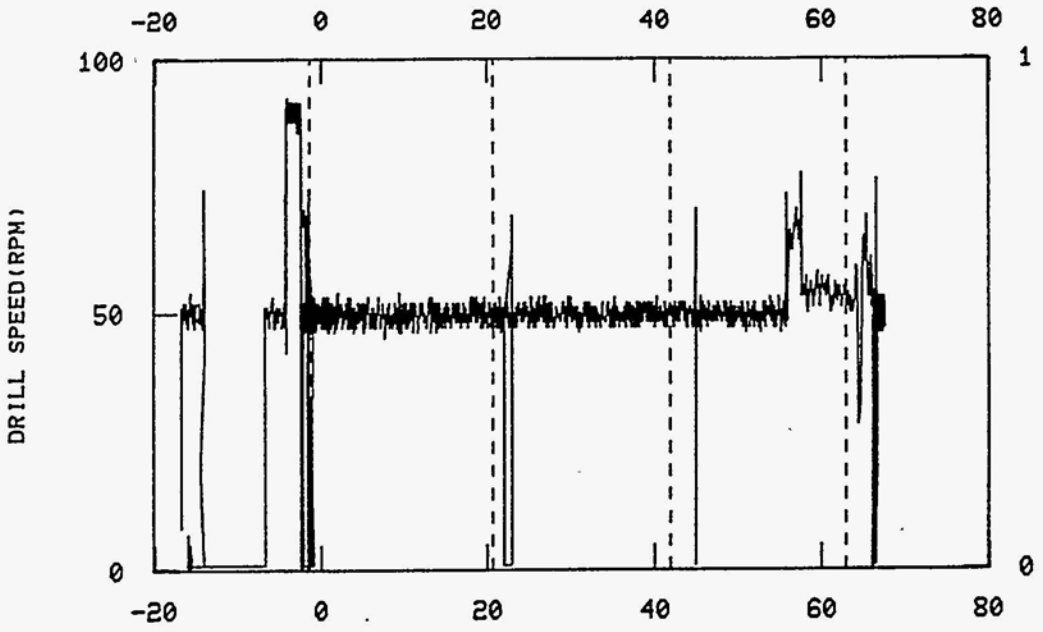

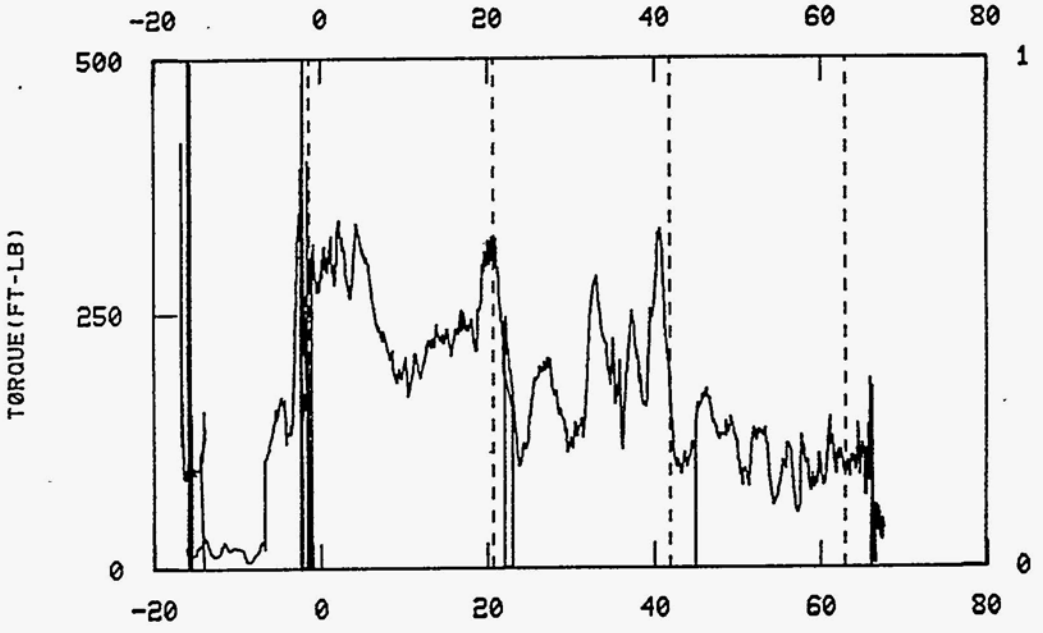

Figure B-14. On-line drilling data for K9.

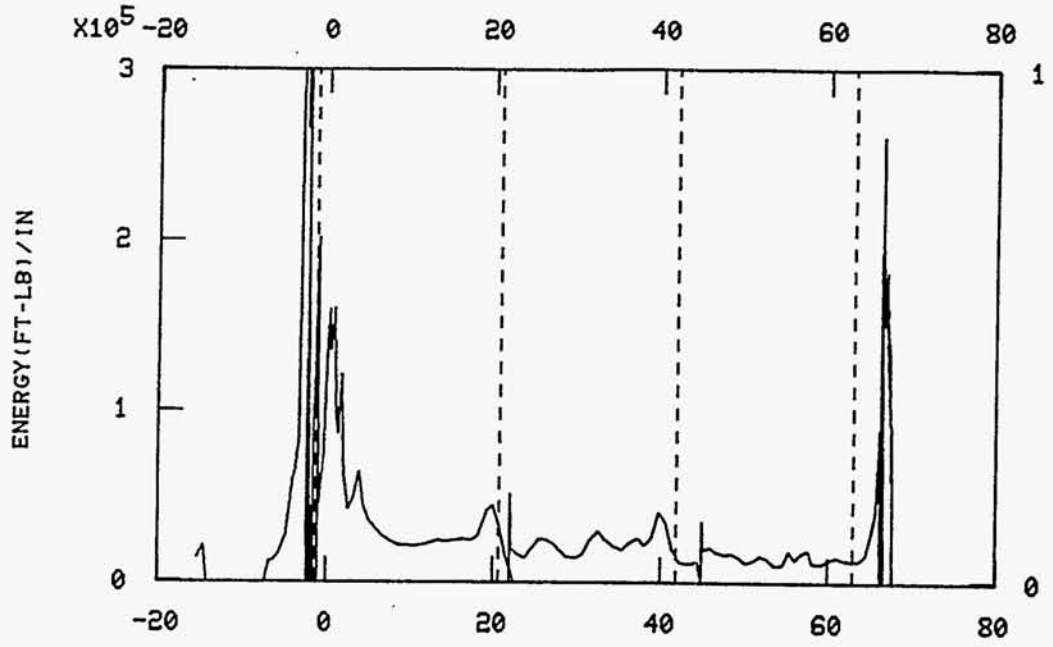

DISTANCE FROM BOTTOM OF FUEL STACK
BORE HOLE K9
DASHED LINES INDICATE MIDPOINT
OF SPACER GRIDS

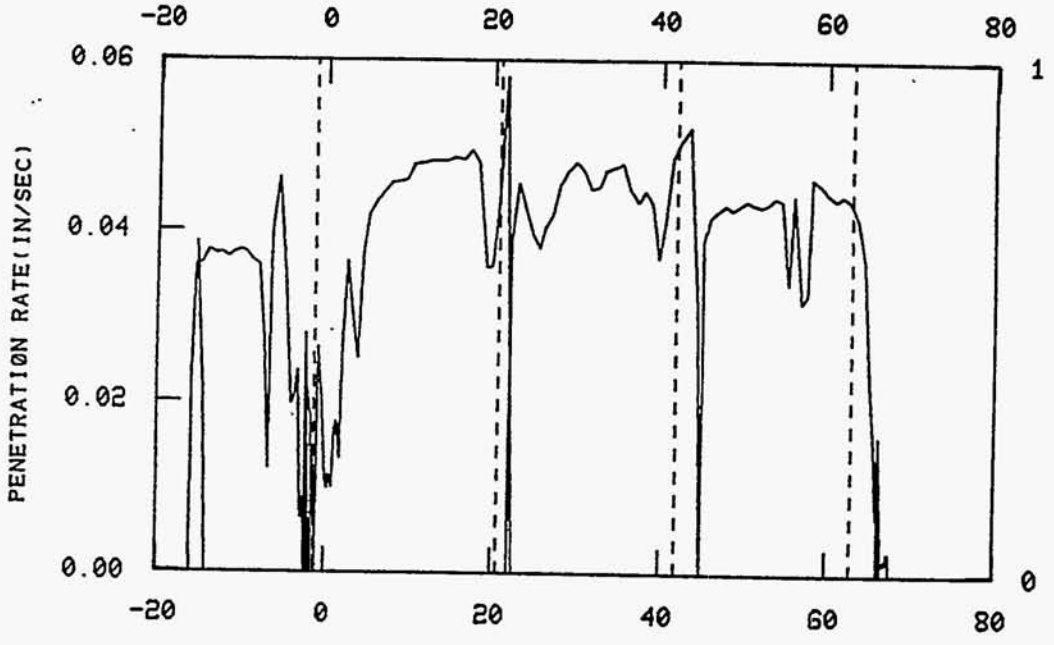

DISTANCE FROM BOTTOM OF FUEL STACK
BORE HOLE K9
DASHED LINES INDICATE MIDPOINT
OF SPACER GRIDS

Figure B-14. (continued)

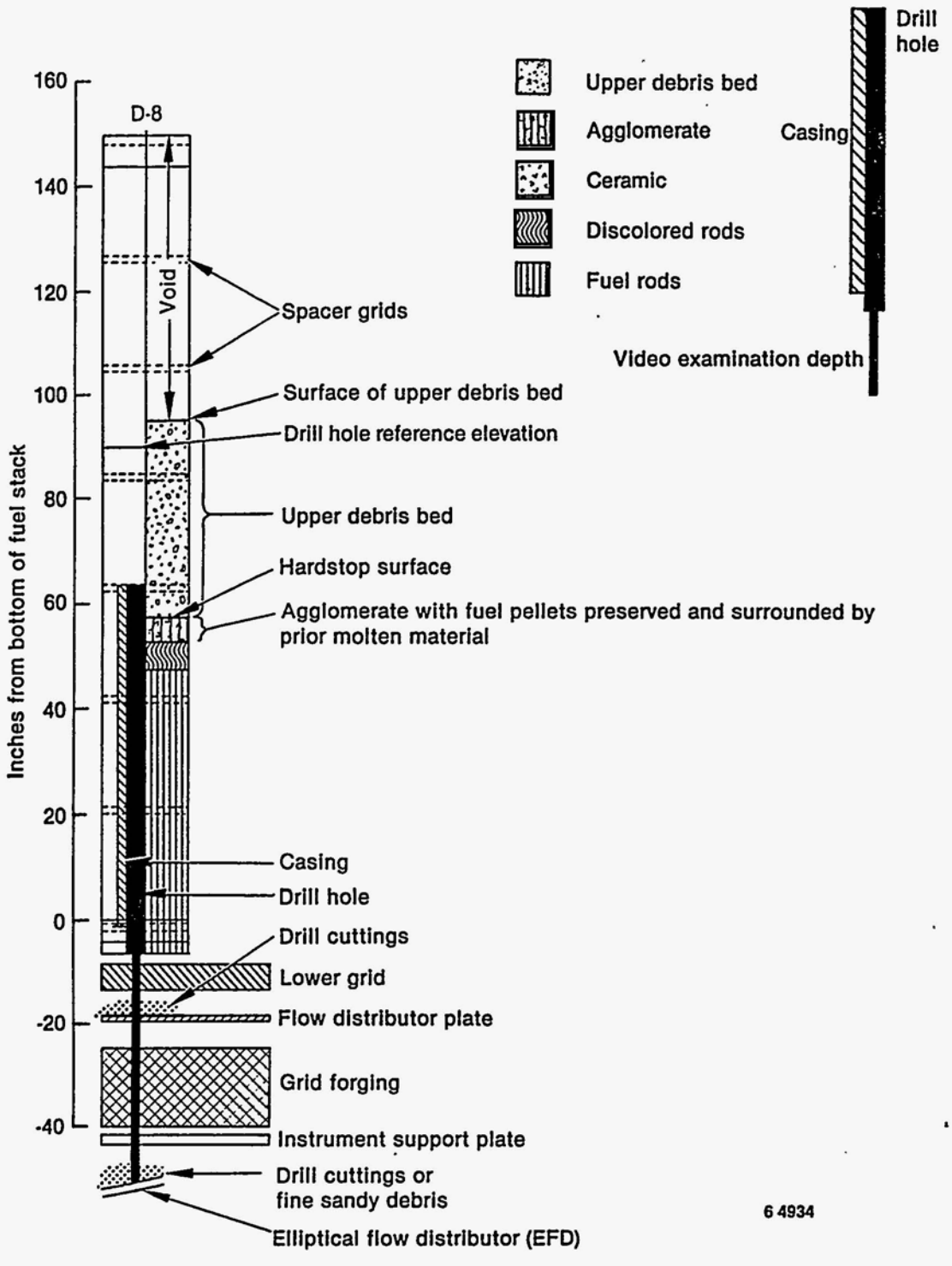

Figure B-15. D8 drill configuration and inspection summary.

View of probable core-boring-generated loose debris on elliptical flow distributor below core position D8 (86-443-4-8)

View of typical condition of elliptical flow distributor and in-core instrument guide tubes from below core position D8 (86-443-4-10)

Core position D8 rod bundle intersection with second spacer grid approximately 26 in. above the fuel rod bottom (86-443-4-11)

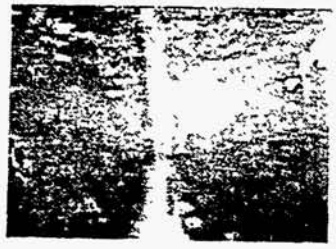

Agglomerated core material approximately 49 in. above the fuel rod bottom at core position D8 (86-443-4-12)

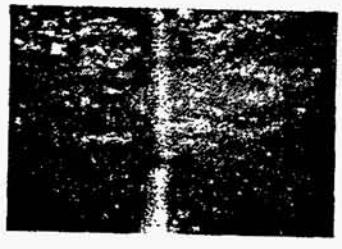

View of the top of small cavity in agglomerated core material approximately 53 in. above the fuel rod bottom at core position D8 (86-443-5-3)

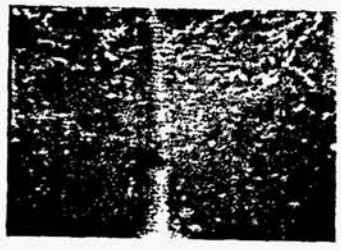

Agglomerated core material approximately 56 in. above the fuel rod bottom at core position D8 (86-443-5-1)

Figure B-16. Enhanced video images about D8.

Core Region Observations

Standing intact fuel rods are observed from the lower fuel assembly endfitting to above the third spacer grid. The upper 6 in. of rods (next to the rod/agglomerate interface) appeared discolored.

The agglomerate region of fuel pellets and/or rods surrounded by previously molten material is only about 5-6 in. thick. The fuel pellets in the agglomerate region are well defined, and in some cases the vertical structure of the fuel pellets is discernible. At about the axial midplane of the agglomerate region, several different metallic-like structures were observed, having various shapes ranging from small, irregular segregations to "vein-like" structures oriented in different directions.

Core Support Assembly Observations

The CSA was inspected down to the top of the elliptical flow distributor. Fine sandy material, probably drill cuttings, was observed on the flow distributor plate and the inside surface of the elliptical flow distributor. No previously molten material were observed in the regions inspected.

Relationship to Other Drill Holes

Metallic segregations were common in this hole and were also observed in the central core locations (G8, K9, K6) and the peripheral location (O9). These fuel assemblies lie in a general east-west band across the core.

No molten ceramic region was observed in D8, consistent with the other peripheral drill location observations. This drill location had the smallest agglomerate thickness of any drill location.

On-line Drilling Data

The automatic mode drilling data are shown in Figure B-17. Automatic drilling started at about 60 in. from the rod bottom, near the top of the agglomerate region. There appear to be significant increases in drill resistance at about 56-58 in. and again at 48-50 in. above the bottom of the fuel rod. These distances are generally consistent with the upper and lower surfaces of the agglomerate.

K6 Data Summary

Figure B-18 summarizes the K6 drilling and inspection regions and major observations. Figure B-19 presents selected video images from the core and CSA regions.

Core Region Observations

Standing intact fuel rods are observed from the lower fuel assembly endfitting to above the second spacer grid. Discoloration of the cladding occurs in the upper regions of the fuel rod stubs below the agglomerate interface. Previously molten material is observed between the lower rod stubs and appears to be present in the lower fuel assembly endfitting. The interface between the lower rod stubs and the agglomerate is not well defined but appears to cover an axial region approximately 5-10 in. below the second spacer grid to approximately 5-10 in. above the second spacer grid, as depicted in Figure B-18.

The molten ceramic region extends from about midway between the second and third spacer grids to the fourth spacer grid (approximately 30-35 in.). Rounded, irregular metallic segregations occur in the upper regions of the molten ceramic.

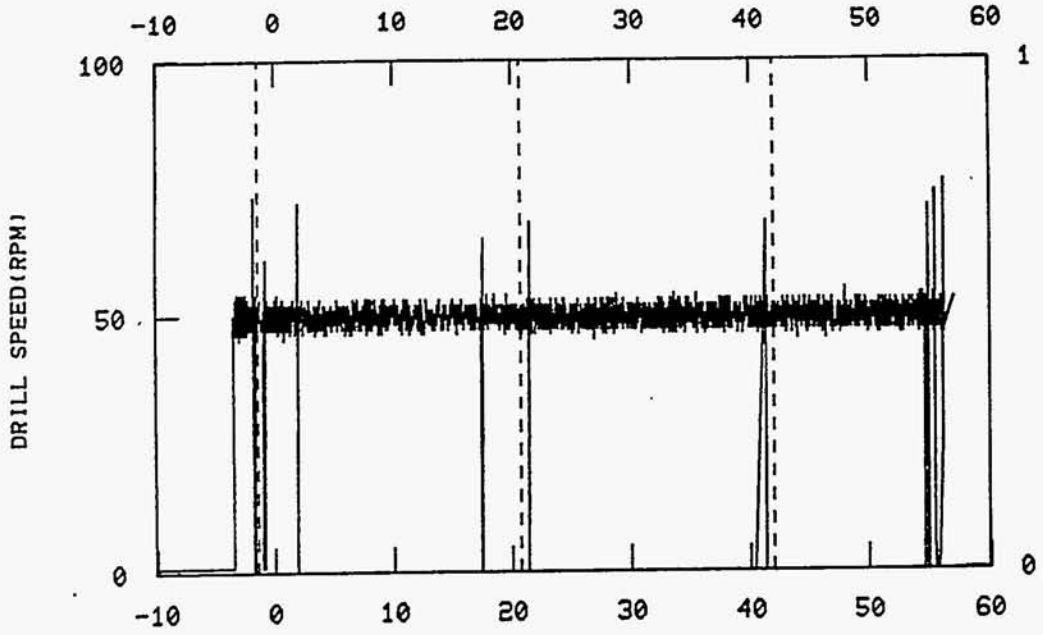

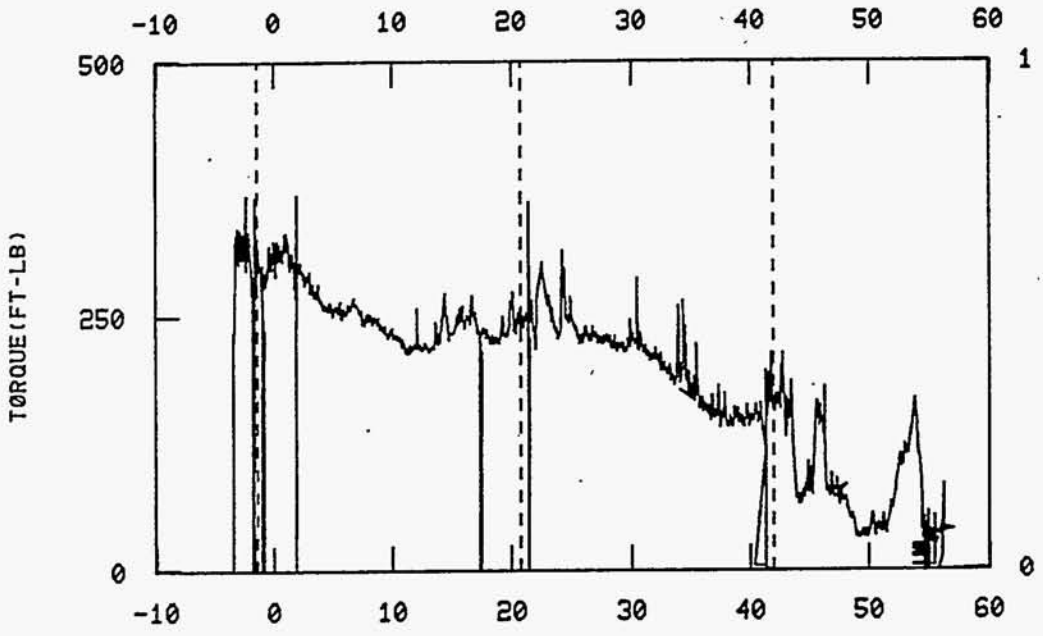

Figure B-17. On-line drilling data for D8.

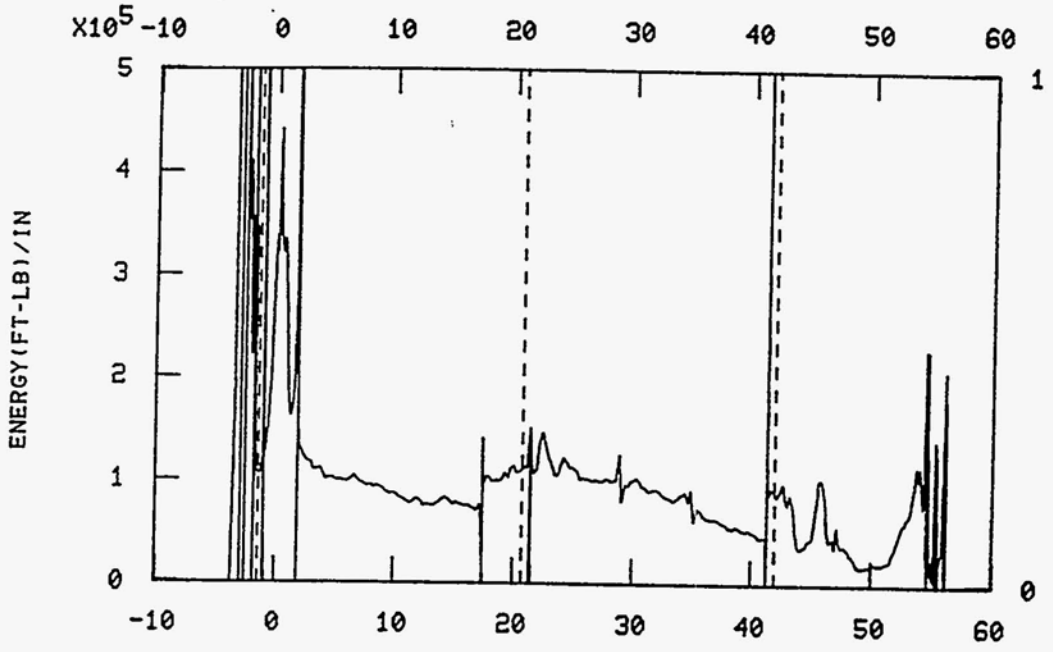

DISTANCE FROM BOTTOM OF FUEL STACK
BORE HOLE D8
DASHED LINES INDICATE MIDPOINT
OF SPACER GRIDS

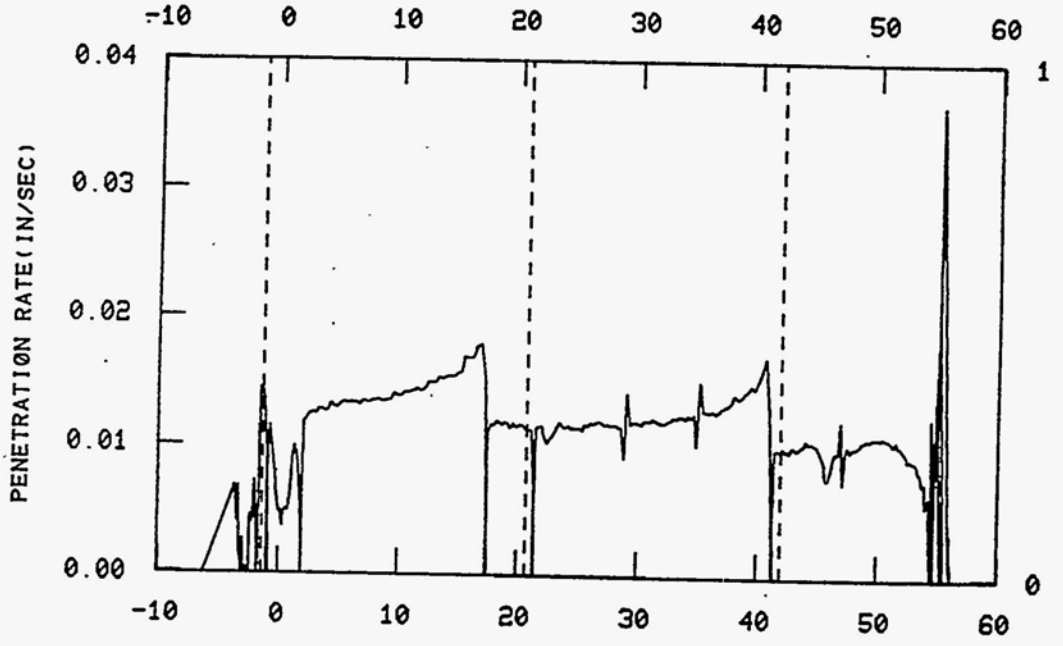

DISTANCE FROM BOTTOM OF FUEL STACK
BORE HOLE D8
DASHED LINES INDICATE MIDPOINT
OF SPACER GRIDS

Figure B-17. (continued)

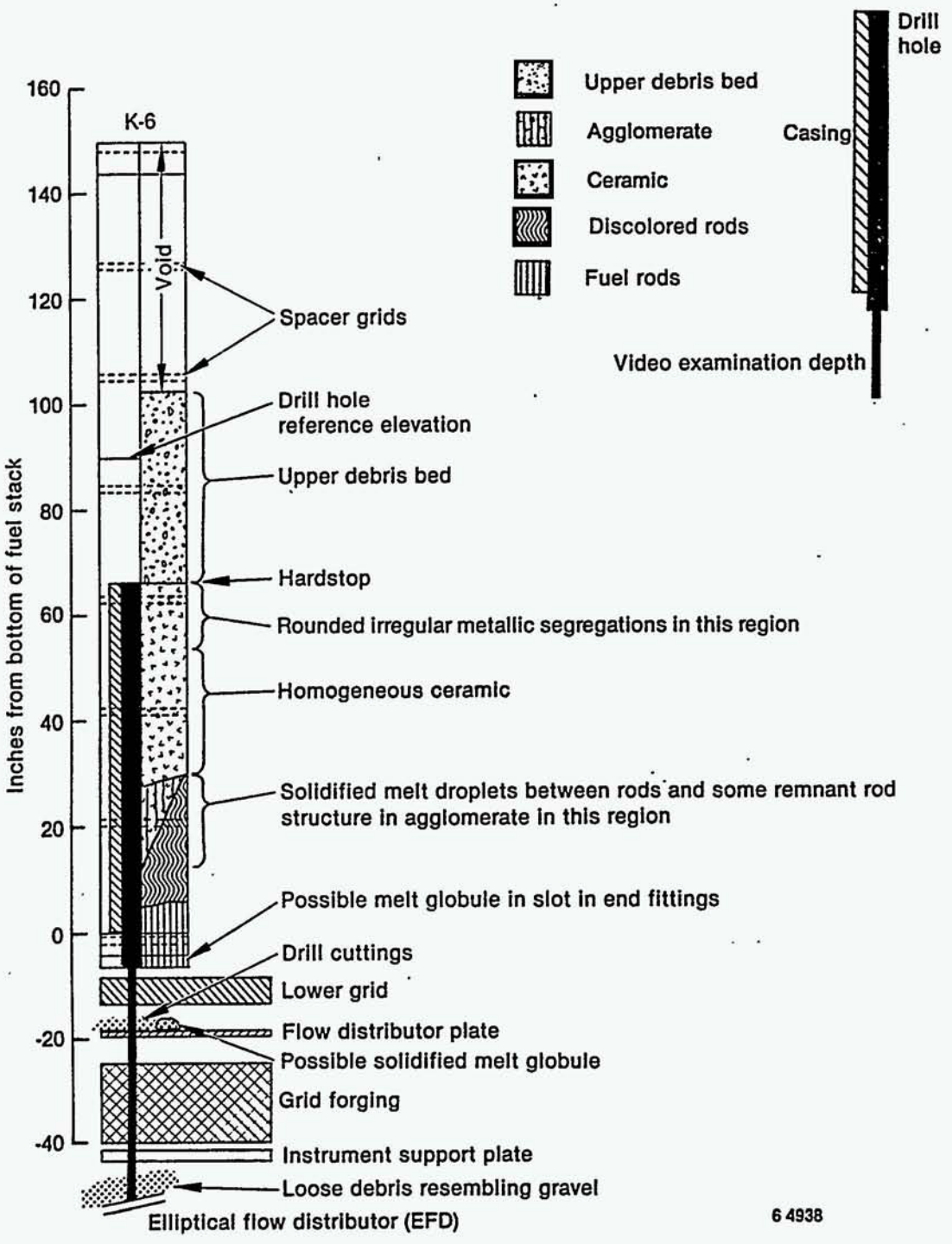

Figure B-18. K6 drill configuration and inspection summary.

View of reactor vessel lower head loose debris top surface below core position K6 with possible overlay of core-boring-generated debris (86-484-7-2)

Possible nugget of previously molten core material on lower lip of lower grid flow distributor hole below core position K6 (86-484-7-5)

Possible previously molten material and horizontal surface ablation on core position K6 lower endfitting (86-484-10-7)

Possible previously molten material behind fuel rods approximately 27 in. above core position K6 fuel rod bottom (86-484-7-6)

Agglomerated core material and fuel rod remnants approximately 60 in. above core position K6 fuel rod bottom (86-484-7-9)

Figure B-19. Enhanced video images about K6.

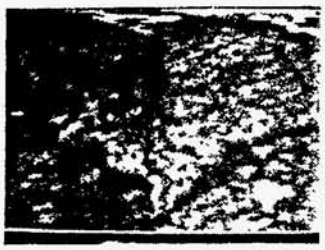

Closeup of previously molten core material with bore casing lower edge at top approximately 48 in. above core position K6 fuel rod bottom
(86-484-7-7)

Possible metallic nuggets in agglomerated core material approximately 60 in. above core position K6 fuel rod bottom
(86-484-7-11)

Figure B-19. (continued)

Core Support Assembly Observations

Loose, gravel-type debris, most likely from the drilling, was observed on the elliptical flow distributor. Similar drill cuttings and a small piece of previously molten material was observed on the flow distributor plate; however, large quantities of previously molten material were not observed in the regions inspected.

Relationship to Other Drill Holes

The observations from locations K6 and K9 (central core region) are similar relative to the material structures in the agglomerate and molten ceramic regions and the oxidation of the lower intact rod stubs. The relocated core materials penetrated to approximately the second spacer grid (approximately 20 in. above the bottom of the fuel rods) in both these locations. The discoloration of the lower fuel rod stubs indicates that the reactor vessel coolant level was below the fuel rods during the initial core heatup.

On-line Drilling Data

The automatic mode data are shown in Figure B-20. Automatic drilling started at about 60 in. from the rod bottom, several inches into the agglomerate region. The data show significant localized variations in the drilling resistance between the second and third spacer grids. This is consistent with the transition region between the agglomerate and intact rods.

D4 Data Summary

Figure B-21 summarizes the D4 drilling and inspection regions and major observations. Figure B-22 presents selected video images from the core and CSA regions.

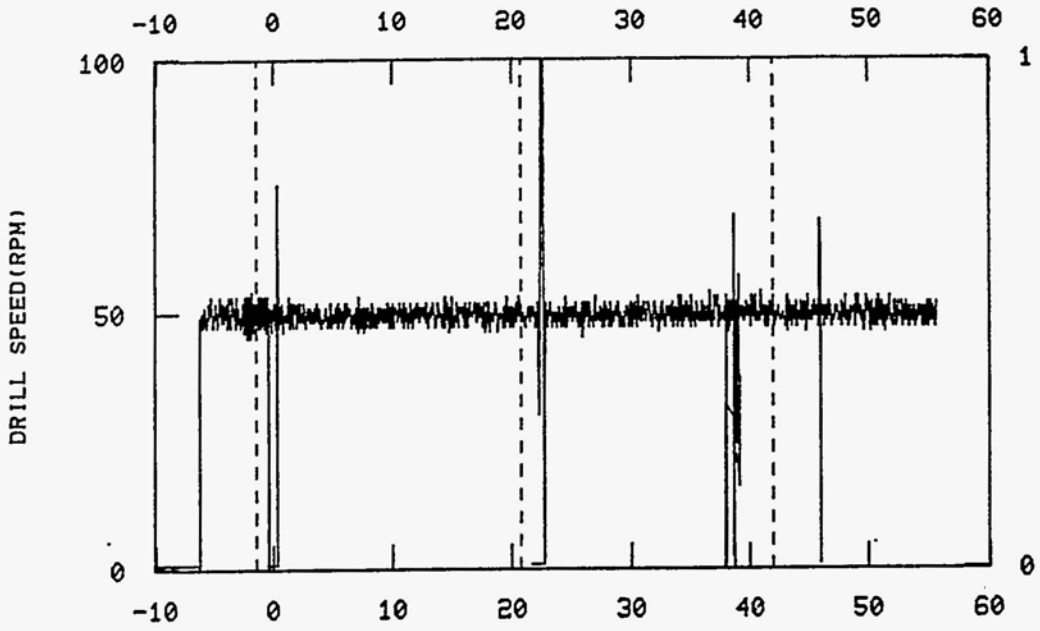

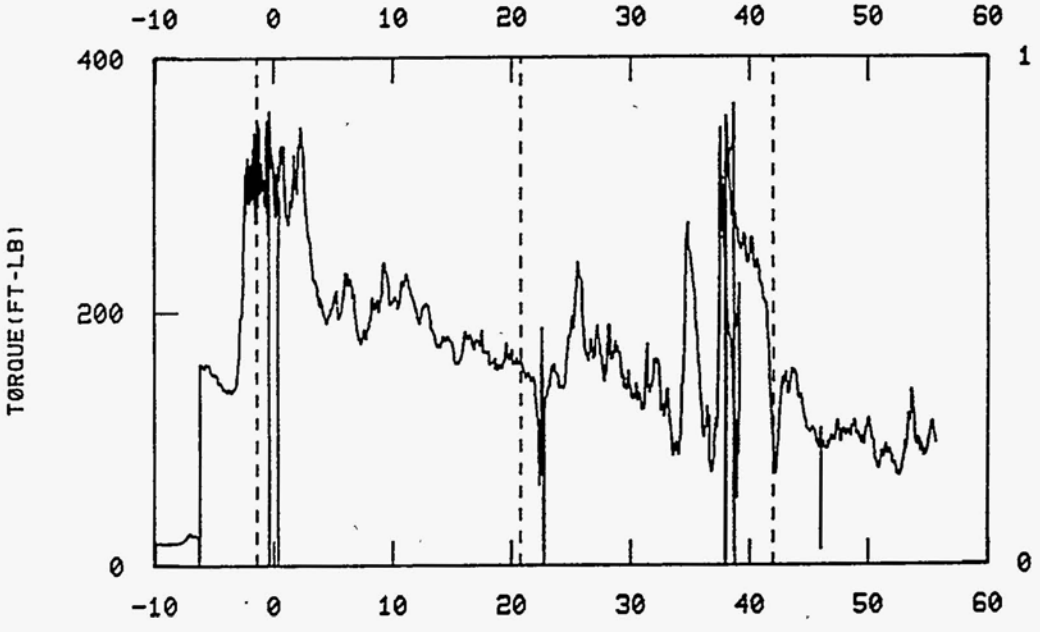

Figure B-20. On-line drilling data for K6.

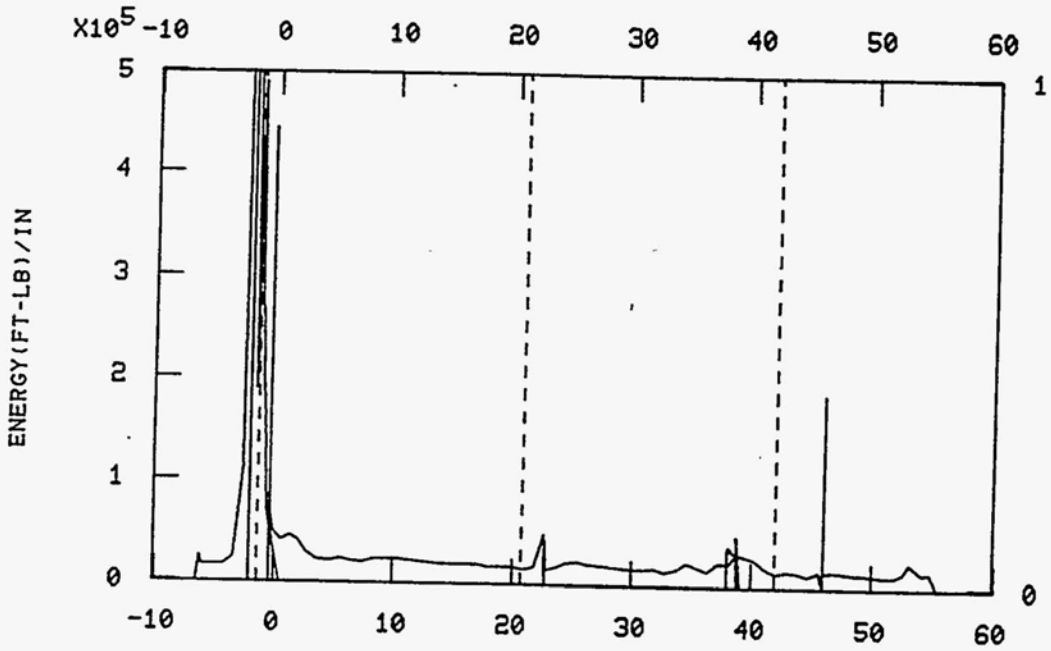

DISTANCE FROM BOTTOM OF FUEL STACK
BORE HOLE K6
DASHED LINES INDICATE MIDPOINT
OF SPACER GRIDS

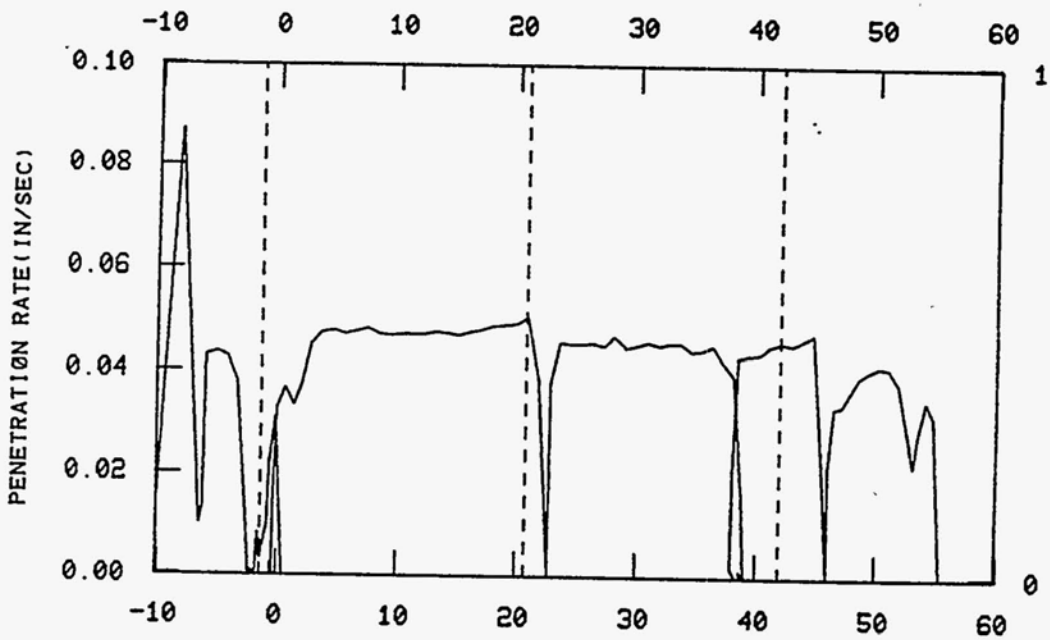

DISTANCE FROM BOTTOM OF FUEL STACK
BORE HOLE K6
DASHED LINES INDICATE MIDPOINT
OF SPACER GRIDS

Figure B-20. (continued)

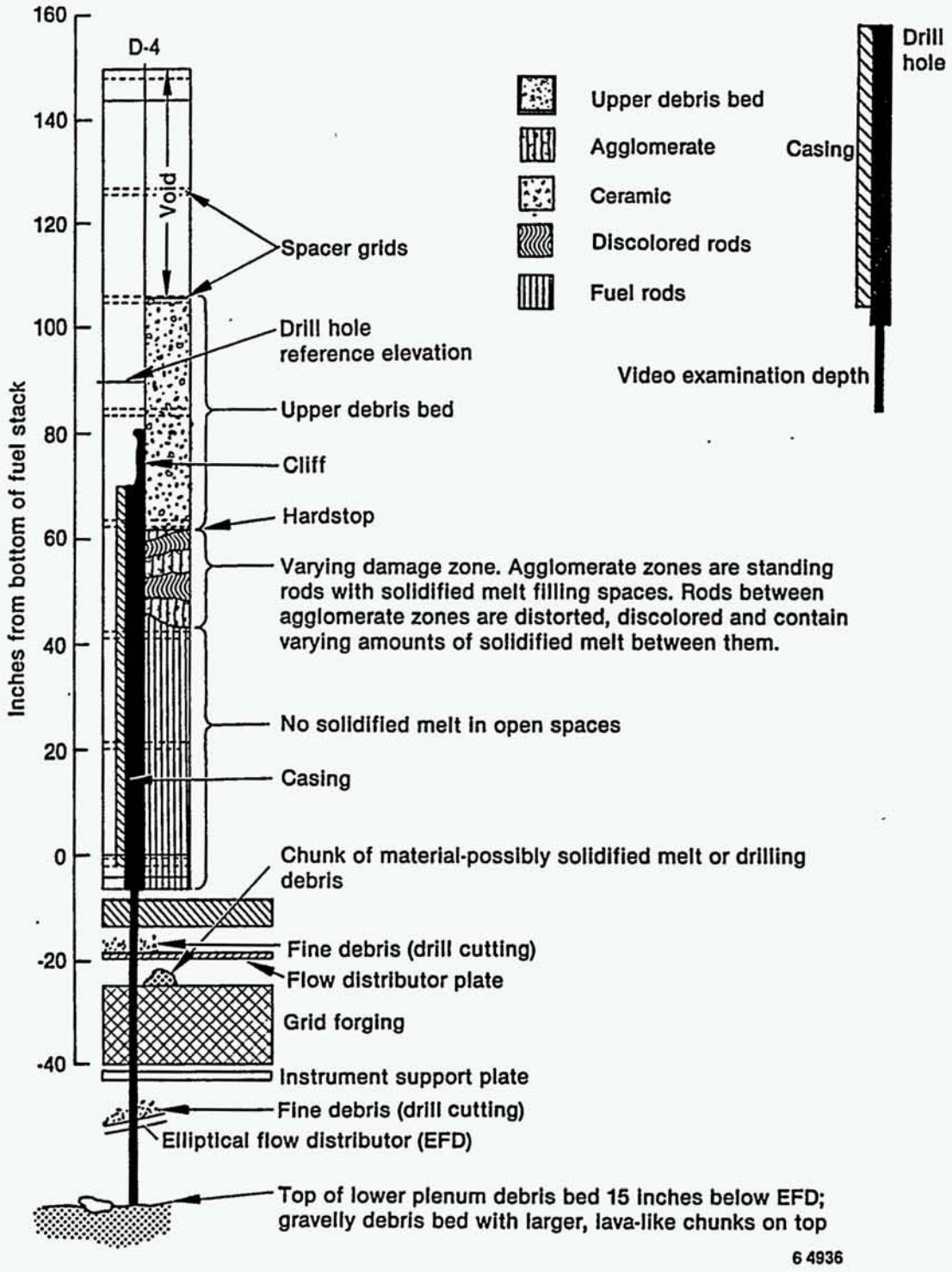

Figure B-21. D4 drill configuration and inspection summary.

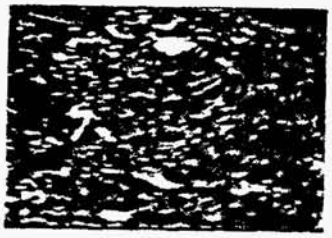

Possible view of loose debris including probable core-boring-generated debris on reactor vessel lower head below core position D4
(86-484-6-2)

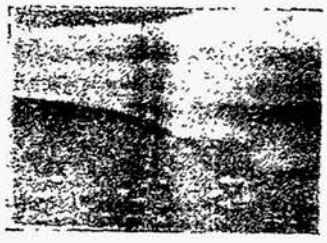

Possible view to north from below core position D4 at loose debris in space below the elliptical flow distributor
(86-484-10-8)

Possible view of the elliptical flow distributor top below core position D4
(86-484-6-1)

Possible chunk of previously molten core material and core-boring-generated debris at top of lower grid forging below core position D4
(86-484-6-4)

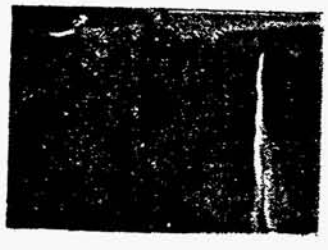

Typical condition of lower grid flow distributor lower surfaces below core position D4
(86-484-6-6)

Figure B-22. Enhanced video images about D4.

Closeup of possible fuel rod damage at top of core position D4 second spacer grid (approximately 48 in. above fuel rod bottom
(86-484-6-9)

Possible previously molten core material at approximately 48 in. above core position D4 fuel rod bottom
(86-484-6-10)

Possible agglomerated core material between 48 and 72 in. above core position D4 fuel rod bottom
(86-484-7-1)

Figure B-22. (continued)

Core Region Observations

Standing intact fuel rods are observed from the lower fuel assembly endfitting to slightly above the third spacer grid. No previously molten material is observed between the lower rod stubs.

The degraded core regions are observed to have alternating axial zones of agglomerate and intact but damaged (oxidized, distorted) rods. A region of agglomerate material was encountered above the upper core hard stop surface (See Figure B-21). This previously molten material was located at the edge of the drill hole and was encountered in two axial elevations. These data suggest that previously molten material exists above the hard stop (in the region of the debris bed) at this drill location.

Core Support Assembly And Lower Plenum Observations

The CSA was inspected down to the top of the elliptical flow distributor. A single, relatively large (1/2 in. across) particle was observed on the grid forging. The particle is thought to be either a piece of drilling debris or previously molten core debris. No significant amount of previously molten material was observed.

Inspection of the lower plenum debris was generally consistent with observations from the other inspection locations. The debris bed appears to consist of loose, rather fine particles. A few larger, solidified pieces (3-4 in. across) were observed on the surface. These larger pieces of lower plenum debris were not observed in the other drill locations. The debris bed height is estimated to be approximately 15 in. below the elliptical flow distributor plate.

Relationship to Other Drill Holes

D4 represents the drill location closest to the west periphery of the reactor vessel. The axial variation in core damage suggests that D4 is near the edge of the degraded core zone.

On-line Drilling Data

The automatic mode data are shown in Figure B-23. Automatic drilling started at about 85 in. from the rod bottom. The data show three unique material regions characterized by abrupt changes in drilling resistance. The first two are located between the fourth and fifth spacer grids (at about 82-85 in. and 72-75 in.), both in the region of the "cliff" material above the core hard stop. The third is located just above the third spacer grid, very near the fuel/agglomerate interface. The drilling data suggest that this interface may have considerable metal content.

07 Data Summary

Figure B-24 summarizes the 07 drilling and inspection regions and major observations. Figure B-25 presents selected video images from the core and CSA regions.

Core Region Observations

Standing intact fuel rods are observed from the lower fuel assembly endfitting to the third spacer grid.

The agglomerate region consists of fuel pellets and/or rods surrounded by previously molten material and is estimated to be about 15 in. thick, between the third and fourth spacer grids.

Core Support Assembly and Lower Plenum Observations

The amount of previously molten core material observed in this location is greater than at any other drill location. The material resembles the molten ceramic materials observed in the core region and looks like it froze in the CSA regions as it flowed downward, thus resembling a "wall" or "curtain." The material appears to encircle the hole in the grid forging plate.

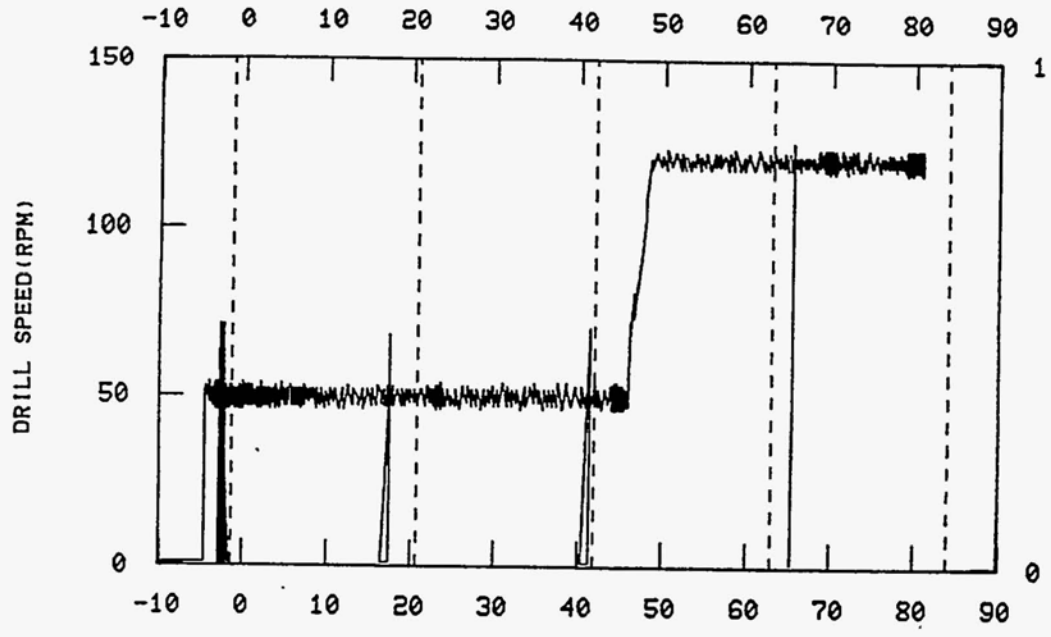

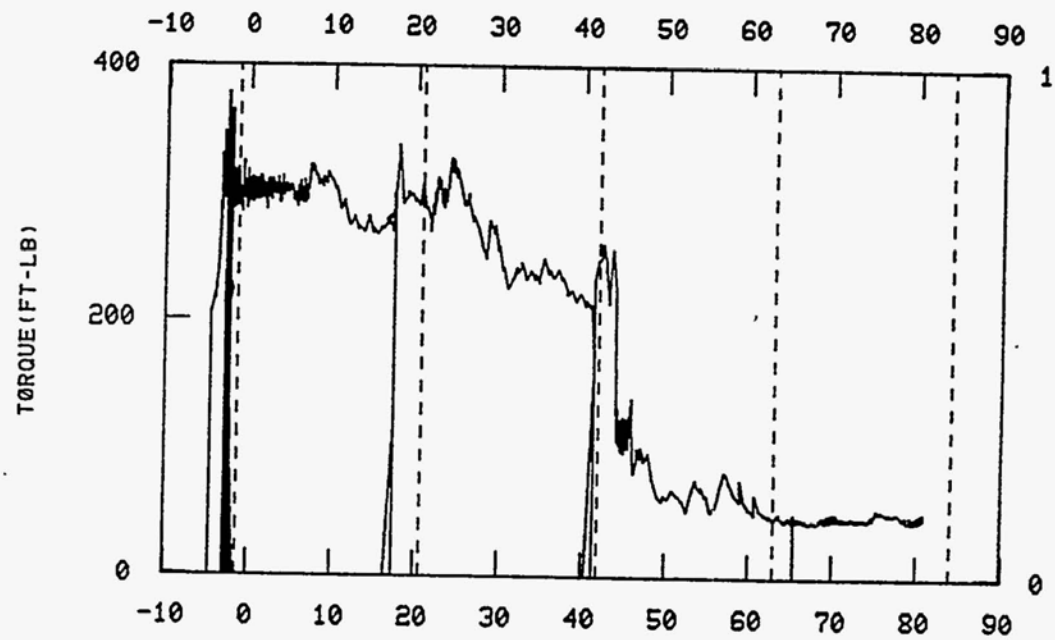

Figure B-23. On-line drilling data for D4.

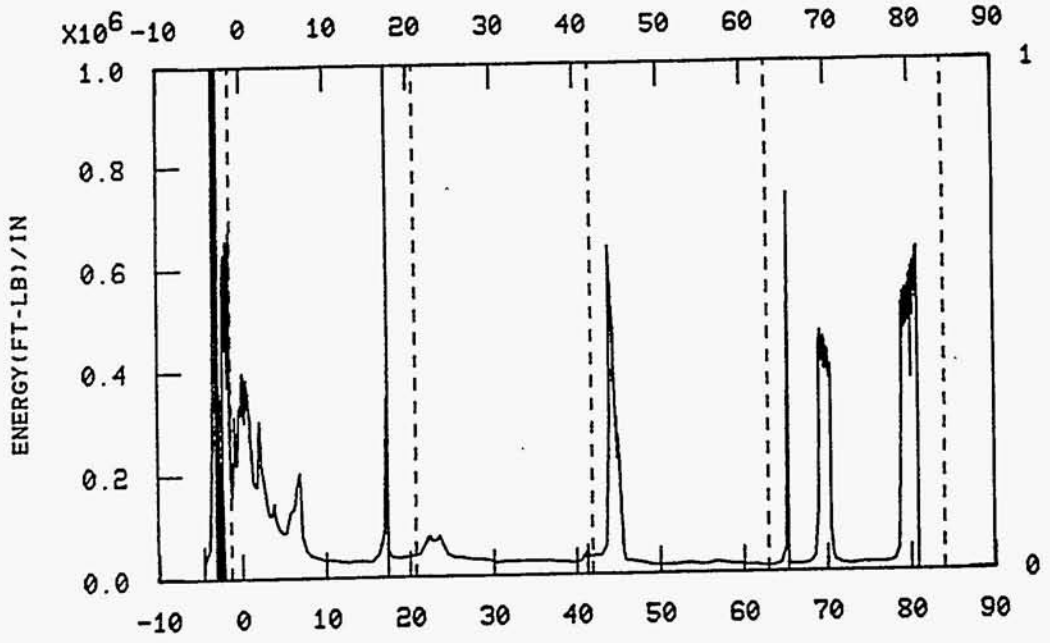

DISTANCE FROM BOTTOM OF FUEL STACK
BORE HOLE D4
DASHED LINES INDICATE MIDPOINT
OF SPACER GRIDS

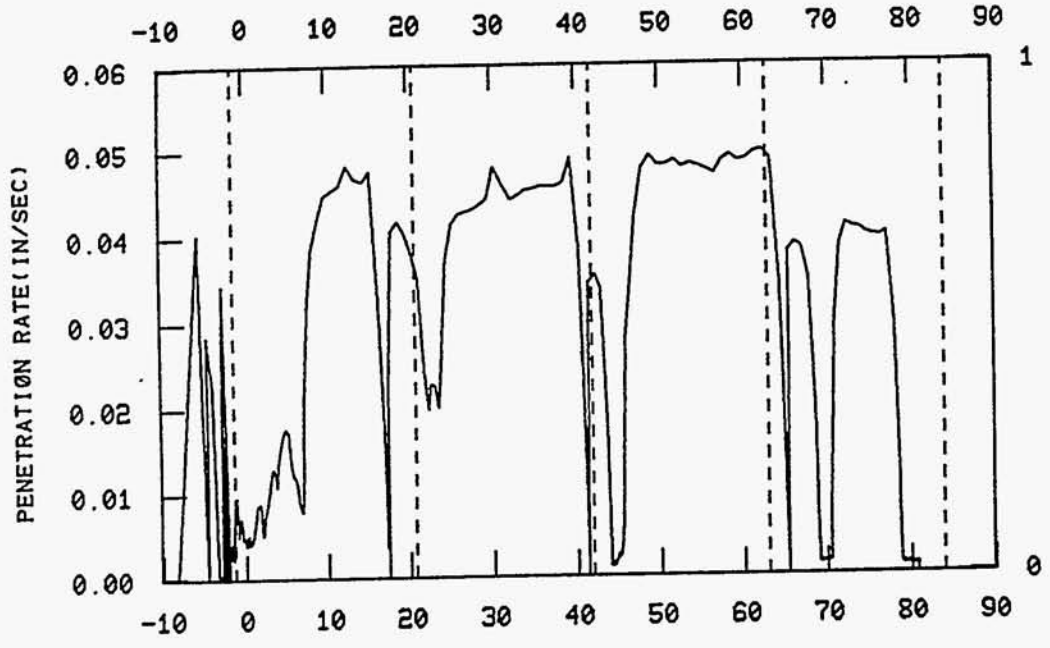

DISTANCE FROM BOTTOM OF FUEL STACK
BORE HOLE D4
DASHED LINES INDICATE MIDPOINT
OF SPACER GRIDS

Figure B-23. (continued)

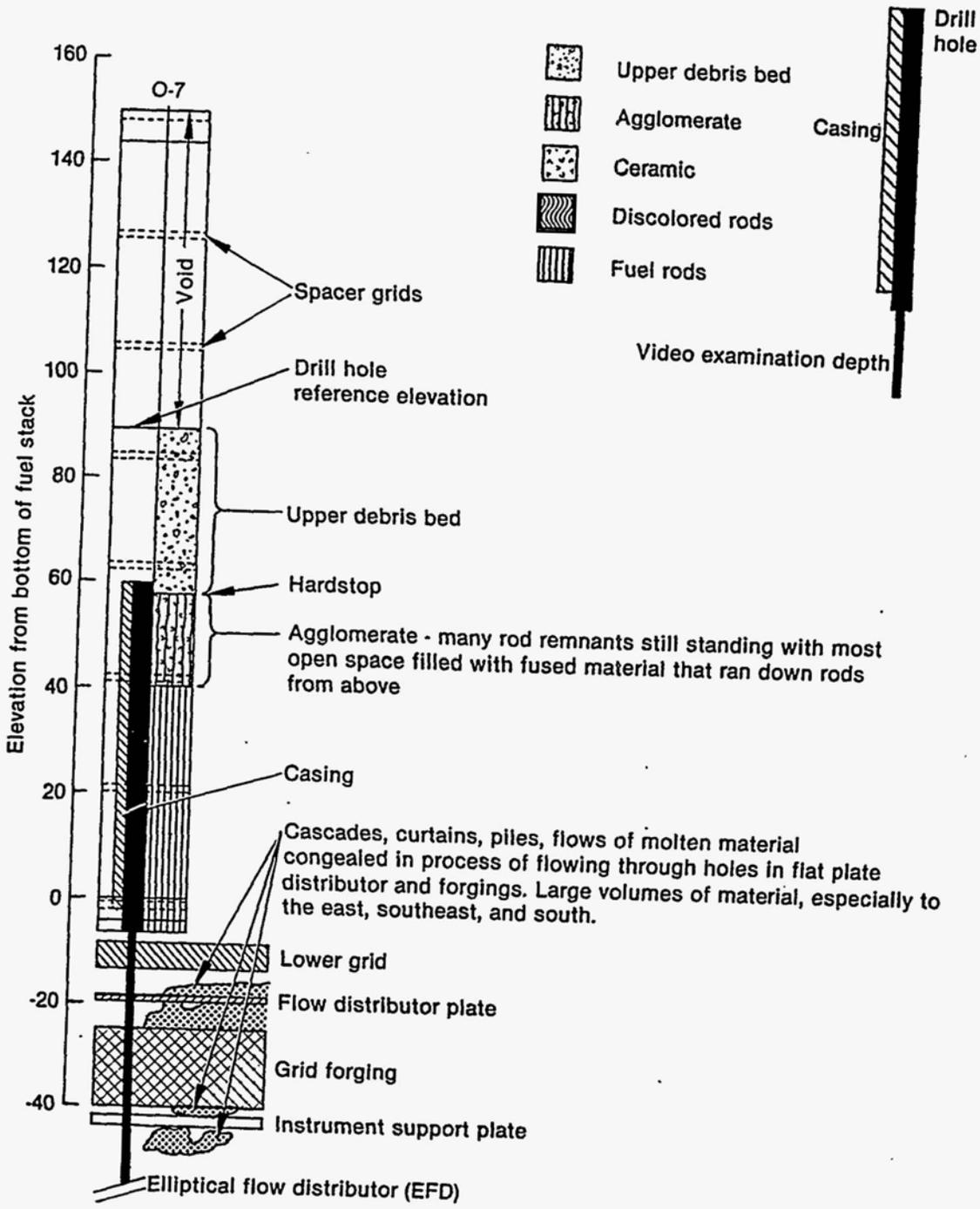

Figure B-24. 07 drill configuration and inspection summary.

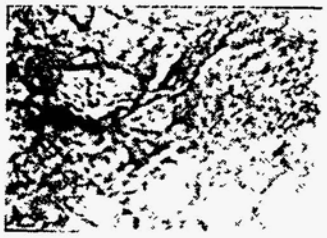

View of loose debris including probable core-boring-generated debris on elliptical flow distributor below core position 07
(86-484-7-12)

Looking south from below core position 07 at previously molten core material on top of elliptical flow distributor
(86-484-8-2)

Looking south from below core position 07 at previously molten core material underneath the in-core instrument support plate
(86-484-8-3)

Previously molten core material in space between in-core instrument support plate and lower grid forging below core position 07 (not continuous all around)
(86-484-8-4)

Possible previously molten core material adhering to wall of lower grid forging below core position 07
(86-484-9-12)

Previously molten core material on top of lower grid forging below core position 07 (typical all around)
(86-484-8-5)

Figure B-25. Enhanced video images about 07.

Looking northeast from below core position 07 underneath the lower grid flow distributor with previously molten core material appearing at right
(86-484-8-7)

Looking northeast by east from below core position 07 at previously molten core material flow underneath the lower grid flow distributor
(86-484-9-9)

Looking east from below core position 07 at previously molten core material underneath the lower grid flow distributor
(86-484-8-8)

Looking west from below core position 07 underneath the lower grid flow distributor with previously molten core material appearing at left
(86-484-8-10)

Possible previously molten core material on top of lower grid flow distributor below core position 07
(86-484-8-11)

Figure B-25. (continued)

Looking east-southeast at possible previously molten core material and support post at top of lower grid flow distributor below core position 07 (86-484-8-12)

Looking south from core position 07 at previously molten core material behind the support post (extreme right) at the top of the lower grid flow distributor. The core instrument guide tube underneath core position 06 is covered or missing (86-484-4-1)

Possible previously molten core material at one corner of the core position 07 lower endfitting (core material not observed at other three corners) (86-484-9-10)

Core position 07 rod bundle at first spacer grid approximately 26 in. above fuel rod bottom (86-484-10-1)

Transition of rod bundle geometry to agglomerated core material approximately 40 in. above core position 07 fuel rod bottom (86-484-10-3)

Figure B-25. (continued)

Based on the CSA observations from N5 and N12, it was anticipated that previously molten core material was likely in the CSA region. The small-diameter drilling hardware was used to sample the material in the CSA region below 07. However, the drilling parameters indicated no significant drilling resistance and no CSA sample material was retrieved in the sample canister.

There appeared to be some damage to a core support post and in-core instrument guide tube above the flow distributor plate. The forging structure was discolored in places, indicating high temperatures.[B-1]

Relationship to Other Drill Holes

The agglomerate region in the core is similar to that in other peripheral drill locations (D4, N5, and N12). The form and pattern of molten material in the CSA are similar to that observed in locations N5, N12, and 09. More previously molten core material was observed in the CSA region at this location than at any other location. The 07 data suggest that a core material flow path to the lower plenum was to the southeast, most likely in fuel assembly P6 and/or P7.

On-line Drilling Data

The automatic mode data are shown in Figure B-26. Automatic drilling started at about 60 in. from the rod bottom, near the top of the agglomerate region. There appear to be significant changes in drill resistance; however, because the drill was stopped several times, inferences relative to material composition are not too meaningful.

09 Data Summary

Figure B-27 summarizes the 09 drilling and inspection regions and major observations. Figure B-28 presents selected video images from the core and CSA regions.

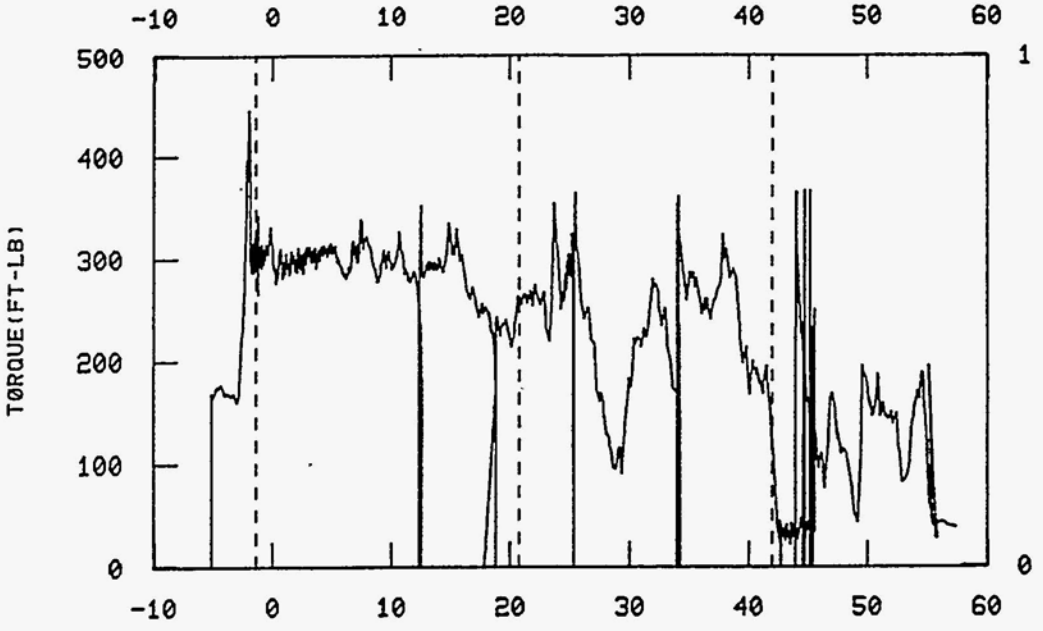

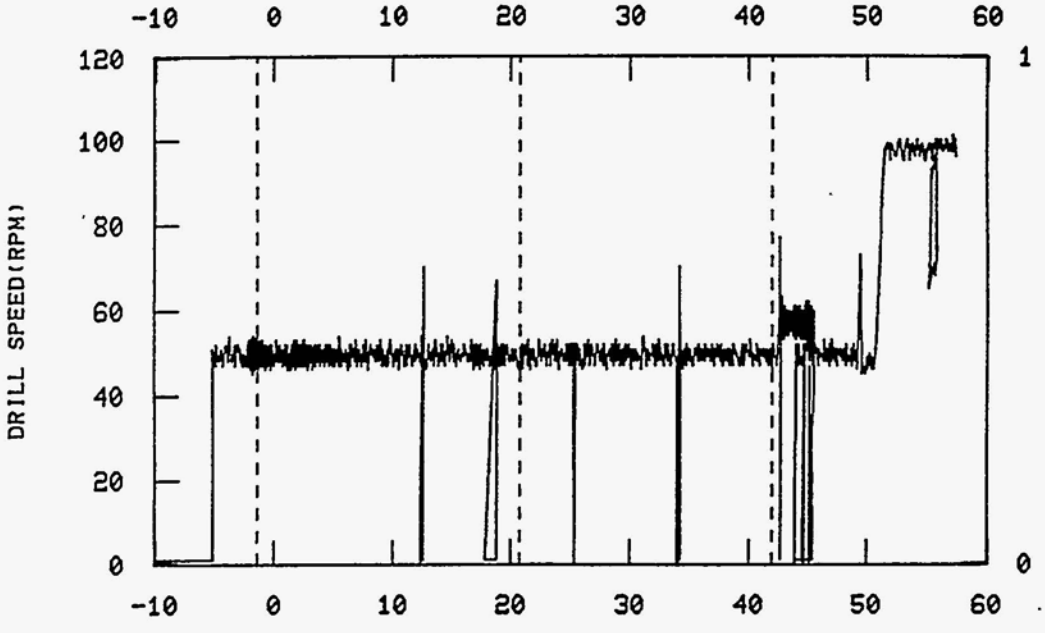

Figure B-26. On-line drilling data for 07.

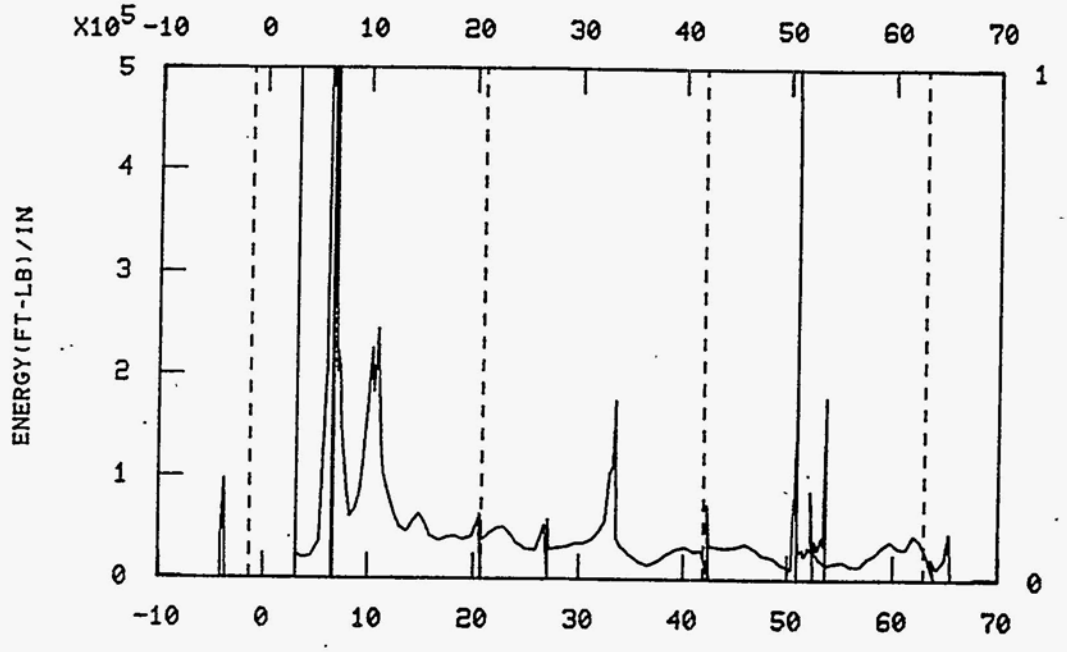

DISTANCE FROM BOTTOM OF FUEL STACK
BORE HOLE 07
DASHED LINES INDICATE MIDPOINT
OF SPACER GRIDS

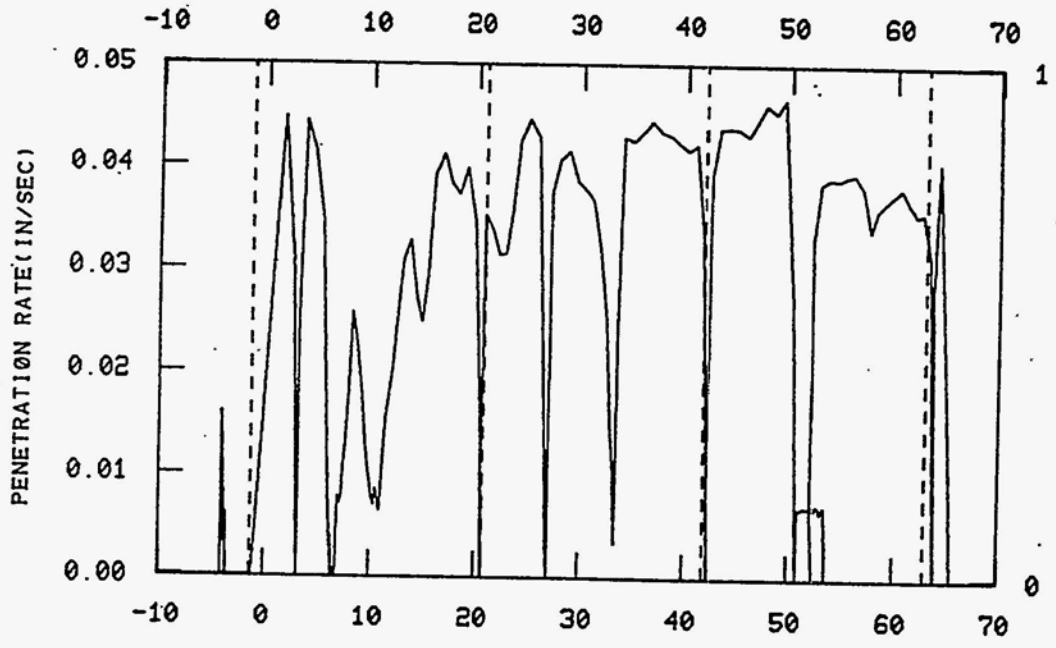

DISTANCE FROM BOTTOM OF FUEL STACK
BORE HOLE 07
DASHED LINES INDICATE MIDPOINT
OF SPACER GRIDS

Figure B-26. (continued)

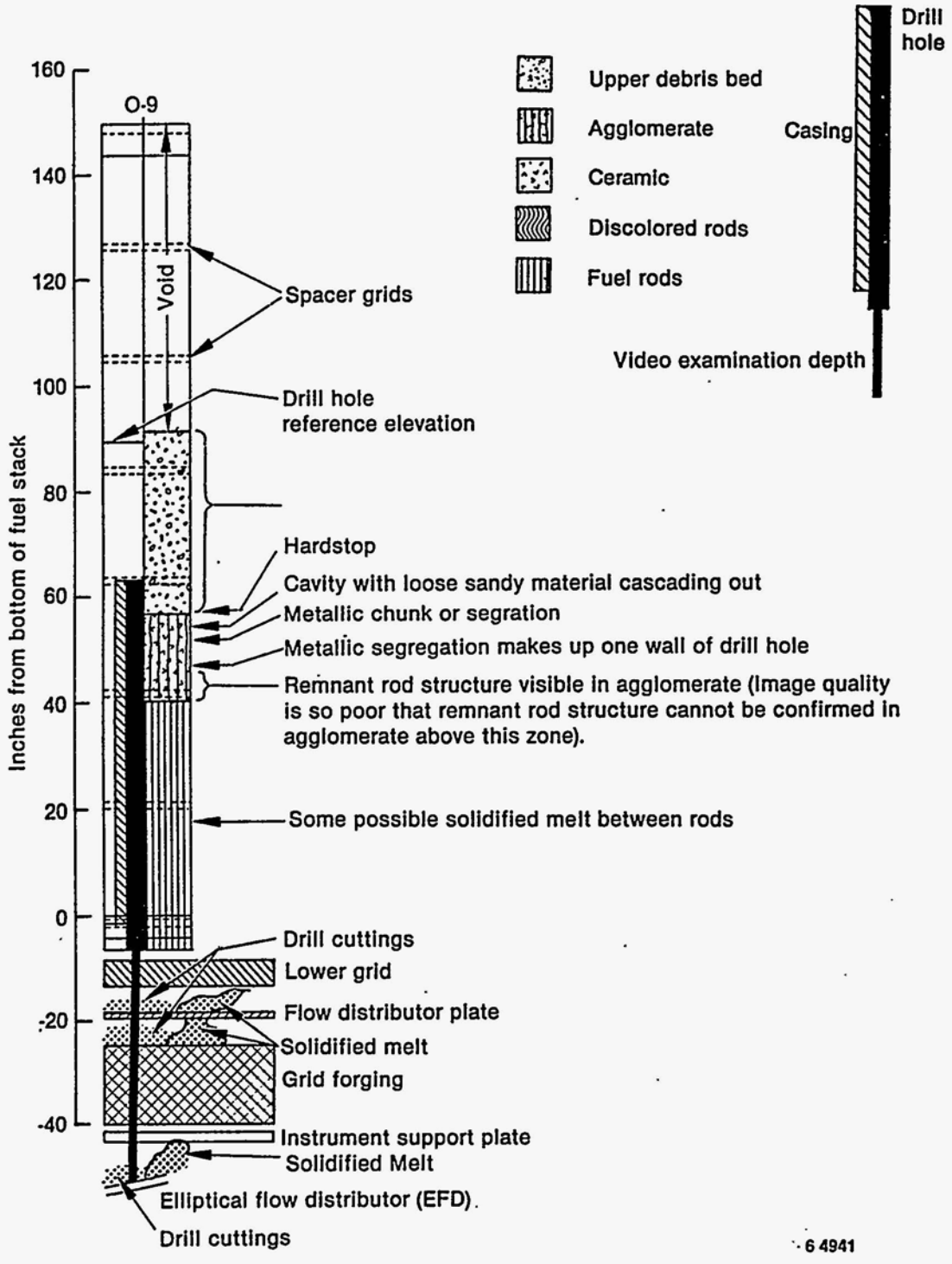

Figure B-27. 09 drill configuration and inspection summary.

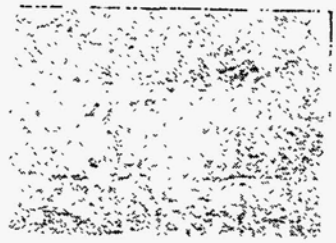

Top of elliptical flow distributor below core position 09
(86-443-1-1)

Possible view of RV lower head loose debris through an opening in the elliptical flow distributor with a core instrument guide tube in lower right quadrant from below core position 09
(86-443-1-2)

Looking east from below core position 09 at previously molten core material below the in-core instrument support plate
(86-443-2-1)

Looking east from below core position 09 at previously molten core material stalagmite on top of lower grid forging
(86-443-1-9)

Possible view looking east from below core position 09 of previously molten core material above lower grid forging underneath core position P9 (86-443-1-4)

Figure B-28. Enhanced video images about 09.

Possible view looking southeast from below core position 09 of previously molten core material below lower grid flow distributor underneath core position P8 (86-443-1-5)

Interface of decomposed fuel rods and agglomerated core material at approximately 46-in. above core position 09 fuel rod bottom (86-443-2-3)

View of agglomerated core material at approximately 48 in. above core position 09 fuel rod bottom with bore casing bottom edge at top (86-443-1-12)

Figure B-28. (continued)

Core Region Observations

Standing intact fuel rods are observed from the lower fuel assembly endfitting to just below the third spacer grid.

The agglomerate region consists of fuel pellets and/or rods surrounded by previously molten material and is estimated to be about 15 in. thick between the third and fourth spacer grids. The rod remnant structure in the lower few inches of the agglomerate is well defined. Because of poor image quality in the upper regions, the structure cannot be determined; however, metallic segregations are observed in the upper regions.

Core Support Assembly Observations

The CSA was inspected down to the top of the elliptical flow distributor. Fine, sandy material, probably drill cuttings, was observed on the grid distributor plate and the inside surface of the elliptical flow distributor. Although no physical damage to the structures is discernible, significant amounts of previously molten material are observed, particularly to the east in fuel assemblies P8, P9, and P10.[B-1]

Relationship to Other Drill Holes

09 is similar to N5 and 07, showing significant amounts of previously molten core material in the CSA regions, particularly in the 'P' row of fuel assemblies. These data suggest that core (crust) failure may have occurred extensively in the east quadrant of the core.

On-line Drilling Data

The automatic mode data are shown in Figure B-29. Automatic drilling started at about 60 in. from the rod bottom, near the top of the agglomerate region. There were several shutdown periods, so possible differences in material structure are difficult to identify. One area between the second

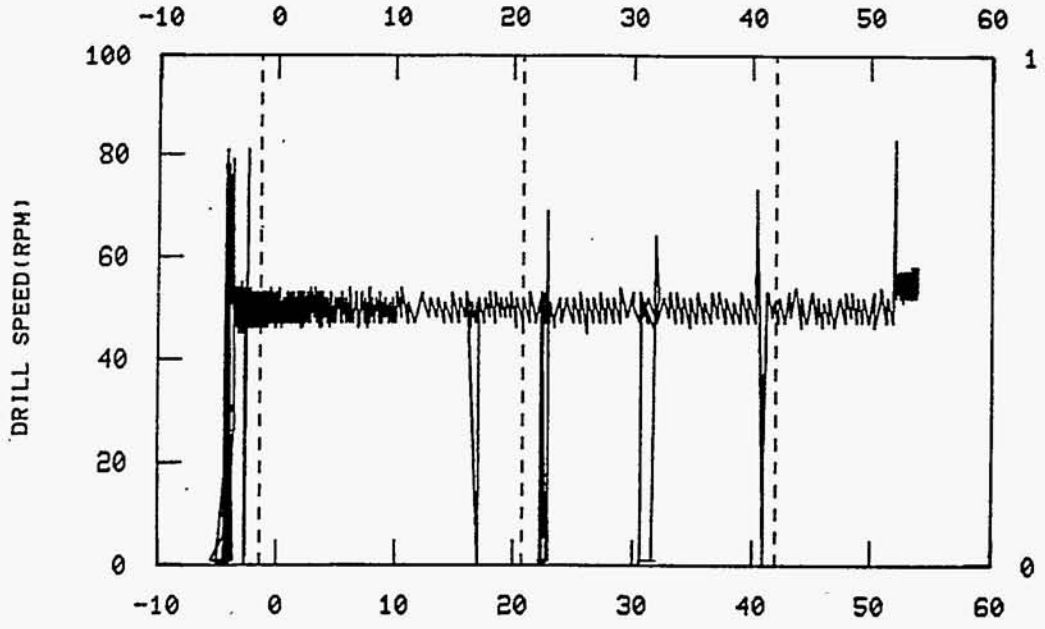

DISTANCE FROM BOTTOM OF FUEL STACK
BORE HOLE 09
DASHED LINES INDICATE MIDPOINT
OF SPACER GRIDS

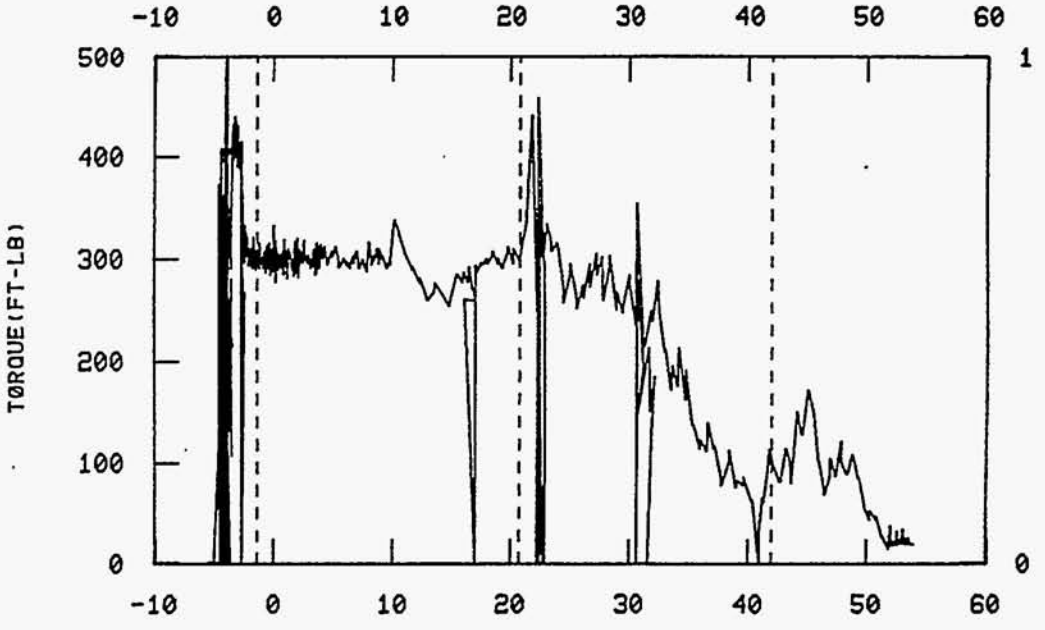

DISTANCE FROM BOTTOM OF FUEL STACK
BORE HOLE 09
DASHED LINES INDICATE MIDPOINT
OF SPACER GRIDS

Figure B-29. On-line drilling data for 09.

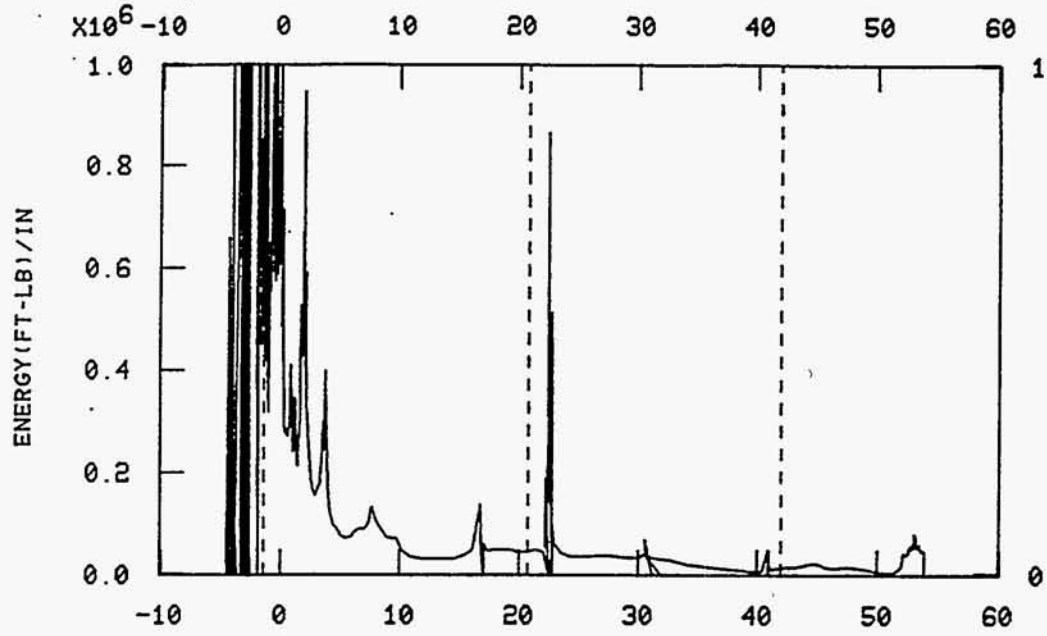

DISTANCE FROM BOTTOM OF FUEL STACK
BORE HOLE 09
DASHED LINES INDICATE MIDPOINT
OF SPACER GRIDS

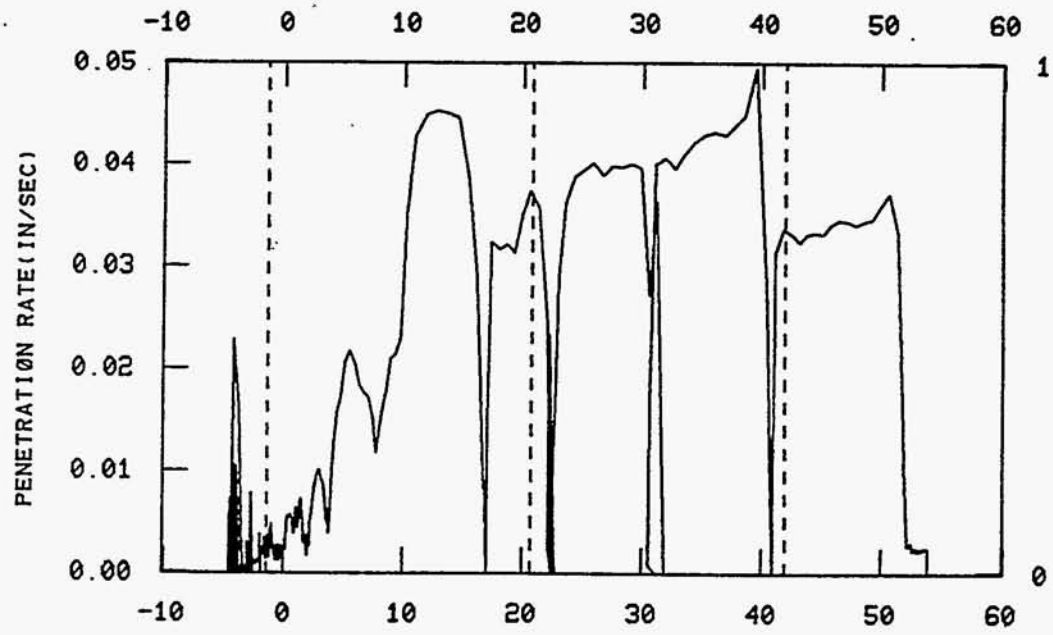

DISTANCE FROM BOTTOM OF FUEL STACK
BORE HOLE 09
DASHED LINES INDICATE MIDPOINT
OF SPACER GRIDS

Figure B-29. (continued)

and third spacer grids, between approximately 8-12 in., appears to have a significant increase in drilling resistance. This area may contain relocated metallic material.

References

1. GPU Technical Bulletin TB-86-35 (Rev. 3), "Core Stratification Sampling Program", August 18, 1986.

APPENDIX C

CONTOUR DATA TO DEFINE UPPER CORE CRUST CONFIGURATION (FROM ROD PROBE DATA)

APPENDIX C

CONTOUR DATA TO DEFINE UPPER CORE CRUST CONFIGURATION (FROM ROD PROBE DATA)

Data have been obtained to define the axial location of the hard stop, or "crust," that is supporting the upper core debris. These data are summarized in Reference 5 of the text. The data are summarized in Table C-1, and contours of the data are shown graphically in Figure C-1. The core bore data showing the axial elevation of the upper crust are also included in Figure C-1. These data are used to define the degraded core cross sections presented in Appendix E.

TABLE C-1. ROD PROBE DATA SUMMARY--HARD STOP (UPPER CRUST) ELEVATIONS

Location		Elevation of Hard Stop (Core Upper Crust)	
Degrees	Radius (in.)	(ft)	(in.)
165	44	304	7.25
180	12	303	9.00
180	24	304	1.75
180	36	303	10.00
180	44	303	7.25
195	36	303	8.25
195	44	303	10.00
210	24	303	9.25
210	36	304	1.00
210	44	304	3.00
225	36	303	9.00
225	44	303	8.00
240	12	303	11.50
240	24	303	7.75
240	36	303	7.00
240	44	303	10.50
255	36	303	5.00
255	44	303	6.50
270	24	304	2.50
270	44	303	7.75
285	36	303	11.50
285	44	304	0.75
300	12	304	11.25
300	24	304	3.25
300	36	303	9.00
300	44	303	10.25
315	36	303	9.75
315	44	303	6.00
330	24	304	1.00
330	36	303	7.75
330	44	302	3.50
345	36	304	8.75
345	44	304	10.75

TABLE C-1. (CONTINUED)

Location		Elevation of Hard Stop (Core Upper Crust)	
Degrees	Radius (in.)	(ft)	(in.)
0	24	303	11.00
0	36	303	11.50
0	44	303	6.00
15	36	304	9.75
15	44	304	4.75
30	24	304	6.00
30	36	304	8.50
30	44	304	5.50
45	36	304	4.00
45	44	304	8.00
60	12	304	10.50
60	24	305	3.50
60	36	304	11.00
60	44	304	11.00
75	36	303	10.00
75	44	304	9.50
90	24	304	7.00
90	44	304	2.50
105	36	304	7.50
105	44	304	6.75
120	12	304	5.50
120	36	304	4.75
120	44	304	4.75
135	36	304	3.00
135	44	304	5.50
150	24	303	7.00
150	36	303	5.00
150	44	304	6.00
165	36	303	6.00
165	44	303	7.50
Center		304	5.50

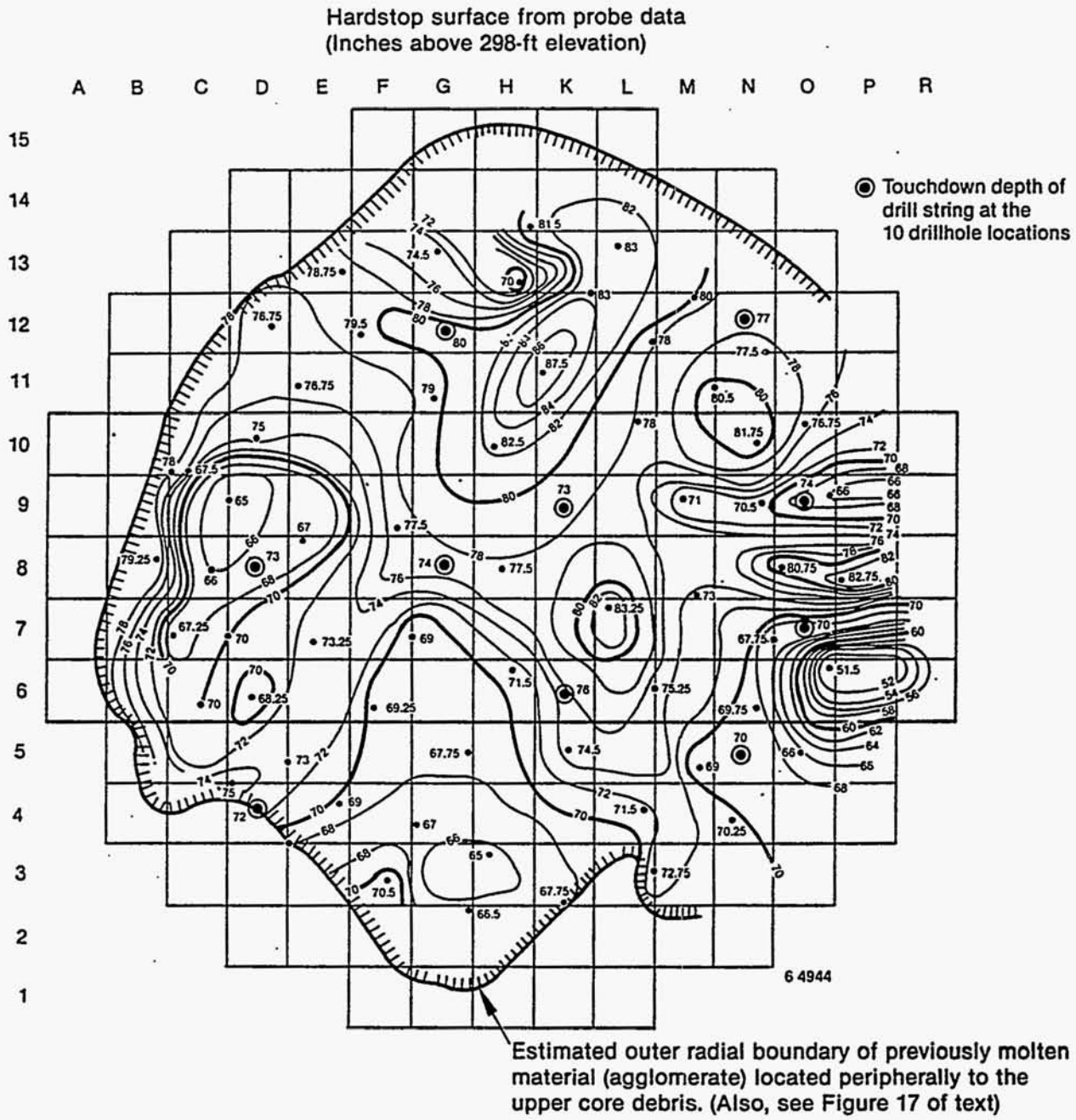

Figure C-1. Core hard stop contour map (from rod probe data).

APPENDIX D

CONTOUR DATA OF UPPER DEBRIS BED SURFACE
(FROM ACOUSTIC TOPOGRAPHY MEASUREMENTS)

APPENDIX D

CONTOUR DATA OF UPPER DEBRIS BED SURFACE (FROM ACOUSTIC TOPOGRAPHY MEASUREMENTS)

Acoustic measurements have been completed to map the surface of the upper core cavity. These measurements are documented in Reference 6 of the text.

The data provide the basis for defining the upper boundary of the debris bed and standing fuel rods near the upper core periphery.

The contour map shown in Figure D-1 represents the top of the upper core debris surface. These data were used to define the core cross sections presented in Appendix B and the text.

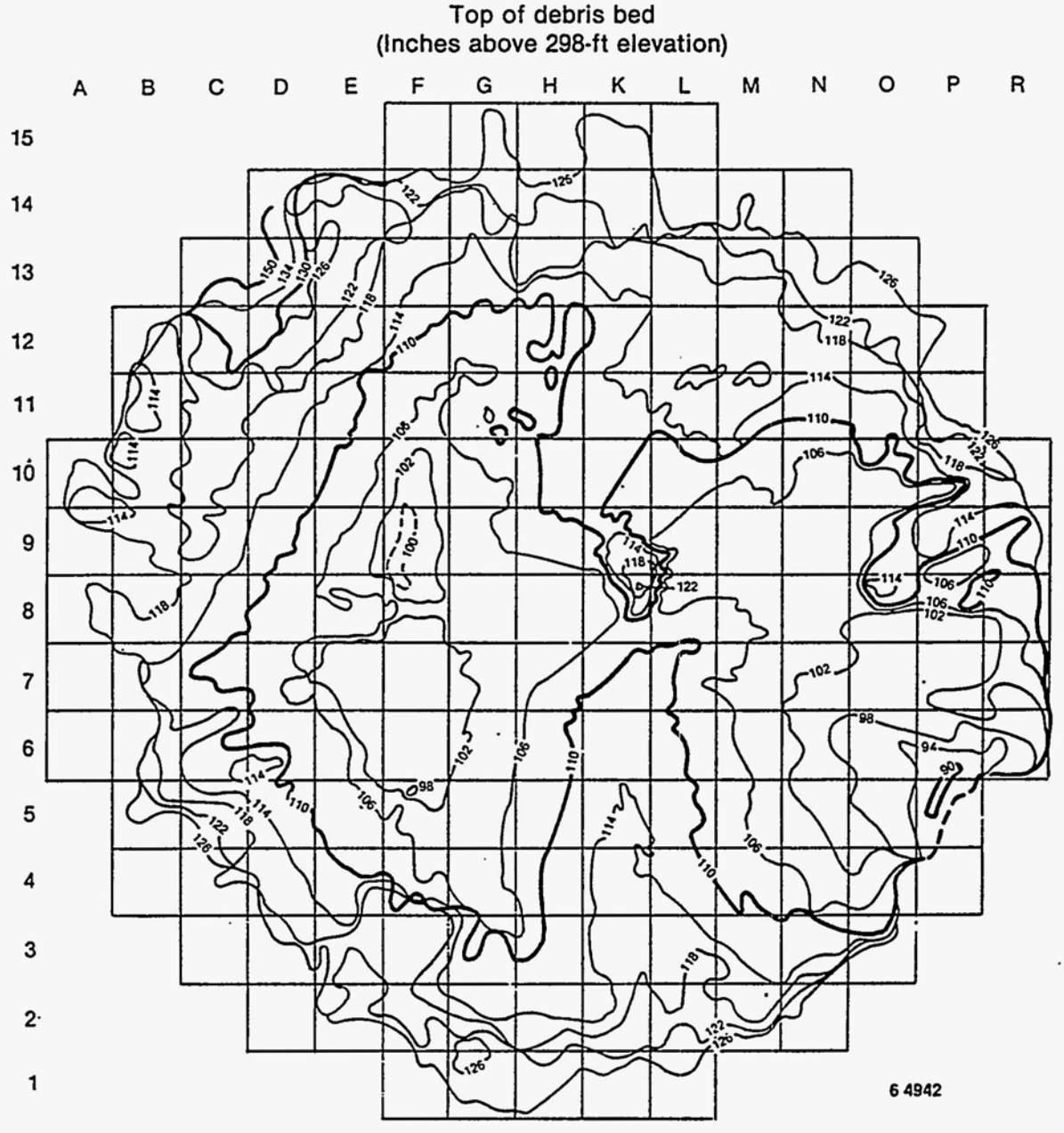

Figure D-1. Core debris upper surface contour map.

APPENDIX E

CORE DAMAGE ZONE CROSS SECTIONS

APPENDIX E

CORE DAMAGE ZONE CROSS SECTIONS

The contour data to define the interfaces between the molten core region and lower intact fuel rods (shown in Figure 7 of the text), together with the contour data in Appendixes C and D to define the boundaries of the upper debris bed, allow core damage cross sections to be drawn. These cross sections through fuel assembly rows B through P are presented in Figures E-1 through E-13.

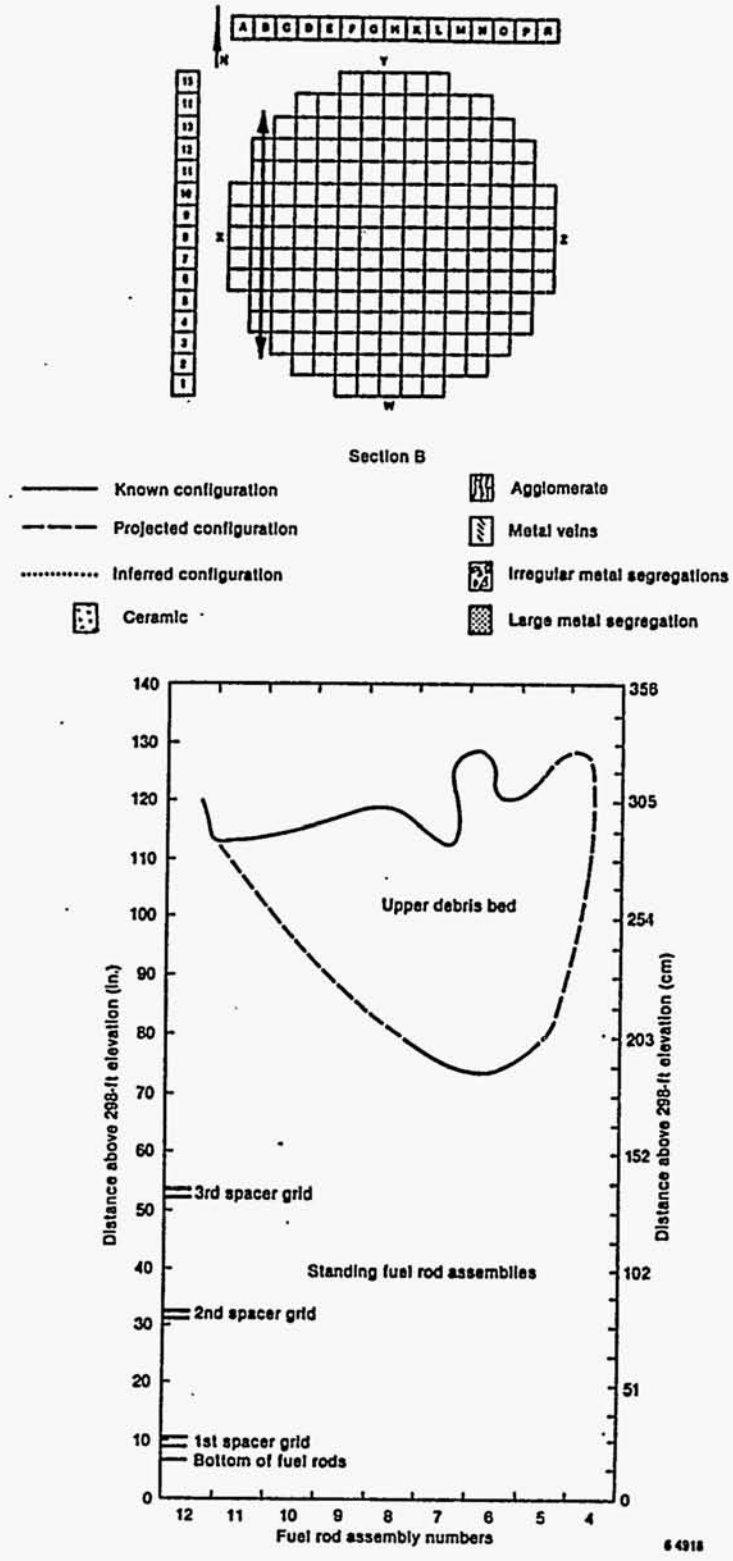

Figure E-1. Core cross section showing end-state damage configuration through B row of fuel assemblies.

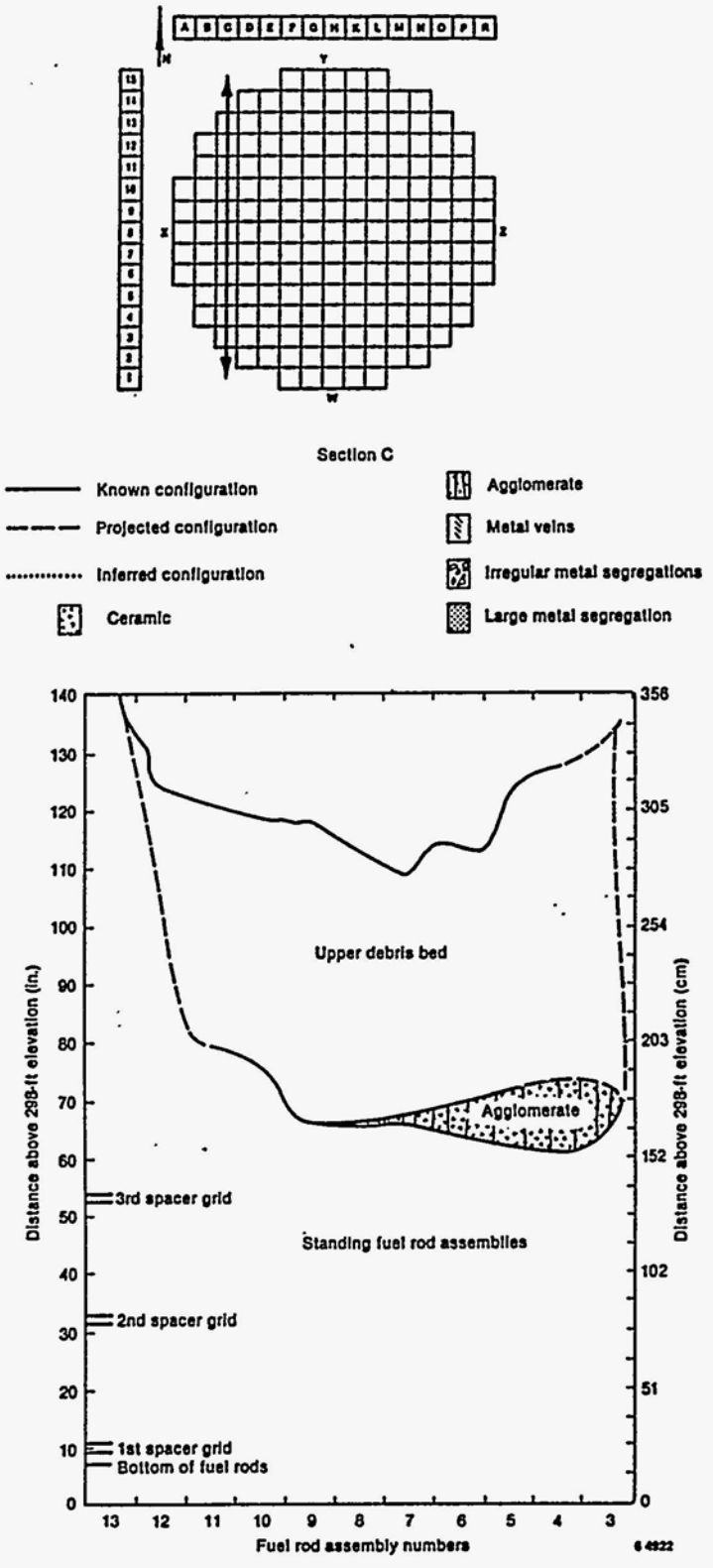

Figure E-2. Core cross section showing end-state damage configuration through C row of fuel assemblies.

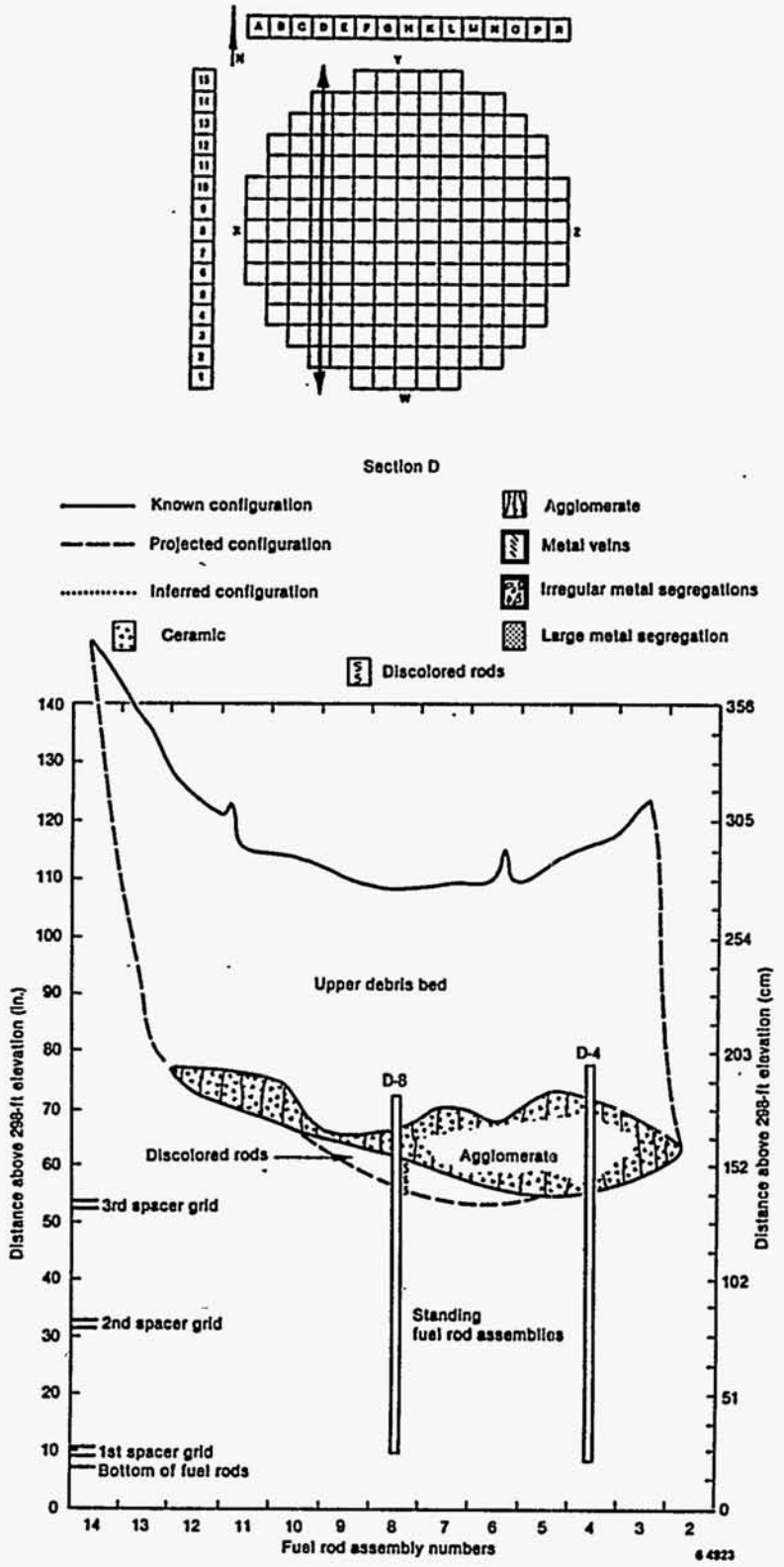

Figure E-3. Core cross section showing end-state damage configuration through D row of fuel assemblies.

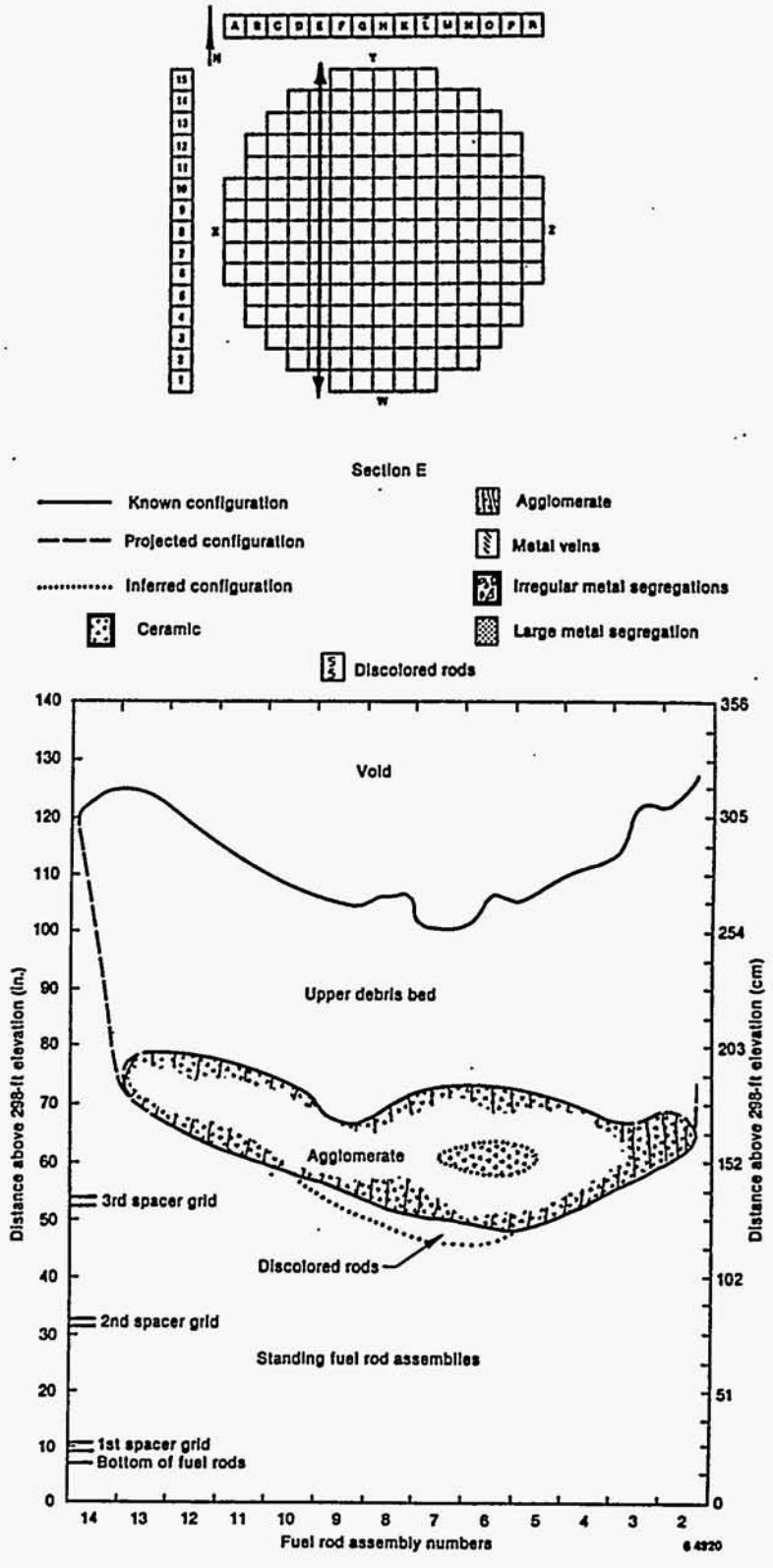

Figure E-4. Core cross section showing end-state damage configuration through E row of fuel assemblies.

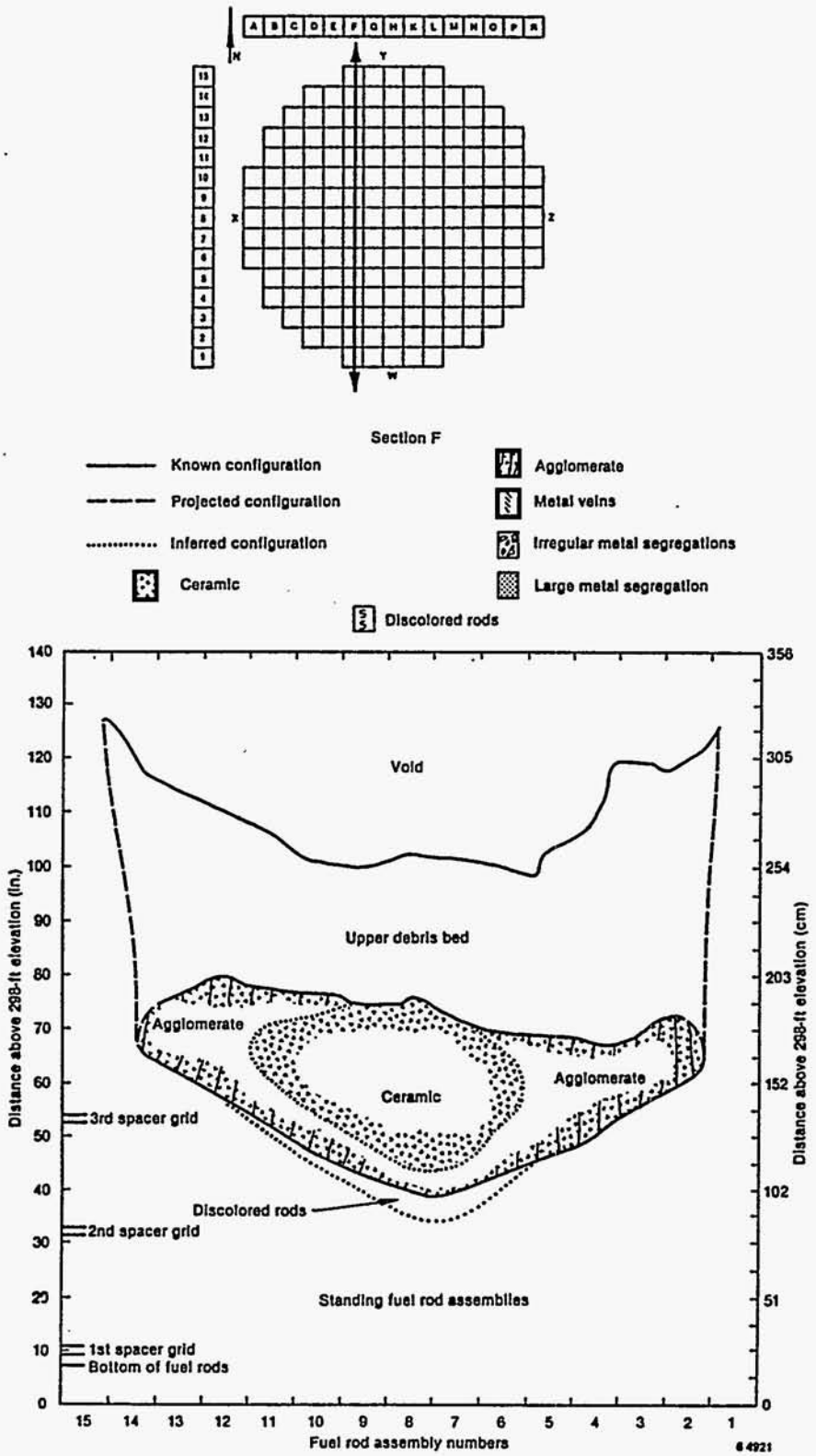

Figure E-5. Core cross section showing end-state damage configuration through F row of fuel assemblies.

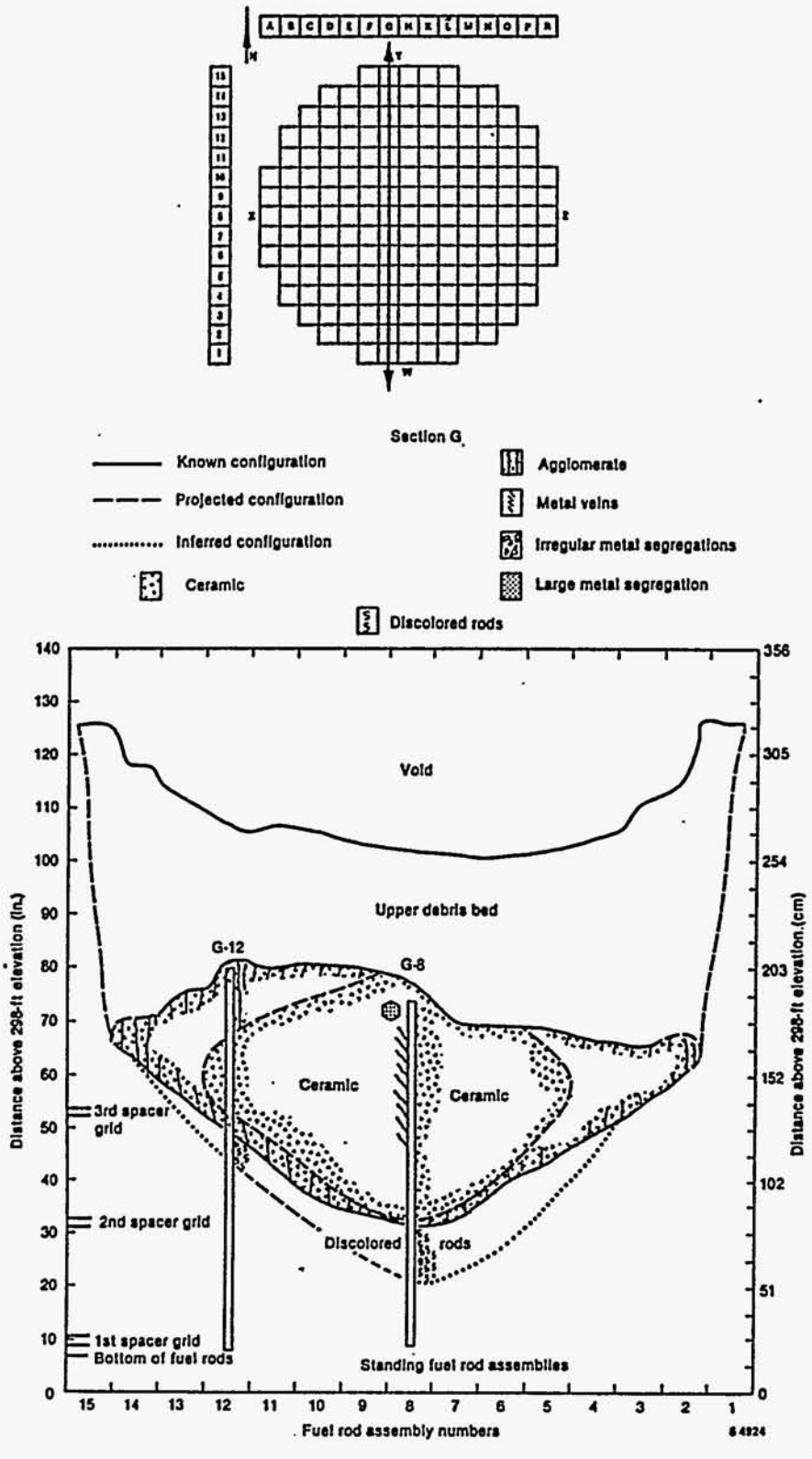

Figure E-6. Core cross section showing end-state damage configuration through G row of fuel assemblies.

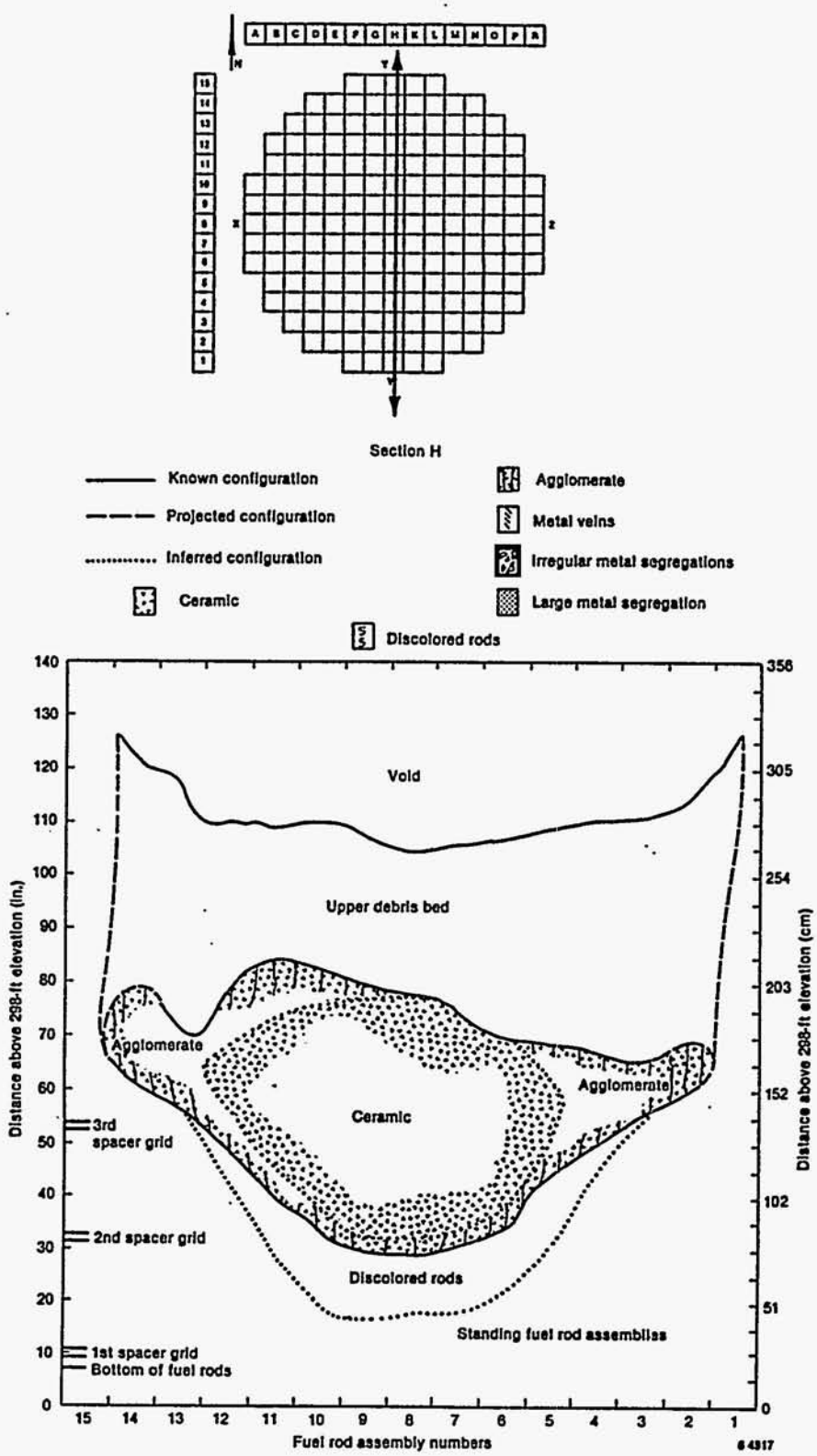

Figure E-7. Core cross section showing end-state damage configuration through H row of fuel assemblies.

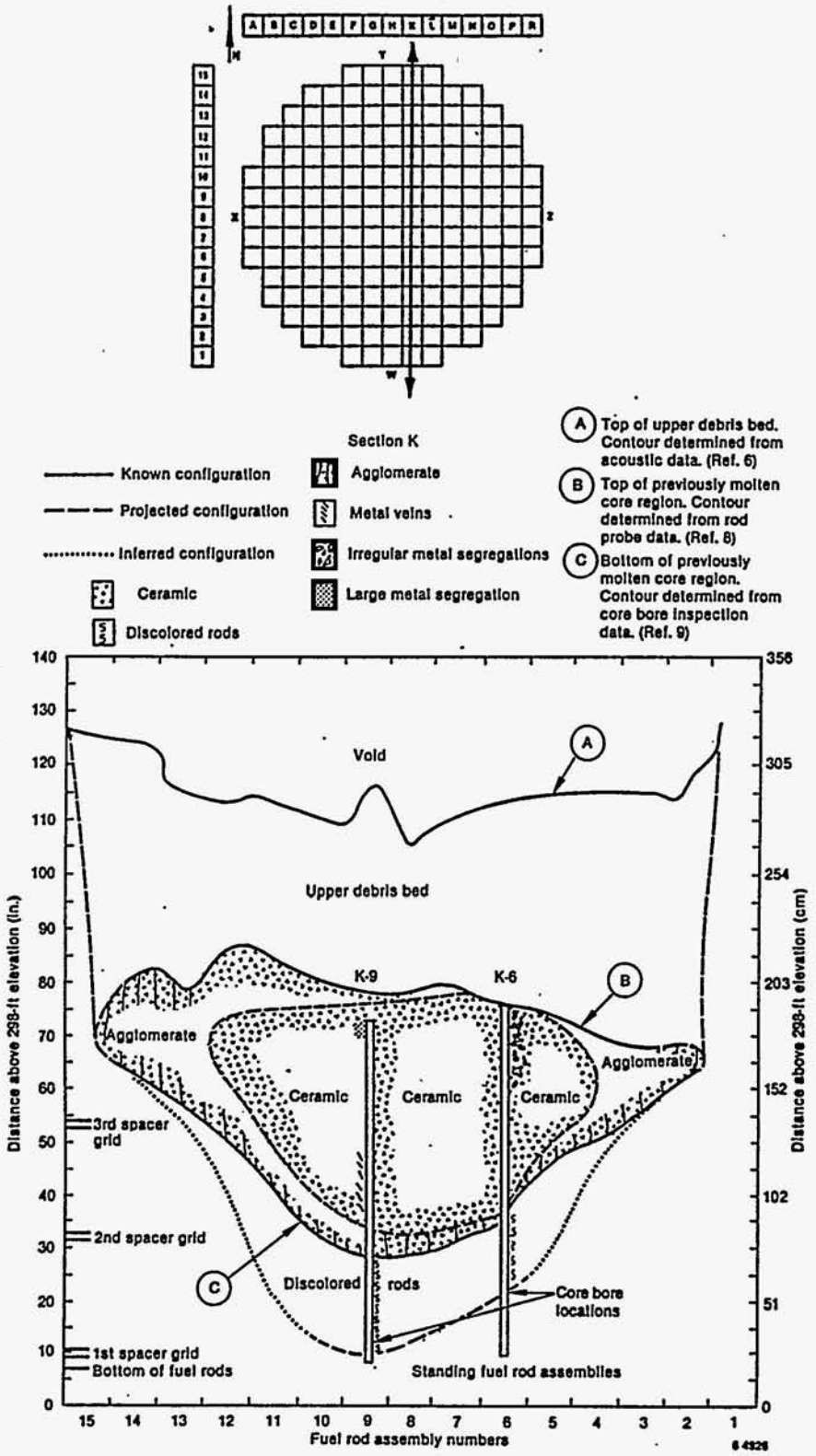

Figure E-8. Core cross section showing end-state damage configuration through K row of fuel assemblies.

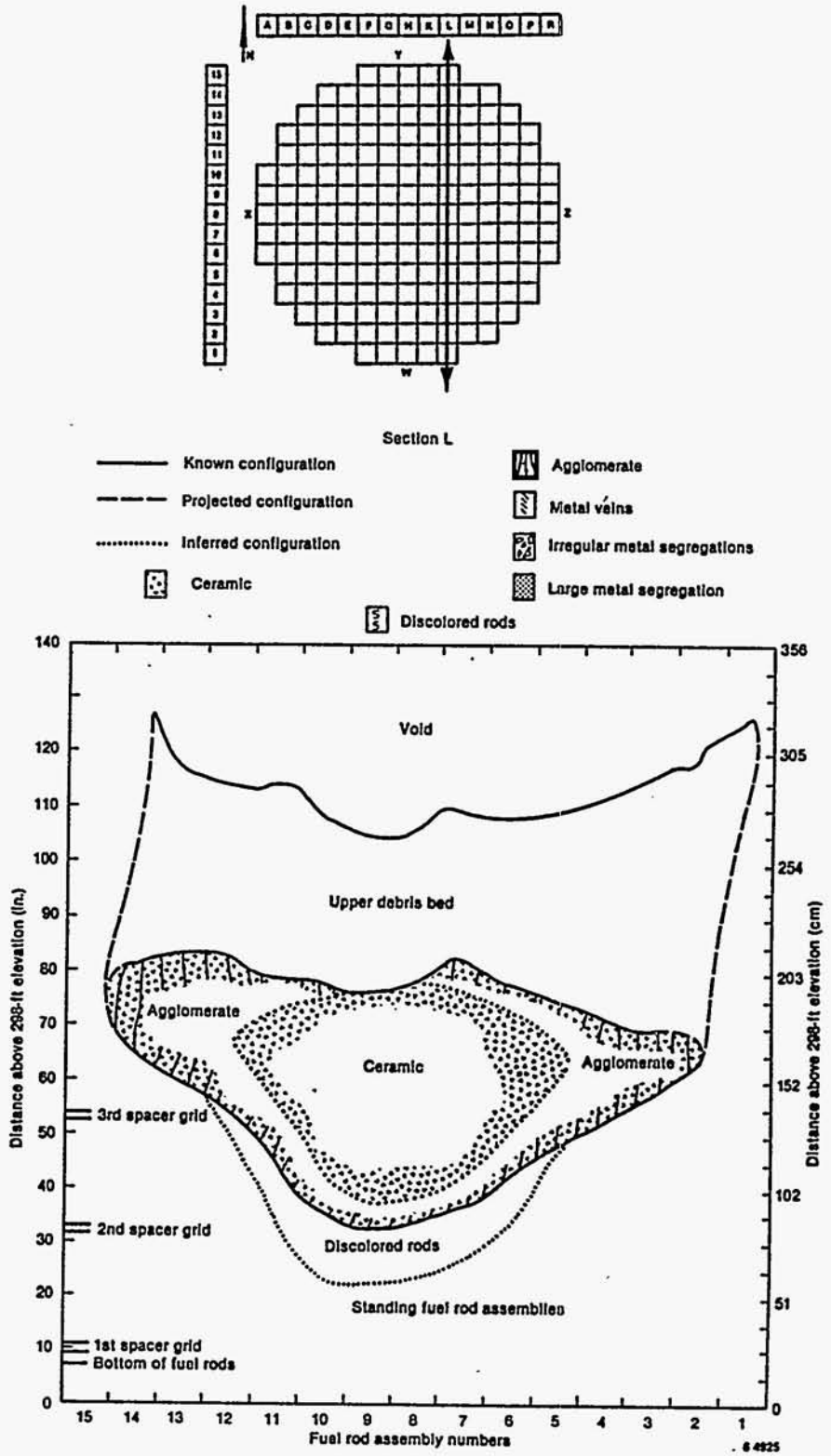

Figure E-9. Core cross section showing end-state damage configuration through L row of fuel assemblies.

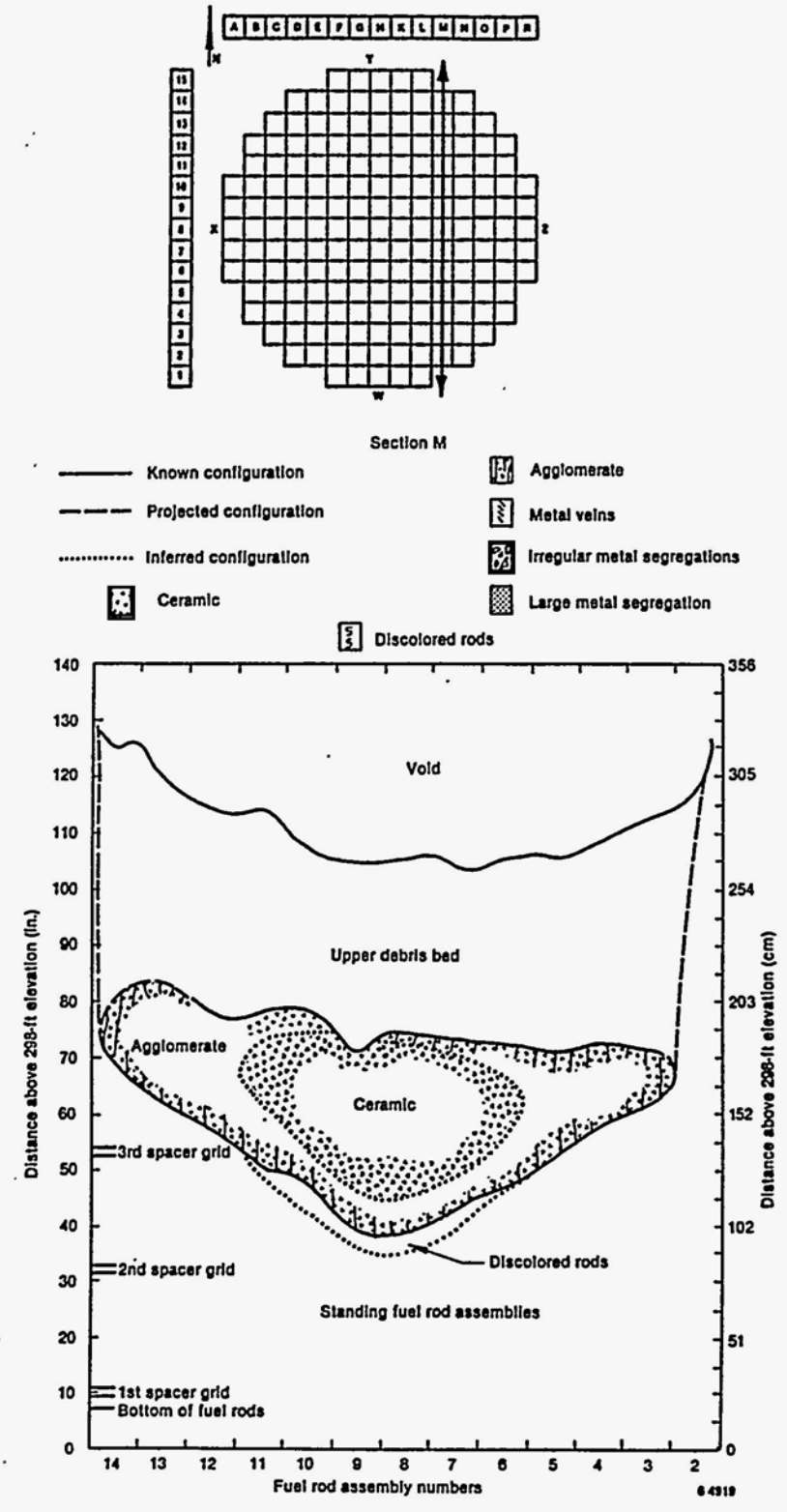

Figure E-10. Core cross section showing end-state damage configuration through M row of fuel assemblies.

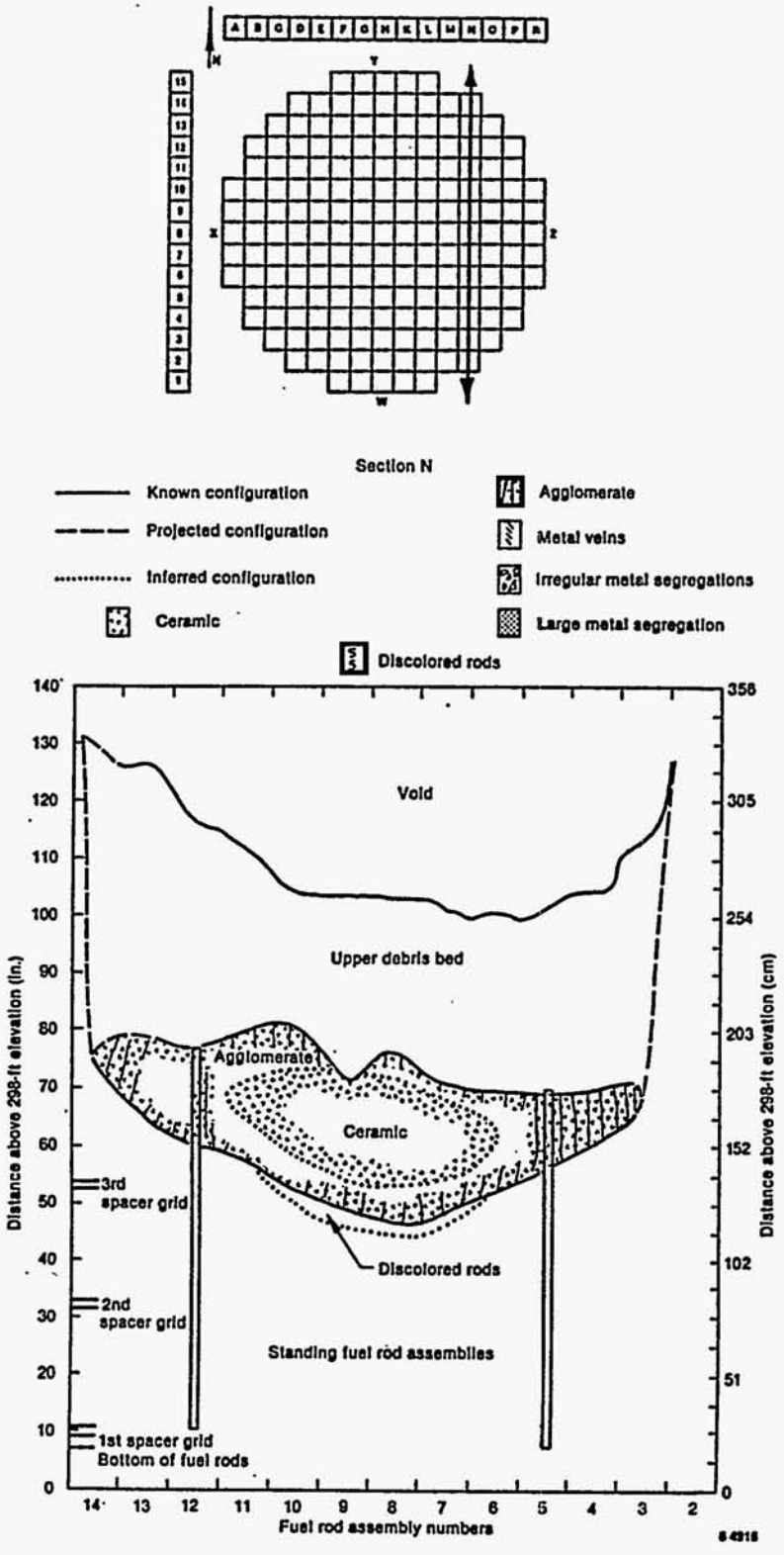

Figure E-11. Core cross section showing end-state damage configuration through N row of fuel assemblies.

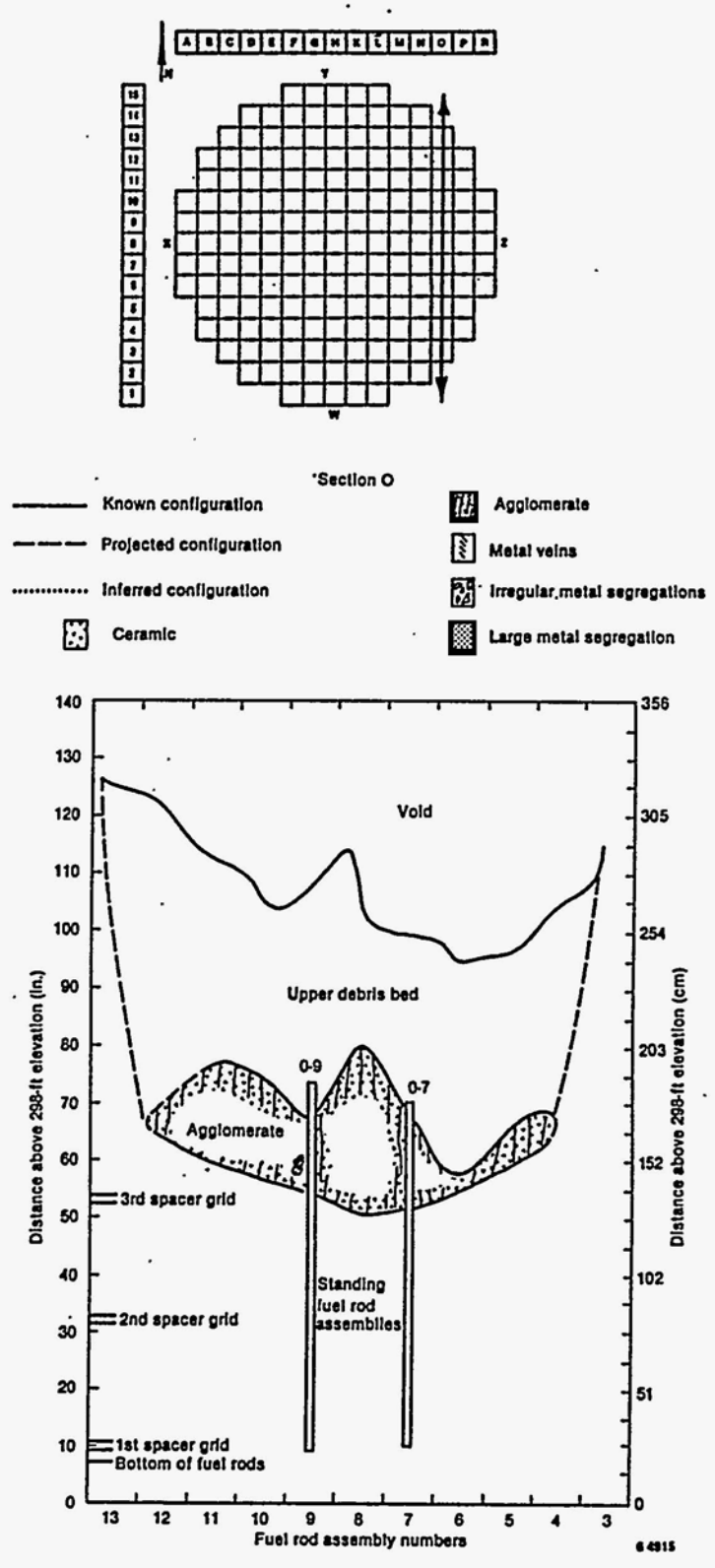

Figure E-12. Core cross section showing end-state damage configuration through O row of fuel assemblies.

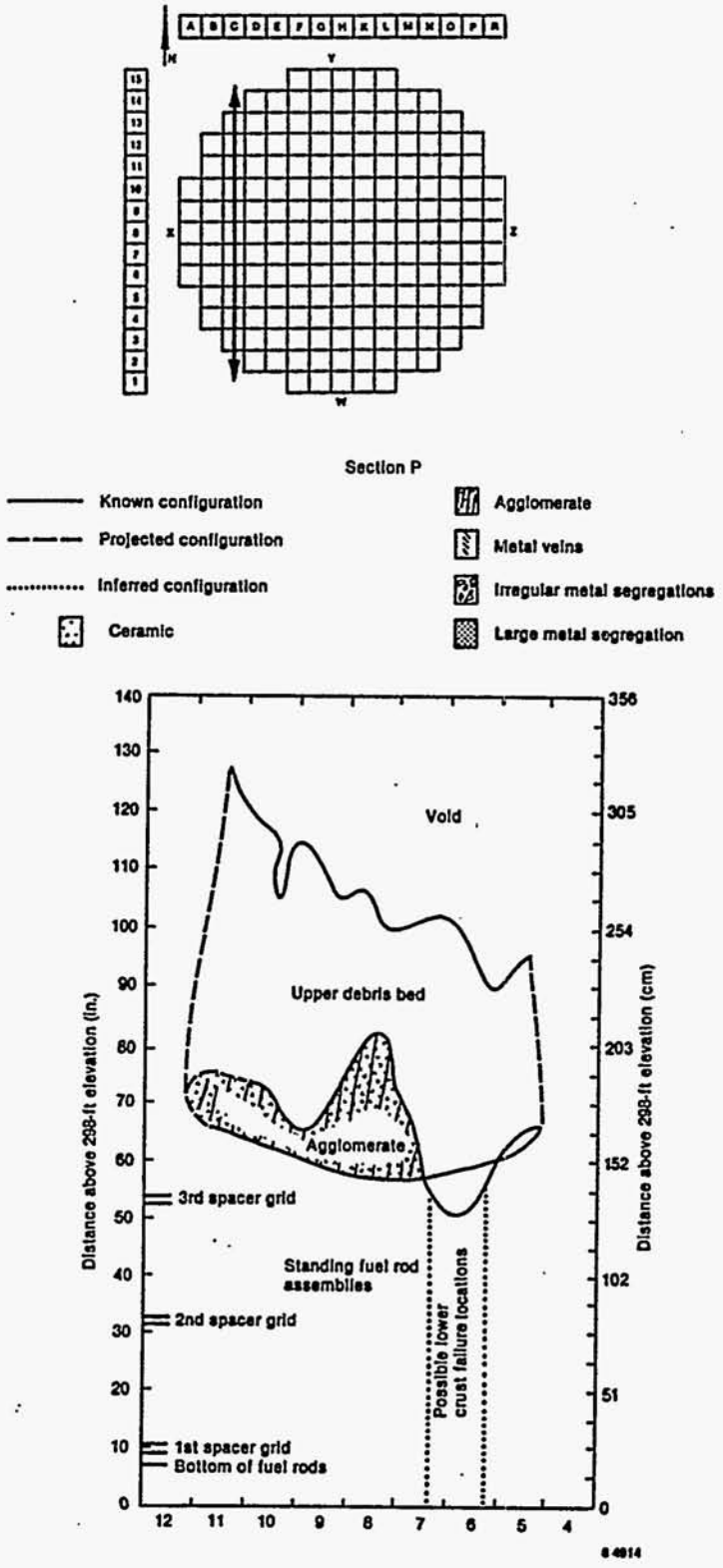

Figure E-13. Core cross section showing end-state damage configuration through P row of fuel assemblies.

APPENDIX F

CORE SUPPORT ASSEMBLY CONFIGURATION AND NOMENCLATURE

APPENDIX F

CORE SUPPORT ASSEMBLY CONFIGURATION AND NOMENCLATURE

The TMI-2 core support assembly configuration and nomenclature are shown in Figure F-1. The nomenclature shown in Figure F-1 has been used throughout the report.

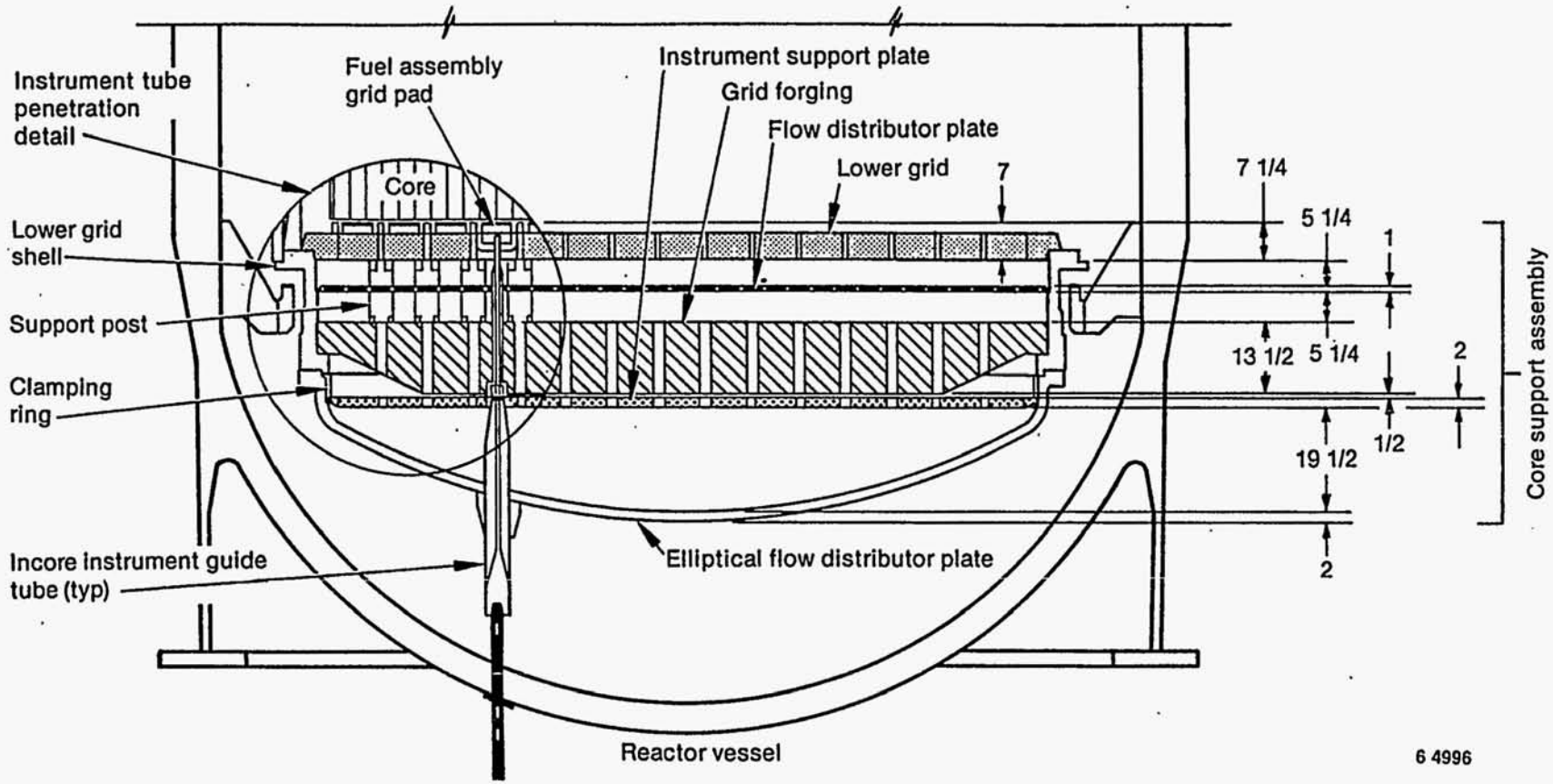

Figure F-1. TMI-2 Core Support Assembly configuration.

APPENDIX G

ESTIMATE OF VOLUME AND MASS FOR THE DEGRADED CORE REGION

APPENDIX G

ESTIMATE OF VOLUME AND MASS FOR THE DEGRADED CORE REGION

This Appendix presents the results of calculations to estimate the volumes and masses for each major region of the degraded core. Using the estimated core region masses and estimated uncertainty in these masses, the mass of the lower plenum debris is estimated. Finally, the best-estimate volume of the lower plenum debris is added to the known end-state volume of the molten core region to estimate the size of the molten core region just prior to the material relocation to the lower plenum.

Original Core Mass

Estimates of the original core material masses are presented in Table G-1 and are based on the original core mass inventory documented in Reference G-1. Also included in the Table is an estimate of oxygen uptake as a result of zircaloy oxidation during the accident.

Core Region Volumes

The core cross sections presented in Appendix E provide the basis for estimating the volumes of the upper debris bed, molten core zone, and intact fuel rods. Using these core cross sections and the fuel assembly cross-sectional area, the volumes of these degraded core regions were calculated and are summarized in Table G-2.

Core Mass Estimates

A core mass balance is possible using the degraded and intact core volumes shown in Table G-2 and assumptions for the density of the various core materials based on available data. Table G-3 summarizes the volumes and masses and their uncertainties.

Based on these estimates, the nominal mass of the lower plenum debris is approximately 23 tons. However, as noted in the Table, the uncertainty

TABLE G-1. ORIGINAL TMI-2 CORE MASS ESTIMATES[a]

Core Component	Zircaloy (lbm)	304 SS (lbm)	Inconel (lbm)	Ag-In-Cd (lbm)	Al_2O_3/B_4C (lbm)	Gd_2O_3/UO_2 (lbm)	ZrO_2 (lbm)	UO_2 (lbm)	Total (lbm)
Full-length control rod assembly (61 assemblies)									
Individual rod	276	37	15	96	--	--	4	1159	--
Total assembly	16,836	2,257	915	5,856	--	--	244	70,699	96,807
Partial-length control rod assembly (8 assemblies)									
Individual rod	276	31	15	26	--	--	4	1,159	--
Total assembly	2,208	248	120	208	--	--	32	9,272	12,088
Burnable poison rod assembly (68 assemblies)									
Individual rod	300	9	15	--	22	72	4	1159	--
Total assembly	20,400	612	1,020	--	1,496	4,896	272	78,812	107,508
Orifice rod assembly (40 assemblies)									
Individual rod	276	11	15	--	--	--	4	1,159	--
Total assembly	11,040	440	600	--	--	--	160	46,360	58,600
Total mass	50,484	3,557	2,655	6,064	1,496	4,896	708	205,143	275,003

a. The mass of the endfittings is not included.

b. A best-estimate of the oxygen uptake during the accident assumes that 70% of the original core zircaloy mass was oxidized; i.e., all zircaloy not contained in the remaining rod stubs. Thus, the oxygen uptake = zircaloy mass x oxidation fraction x atomic ratio of O_2/Ar = (40,484 lbm)(0.6)(32/91.22) = 10,600 lbm. The 2σ uncertainty is estimated to be ±50%, or 5300 lbm. This would give a nominal postaccident core mass of 285,603 lbm.

TABLE G-2. SUMMARY OF CORE VOLUME FROM CORE CROSS-SECTION FIGURES IN FT^3

Fuel Assembly Row	Intact Rods	Molten Core Region	Upper Debris
A	33.0	0	0
B	38.5	0	10.2
C	36.8	1.6	19.0
D	42.4	4.1	21.0
E	31.0	8.1	21.3
F	38.9	12.3	18.7
G	32.0	15.5	20.8
H	33.0	17.0	21.5
K	32.2	18.2	22.2
L	38.2	16.4	18.1
M	30.4	12.0	18.6
N	35.1	8.9	17.5
O	31.0	5.0	15.4
P	33.2	2.7	11.3
R	13.1	0	0
Total[a]	498.8	121.8	235.6

a. Total volume of intact rods, molten core region, upper debris, and upper core void = 1184.6 ft^3.

TABLE G-3. TMI-2 END-STATE FUEL REGION VOLUMES AND MASSES

Region	Estimated Volume (ft^3)	Estimated Material Density (lbm/ft^3)	Estimated Mass (lbm)	Comments
Upper core debris	236 ± 47[a]	280 ± 60[b]	66,080 ± 20,000	Based on core defueling and core bore data
Molten core zone	122 ± 24[a]	436 ± 60[c]	53,190 ± 13,000	
Standing rods	499 ± 50[a]	241 ± 5[e]	120,259 ± 12,300	
Lower plenum debris	105 ± 64	436 ± 60	46,070 ± 27,000	Based on postaccident core mass (Table G-1) and above data

a. From Table G-2. Uncertainties are engineering estimates.

b. Mid-point value between the ranges of measured upper debris bulk densities of 3.5 to 5.5 g/cm^3.

c. Assumed to be the same as the lower plenum debris (7.0 g/cm^3).

d. Obtained from Table G-1 and the original core volume = 1,182.1 ft^2.

in this value is approximately 50%, due largely to the uncertainty in the masses of the upper debris bed and the material in the previously molten core regions.

Estimate of the Molten Core Zone Prior to Lower Plenum Relocation

For estimating the molten core zone prior to the core material relocation to the lower plenum, it is assumed that the nominal lower plenum debris volume can be represented as a right-circular cylinder near the top of the end-state molten core region. The height of the additional molten core material is dependent on the assumed diameter of the cylinder, as shown below:

Cylindrical Region Diameter (ft)	Increased Height of Molten Zone (ft)	
8	2.0[a]	0.8[b]
7	2.7[a]	1.1[b]
6	3.7[a]	1.5[b]

Based on these assumptions, it is conceivable that the upper height of the molten core zone, before lower plenum relocation, was likely from one to several feet higher than the end-state molten core upper surface.

References

G-1. TMI-2 Accident Core Heatup Analysis (A Supplement), NSAC-25, June 1981.

G-2. D. Akers et al., "TMI-2 Lower Vessel Debris Examination," Proceedings of the 14th Water Reactor Safety Information Meeting, Gaithersburg, MD (to be published).

---

a. Based on a lower plenum volume of 103 ft^3.

b. Based on a lower plenum volume of 41 ft^3 (lower-based estimate).